PERFORMANCE EVALUATION OF A FREQUENCY MODULATED SPREAD-SPECTRUM SYSTEM

by
Yash M. Vasavada

Thesis submitted to the Faculty of the
Virginia Polytechnic Institute and State University
in partial fulfillment of the requirements for the degree of

MASTER OF SCIENCE
in
Electrical Engineering

Approved:

Dr. Jeffrey H. Reed
(Chairman)

Dr. Brian D. Woerner

Dr. Dennis G. Sweeney

May 1996
Blacksburg, Virginia

Performance Evaluation of a Frequency Modulated Spread-Spectrum System

by

Yash M. Vasavada

Committee Chairman: Dr. Jeffrey H. Reed

Electrical Engineering

Abstract

Analog frequency modulated (FM) systems offer advantages of reliable speech quality and simplicity, whereas code division multiple access (CDMA) systems promise high capacity, resistance to multipath fading, and simplified frequency planning. In this thesis, we investigate the performance of a wireless local loop (WLL) system that uses the frequency modulation with the CDMA technique.

The performance of the FM CDMA system is affected by the choice of the frequency demodulation method. Performance of different state-of-art DSP based FM demodulators is evaluated. Design improvements with threshold extension, pre-deemphasis, and voice companding techniques are explored, and the limitations of the DSP based FM demodulation methods are identified .

The transmitter, the channel, and the receiver of the FM CDMA system are simulated for particular values of FM bandwidth and spread-spectrum processing gain. The capacity supported by the FM CDMA sysem is estimated with different levels of orthogonal as well as non-orthognal multiple access interference. The performance of the FM CDMA system in AWGN, multipath fading, Doppler spread, and nonlinear signal processing effects is predicted. A power control algorithm for the FM CDMA system is proposed, and its effect on the system performance is studied.

The capacity of the FM based wireless system may saturate as the system evolves. An adaptive FM CDMA interference cancelation technique and a digital modulation with CDMA are two approaches investigated as ways to improve system capacity.

Acknowledgments

I wish to express my sincere thanks towards Dr. Jeffrey H. Reed, my advisor. His knack of solving the technical difficulties has truly amazed me. I also appreciate the time he devoted after me inspite of following a busy schedule. I immensely value his technical support, and also his nice nature.

I thank Drs. Woerner, and Sweeney on being my committee. Dr. Woerner has been very encouraging during the monthly progress meetings. Dr. Sweeney has provided excellent suggestions while carefully reviewing my thesis work.

I have the pleasure of acknowledging Sigtek, Inc. as the sponsor of the research project. I thank Mr. Royce Bunce and Mr. James Shea for providing the technical guidelines, and the suggestions regarding the line of the research. I enjoyed discussing the research progress during their monthly visits.

I would like to thank Tianshi Li, my project partner. Technical discussions with him have given me valuable insights related to our research.

I acknowledge the technical help from Milap Majmundar, Nitin Mangalvedhe, Paul Petrus and Nevena Zecevic, the graduate researchers at MPRG laboratories. I also thank the MPRG staff for their help during the course of the research.

I wish to express my deep gratitude towards my uncle and aunt, Drs. Ashwin and Kalpana Nanavati. Without their encouragement and support, my dream of obtaining an M.S. degree would have never fructified.

I dedicate this effort to my parents. I believe it is equivalent to an offering to the God.

Contents

List of Figures

List of Tables

Chapter 1

Introduction

Wireless local loop (WLL) enables a flexible connection of fixed subscribers to the network operations, and has become an economical tool for implementing subscriber loops in low density, rural, or third world areas. Driven by a strong customer need for the tetherless access to telephone network, many organizations are spending time, money, and effort at research and development in the wireless local loop services [Cox91]. As economical advantages of wireless access to subscribers fuel the ambitions of service providers, rapid advances in RF semiconductor devices, digital signal processing technology, and VLSI methods continue to sustain the technological demands of wireless local loop implementations [Cox86].

This thesis investigates an analog frequency modulated code division multiple access (FM CDMA) scheme aimed at providing wireless access to the telephone network. The primary goal of the research is to estimate the capacity of such a system in a variety of channel distortions. The thesis also compares different DSP implementations of the FM receiver, and identifies possible approaches for achieving capacity improvement over the FM CDMA technique.

This chapter presents a survey of different WLL system architectures. The background, and the motivation for the FM CDMA approach are also discussed in this chapter.

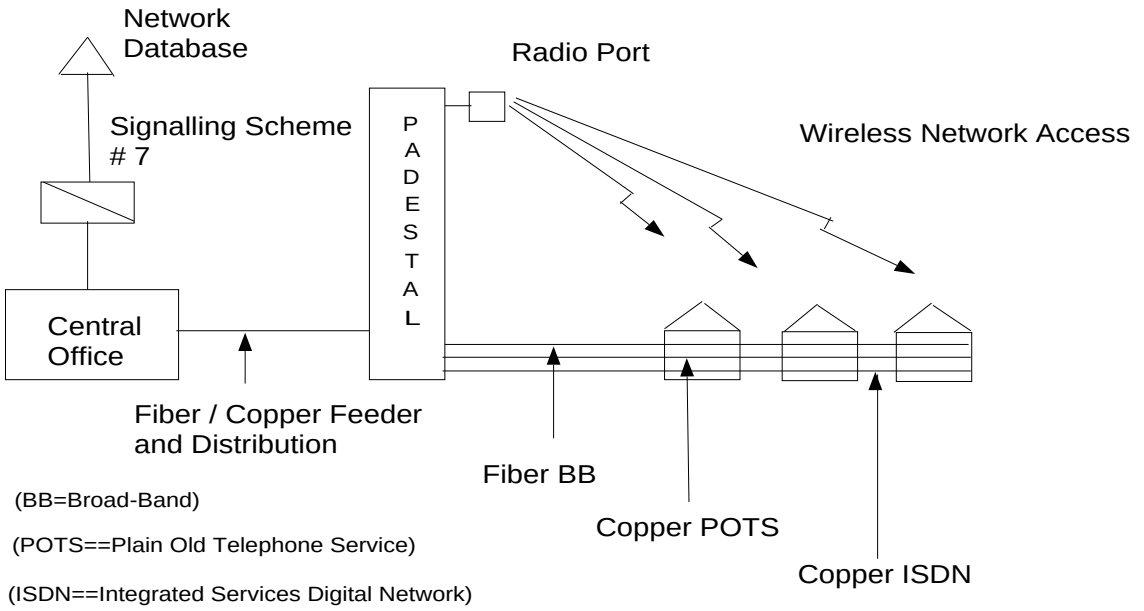

Figure 1.1: Bellcore's Digital Radio Scheme

1.1 Status of Wireless Local Loop Services

Wireless local loop design and development has attracted attention of many organizations, including Bellcore, Interdigital Corp., BNR, Qualcomm, and Analog Devices.

Figure 1.1 shows a low power digital radio scheme developed by Bellcore. The system includes a fiber or a copper feeder for providing private branch exchange (PBX) connection to several radio ports located in a central area. The digital radio system provides several wireless lines from the distributed radio ports, and co-exists with the wireline services. Depending on the status of the local loop in a service area, and the level of network control sophistication, the digital radio service can be merged to a set of Personal Communication Services (PCS) [Cox91].

D.L.Schilling, in an article on broadband CDMA, describes a WLL service developed by Interdigital, first implemented for commercial purposes by GTE in Quitaque, Texas. The Interdigital WLL product, Ultraphone, is based on a 16 PSK TDMA system and supports four time division multiplexed channels per 25 KHz band allocation [Sch94].

A simplified view of WLL architecture proposed by BNR is shown in Figure 1.2 [Jav94]. BNR approach towards WLL implementation is similar to Bellcore's system

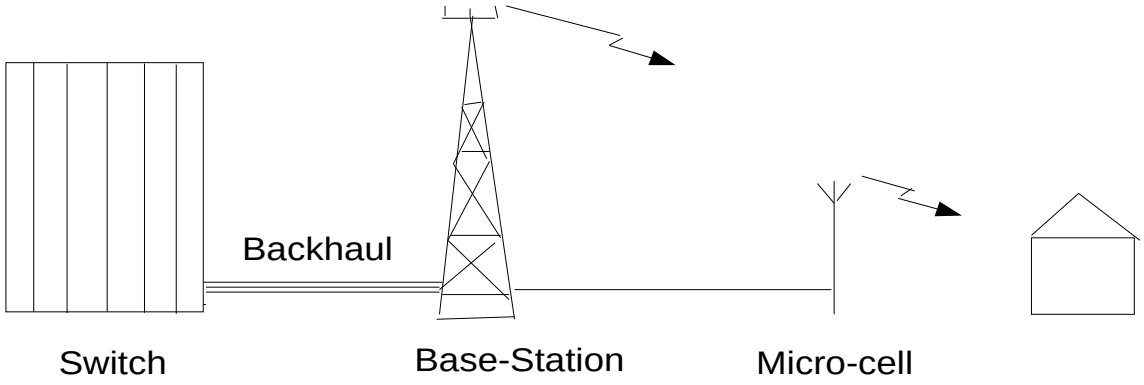

Figure 1.2: BNR's WLL system based on Fixed Cellular Concept

in terms of wireline interface with PBX. However, the BNR WLL system allows larger coverage areas for each base radio relay system, and hence is comparable to fixed cellular services, unlike Bellcore approach which is based on the philosophy of extending cordless telephone technology.

Qualcomm, Inc. has developed a fixed CDMA cellular system based on IS-95 standard. Qualcomm's product, commercial CDMA Base Station (CBS), for cellular and PCS systems has also been used for WLL implementations in third world countries.

Analog Devices Inc. is sponsoring a research effort at Indian Institute of Technology (I.I.T.), Madras, India to investigate extension of the Digital European Cordless Telephony (DECT) standard for WLL implementations [Ram94]. DECT based systems are economical, less complex, secure, and have a lower power requirement resulting in an improved battery life. These and several other characteristics of DECT, including a well-defined air interface protocol, dynamic channel allocation strategy, provision for ISDN services etc. have caused this standard to be a popular choice for WLL applications. Different implementations of DECT based WLL systems are discussed in [Owe93, Kid95]. The architecture proposed in [Owe93] is shown in Figure 1.3. User mobility supported by DECT systems is exploited in this architecture by including portable WLL terminals, besides fixed WLL terminals. A number of radio frequency ports (RFP) located at different points in the service area are connected to PSTN by means of network interface/concentrator. The network interface/concentrator acts as a part of central networking unit, and it is in direct or indirect control of network managment, and authentication and billing center.

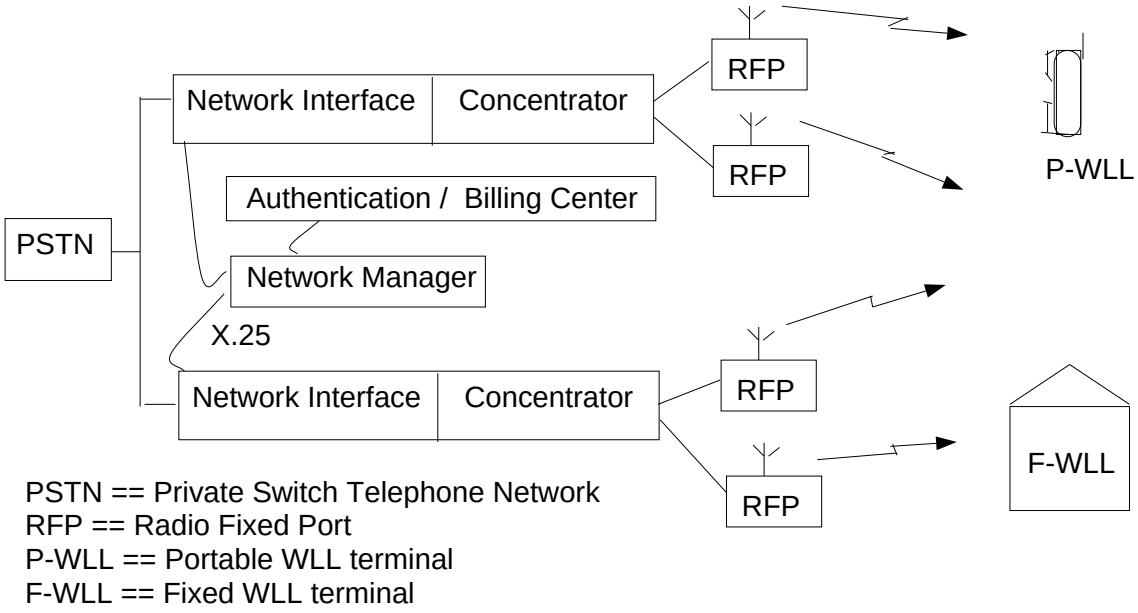

Figure 1.3: DECT based WLL System Architecture

Besides the Bellcore Digital Radio system, and DECT based systems, United Kingdom's cordless telephone standard, CT-2, has also been investigated for WLL applications [Mer93]. In general, WLL systems based on cordless telephony standards are attractive for short range, high density, urban and suburban areas, but the limited coverage area supported by such systems hinders their application to rural or low density regions. Susceptibility to multipath and intersymbol interference (ISI) is another disadvantage associated with narrowband Time Division Multiple Access (TDMA) based cordless telephone systems. Narrowband cordless telephone technologies, including CT-2 systems, do not support high data rates causing difficulties in interface with existing high data rate digital networks.

Fixed, or low mobility wireless access to PBX can also be achieved by existing cellular standards [Hau94]. Cellular systems are characterized by wide service areas with up to 10-35 km radii. Analog cellular systems, such as AMPS and ETACS, are less complex, economical, and provide high quality voice service, but are comparatively less secure systems. Digital cellular systems, such as GSM, offer state of the art technology, and provide multimedia applications with high security, and flexibility. However, the digital systems are more complex, and rely on voice coding techniques

which are sensitive to the rapidly varying wireless environment.

WLL systems based on cellular standards are appropriate for scattered distribution of users in rural, or suburban service areas, particularly for the areas already established with cellular infrastructure [Hau94].

Microwave Link for Point to Multi-Point (MLMP) systems offer an another option for implementing WLL systems. MLMP system has advantages of simplicity, low cost of implementation, good range of service, support of high data rates, and an easier interface to PSTN. Disadvantages of the MLMP system are spectrum inefficiency, Line of Sight (LOS) requirements, and non-standard air interface protocols. MLMP systems have been preferred for providing PBX access to clustered sets of subscribers [Hau94].

Satellite services have also been considered for wireless PBX access. A satellite based scheme, namely Demand Assigned Multiple Access (DAMA), adopted by Alcatel has been proposed for WLL application [Hau94]. Satellite based WLL services are expected to serve regions with many remote villages.

A generic study of radio propagation effects on WLL systems operating at 2 GHz is detailed in [Wer94]. The author evaluates the effect of Doppler shifts due to moving scatterers, and mentions that resulting short-term fading effects are not so disturbing for WLL applications as compared to a mobile application. The author also discusses TDMA/CDMA air interface standards, signal processing, and radio link engineering applied to WLL implementation. Claessens, in [Cla95], describes various tools for evaluating effectiveness of a local loop transmission system. Chandler et.al. [Cha93], examines the network engineering aspects of WLL systems, and analyzes and simulates blocking probability and connectivity in terms of average load, and average neighbors. The authors describe the routing and transport level issues for a well-integrated WLL service.

1.2 Design Choices

The subject of wireless local loop engineering can be investigated from many different aspects, such as propagation and cell-planning issues, PSTN and air standard interface design, and system level design aspects including choice of modulation and multiple access schemes. This thesis aims at studying viability of the FM CDMA

based WLL system from a system designer's perspective.

A brief discussion on the theory behind frequency modulation, and code division multiple access is warranted before explaining the motivation behind the FM CDMA wireless system.

1.2.1 An Overview of Frequency Modulation

Concept of Frequency Modulation (FM) is very old, and first became popular due to an erroneous belief that FM signals require smaller transmission bandwidth compared to AM signals [Lat89]. In 1922, J. Carson, by careful mathematical analysis, showed that bandwidth of FM systems is actually larger than AM systems, a result widely known now as Carson's rule [Car22]. However, Carson wrongly concluded that the FM introduced inherent distortion, and had no compensating advantages. Hence, it was not until 1936, a year in which Major Edwin H. Armstrong introduced noise-suppressing effects of wideband FM systems [Arm36], that many advantages of FM system were appreciated and the interest in FM systems was rekindled.

An expression for analytic (complex) FM signal is

$$g(t) = A_c e^{j\theta(t)}. \tag{1.1}$$

The phase of the FM signal is given by $\theta(t) = D_f \int_{-\infty}^{t} m(\sigma)\, d\sigma$. Frequency of the FM signal varies linearly with the amplitude of message signal, $m(t)$. The frequency deviation constant, D_f, has units of radians/volt-second. Its value determines the peak frequency deviation, $\Delta F = \frac{D_f V_p}{2\pi}$, where V_p is the peak value of the modulating signal $m(t)$. A related parameter widely used to characterize FM signals is the frequency modulation index $\beta = \frac{\Delta F}{B}$, where B is the message signal bandwidth [Cou93].

Frequency modulation is classified as a nonlinear modulation technique, since the amplitude of FM signal has a constant value, and is not a linear function of the modulating signal. It is generally difficult to precisely determine bandwidth of nonlinearly modulated signals. FM bandwidth, B_T, is usually approximated as $2(\beta + k)B$. The value of constant k depends on β. Narrowband FM signals, for which $\beta << 0.5$, the value of k is nearly unity. The resulting formula is the Carson's rule. However, Carson's rule is inaccurate for wideband FM signals, and better approximation to B_T results, if value of k is chosen between 1 and 2 [Lat89].

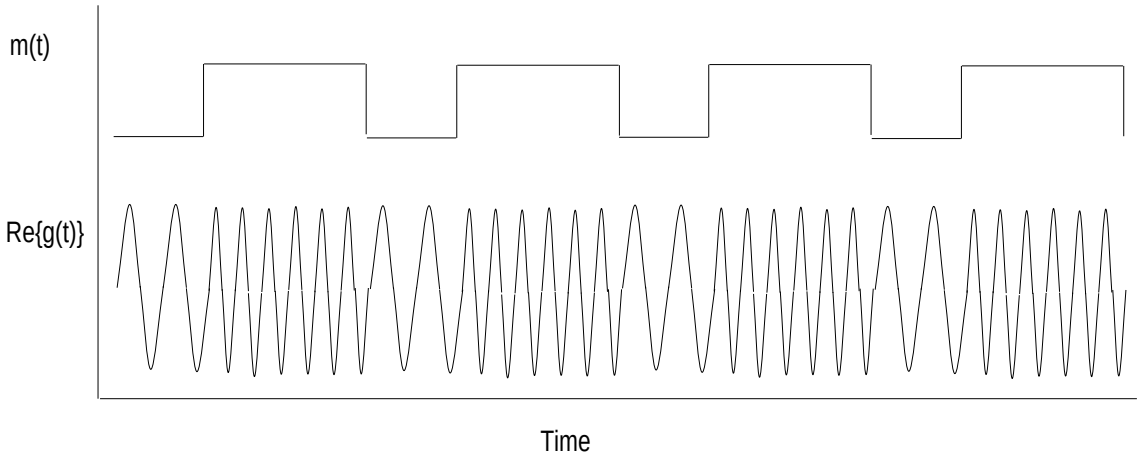

Figure 1.4: An Example of Frequency Modulation

For narrowband FM signals, higher order terms in Taylor's series expression of Equation 1.1 are negligible. The resulting form of NBFM signal is similar to that of an AM signal (except for a quadrature term). Hence, methods for generating NBFM are similar to AM signal generation techniques. Wideband FM signal may be generated by an indirect method in which the bandwidth of a NBFM signal is successively increased using frequency multipliers. A direct method for WBFM signal generation is based on varying a parameter of circuit component, usually capacitance, causing output signal frequency to vary in linear proportion to the amplitude of the modulating signal [Cou93].

There are many different FM demodulation methods all of which extract the message signal from the phase of FM signal. A study of different FM demodulation methods is detailed in Chapter 3.

1.2.2 An Overview of Code Division Multiple Access

An ideal communication system would maximize the output signal to noise ratio (SNR) while minimizing the spectrum usage. Information theory, in agreement with our intuitive and philosophical senses, denies achieving both the goals in a system. Shannon's theorem sets a direct relationship between the performance of communication systems, in terms of output SNR, and the cost of the communication systems,

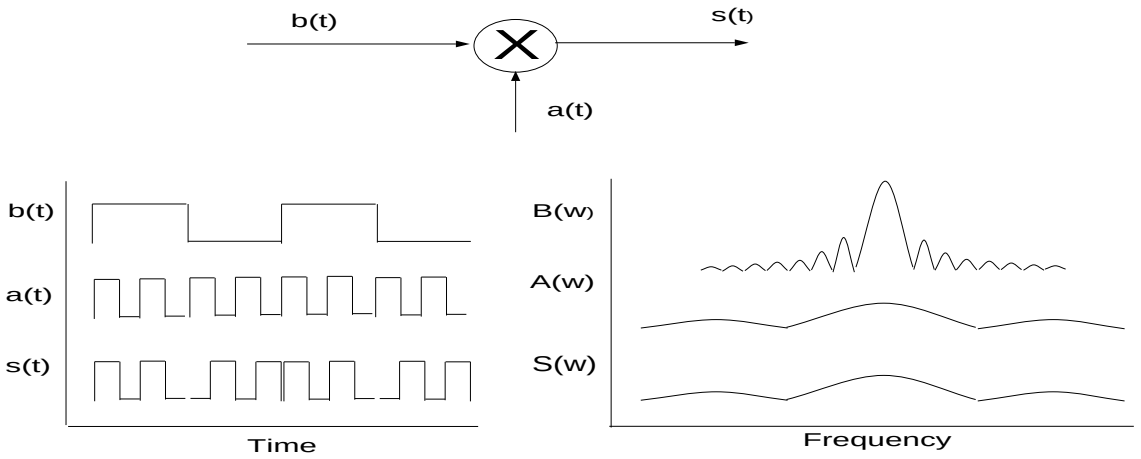

Figure 1.5: An Example of Spread-Spectrum Signal Generation

in terms of bandwidth requirements.

$$\frac{E_b}{N_o} = \frac{2^{R/W} - 1}{R/W}, \tag{1.2}$$

where E_b/N_o is signal to noise ratio (SNR) per bit, R is the data-rate in bits per second, and W is the channel bandwidth in Hertz. Accordingly, it is possible to achieve very high SNR values by increasing the transmission bandwidth W. Frequency modulation is one practical method in which better SNR values are obtained for wideband FM signals. Another practical method is the spread spectrum technique which uses a very high frequency spreading signal to modulate the transmitted signal. United States' digital cellular standard, IS-95, is based on spread-spectrum principle. IS-95 utilizes 64-ary orthogonal modulation on the signals transmitted by the cellular phones [Rap95]. However, the initial applications of spread-spectrum systems were rooted in entirely different characteristics of such systems. In the mid-1950's, the spread-spectrum systems were developed for military antijamming tactical communications [Pic92]. Figure 1.5 shows the process of spreading a binary data signal. The resulting signal is spread over a wideband and appears like a noise signal to a causal observer. It is not possible to evesdrop on, or jam the spread signal without the knowledge of the spreading signal.

Another application of spread-spectrum technique is code division multiple access (CDMA) scheme. CDMA gained attraction of the cellular communications industry

when the capacity of analog cellular systems started showing saturation. Many different users of a CDMA cellular system are allowed to use the same frequency band, and the same transmission time, resulting in a better frequency reuse efficiency and improved system capacity. Isolation among all simultaneously transmitted co-channel signals is provided by spreading each user's signal with a different spreading code. The spreading codes for different users achieve the necessary orthogonalization required for multiple access, and hence the name CDMA. For a CDMA based receiver, spread-signals of different users act as noise whose detrimental effects can be reduced by spreading the desired signal to a wide bandwidth. Processing gain of the spread spectrum system is defined as $N = W/R$, where W is the spread bandwidth, and R is the bandwidth of the original signal. The larger the value of the processing gain, N, the better the interference rejection capability of the system.

There are many classes of CDMA systems [Woe96]. In direct sequence spread-spectrum (DS-SS) systems, the spreading code directly modulates the time domain transmitted signal. Frequency hopped spread-spectrum (FH-SS) systems change the transmission frequency based on the structure of the spreading code. Depending on the rate of the change in transmission frequency relative to the data rate, FH spread spectrum systems are classified either as fast frequency hopping (FFH) or slow frequency hopping (SFH) systems. Frequency hopped spread-spectrum systems offer advantages of immunity to the near-far problem, e.g., the degradation in system performance when received power from any one user is much higher than remaining users. European digital cellular standard, *Groupe Speciale Mobile* (GSM), and cellular digital packet data (CDPD) standard use frequency hopping principle. However, in general FH-SS systems are less popular than DS-SS systems, due to less attractive modulation scheme that is used with FH-SS systems, and an increased system complexity. Time hopped spread-spectrum (TH-SS) systems change the transmission time in a pseudo-random manner. Spread-spectrum systems employing more than one of the above techniques are also possible, but such hybrid systems are yet to find a major commercial application.

1.2.3 Motivation behind the Design Choices

Advantages of FM systems

Frequency Modulation offers two-fold advantage over other analog modulation techniques, including Amplitude Modulation. One advantage for FM systems is realized due to the constant envelope nature of FM signal. Since all the information is contained in the phase of the FM signal, it does not suffer from amplitude fading and non-linearity effects, unlike AM signals whose performance deteriorates in such conditions. FM systems also offer an inherent way of increasing the SNR by trading band occupancy, whereas AM systems do not offer such an exchange between SNR and bandwidth.

Besides, the two most attractive properties of the FM system, there are many other factors in favor of the choice of the FM system. FM signals are characterized by the *capture effect*, a phenomena in which a weak co-channel interferer is suppressed by a stronger signal. Another attractive feature of FM systems is the *quieting effect*, or the reduction of the effect of noise during periods of silence due to the presence of a strong unmodulated carrier. Cellular systems based on FM modulation use companding, e.g. nonlinear amplitude compression at the transmitter, and corresponding amplitude expansion at the receiver, to further reduce the noise effects when the amplitude of message signal is low.

FM systems show drastic performance degradation below a certain threshold of input SNR. It is important to ensure that the FM receiver operates above this threshold to obtain a high fidelity demodulated signal. PLL based FM demodulation, or FM demodulation with Feedback (FMFB) are the improved FM demodulation techniques for lowering the threshold value of input SNR, and increasing the dynamic range of the system operation.

An important feature of the conventional FM demodulator is its unique effect on frequency spectrum of output noise signal. Since, FM demodulators take time derivative of the received signal, high frequency components of the noise are amplified [Tau86]. A popular technique, pre-deemphasis (PDE), combats deteriorating effects of noise by emphasizing the high frequency components of the message signal prior to the FM modulation. An inverse law is used at the receiver to deemphasize the high frequency components. Deemphasis operation mitigates the high frequency noise

effects at the FM demodulator output, resulting in an improved receiver performance.

Since advantages of FM systems over AM systems are widely recognized, a more interesting and relevant topic is the comparison of FM systems with the digital modulation schemes. Digital systems convert continuous time analog message signals into discrete time, discrete amplitude signals before modifying either amplitude, phase, or frequency of the carrier signal. Digital wireless systems are increasingly replacing analog systems because of their many attractive features including feasibility for bandwidth-SNR exchange, improved bandwidth efficiency due to data compression, improved system performance due to error correction and detection techniques, easier interface with existing digital networks etc [Woe96]. Inspite of such advantages of digital modulation techniques, selection of the FM technique for wireless applications is also well justified. The FM based wireless system, specifically with simple DSP based implementations, is less complex, and is easily upgradable. Such a system also has a reliable perceptual voice quality, unlike several voice coding techniques. Due to their simplicity, FM receiver structures are easier to implement and understand, and are economically viable. Hence, FM based wireless systems are still considered a good choice, especially in rural or suburban service areas, where the user density is not usually very high, or in third world countries where initial subscriber base is not very large.

Advantages of CDMA Systems

The CDMA technique for wireless applications is increasingly gaining popularity due to the possibility of an increase in the capacity relative to the frequency division multiple access (FDMA), or the time division multiple access (TDMA) techniques. The universal frequency reuse available with the CDMA systems gives them a capacity advantage over other cellular systems. The frequency planning becomes easier due to very high frequency reuse efficiency, and coverage holes are minimized. Since the CDMA is an interference limited technique, several interference reduction methods such as cell sectorization with use of directional antennas, and voice activity exploitation further improve the capacity of such a system [Gil91].

Even when the capacity of the wireless system is not a main issue, the choice of the CDMA technique is justified. An important attribute of the CDMA wireless systems is their inherent resistance to the multipath fading. Multipath components with

interarrival times greater than the inverse of signal bandwidth are highly uncorrelated and resolvable. Hence, the multipath combining can be incorporated to actually improve system performance. Better understanding of the robustness of the CDMA systems to the multipath fading is possible by viewing this phenomenon in frequency domain. Typical multipath wireless channels resemble a notch filter with a width (coherence bandwidth) of the order of several hundreds of KHz. While such a notch is sufficient to impair a narrowband transmission, as in FDMA or narrowband TDMA systems, it corrupts only a small fraction of the spread-spectrum band and does not cause substantial performance degradation [Kau95].

A CDMA system undergoes a graceful degradation when the number of users increase beyond the designed value. Such a soft capacity offered by the CDMA systems is a useful feature, since the TDMA or FDMA systems do not support the $K + 1^{th}$ user, if the system is designed for K users.

Since the transmitted signal in the CDMA system is spread over a wide bandwidth, it causes only a small increase in the noise floor for an existing narrowband system. Hence, it is possible to overlay a broadband CDMA signal on top of a narrowband spectrum. Another advantage of the CDMA system, though not necessarily applicable for local loop systems, is due to the possibility of soft handoff wherein several base-stations combine the energy received from a mobile user to achieve better performance.

Several negative aspects of the CDMA systems should also be understood before designing such systems. One is the complexity of such systems which arises due to the need for synchronizing and tracking the spreading code at the receiver. Misalignment of the spreading code at the receiver results in imperfect despreading operation which greatly impairs the system performance. Another limitation of CDMA systems is the near-far effect. In wireless channels, the signal attenuates at the rate of 20-40 dB/kilometer. Thus, if an undesired user is much closer to the receiver than the user of interest, the undesired user can easily swamp the desired user at the receiver. The near-far effect requires very stringent power control at the transmit and receive ends. Unfortunately, due to fading effects, and component gain variations perfect power control is very difficult to attain. Besides imperfect power control, the capacity of CDMA system also suffers from self-jamming or poor interference cancelation, since in practical conditions received signals from different users are never perfectly orthogonal

[Dix84].

1.3 Purpose of Research

Advantages of digital CDMA systems are now widely accepted, and are on the verge of practical realization. However, the advantages of analog CDMA systems are less understood. The purpose of the this research is to evaluate the performance, and the capacity of such systems by simulating the FM CDMA system.

The first task of the research is identification of an optimum FM demodulator based on digital signal processing techniques. Improvement in output SNR for FM demodulators by means of pre-deemphasis (PDE), and companding techniques are estimated. A lower limit, or threshold, on the operation of FM demodulators is determined, and an estimate of the extent of threshold extension possible due to the phase-locked loop (PLL) based FM demodulation is formed. Voice quality for an FM receiver operating above the threshold is evaluated. Various objective voice quality measures, such as mean squared error (MSE) and SNR at the output, segmented SNR, and distribution functions of segmented SNR values are used, apart from the subjective voice quality evaluations.

The second task of the research involves estimation of the capacity supported by the FM CDMA system. System level simulations are performed, and the output voice quality for the FM CDMA system with different levels of multiple access interference (MAI), and various channel impairments is identified. A novel power control algorithm for the FM CDMA system is developed, and the stability of such an algorithm is shown. The system performance with such a power control scheme is also studied.

The third task of the research is to suggest the direction of possible evolution of the FM CDMA based WLL system. Examples of the performance improvement possible with the advanced adaptive FM CDMA receivers operating in multipath fading effects are presented. The capacity gains realized by the adaptive interference cancelation algorithms with imperfect power control, or with non-orthogonal spreading codes, are also estimated. Another approach proposed for future system upgrades is based on digital modulation format with the CDMA technique. The capacity supported by such a system is estimated using analytic tools, and is compared with the capacity of the FM CDMA system.

The remainder of the thesis is organized as follows. Chapter 2 presents an overview of the FM CDMA system from hardware perspective. It also describes the simulation strategy adopted in this research. Chapter 3 focuses on the DSP based FM demodulation techniques. A comparative study of various FM demodulators, in terms of their output SNR characteristics is detailed. Effects of PDE and companding on SNR curves are shown. Various methods of calculating the output SNR are also discussed in Chapter 3. Chapter 4 presents the test cases illustrating the performance of the FM CDMA system in AWGN, multipath fading, nonlinear amplification, and imperfect power control environment. The capacity of the FM CDMA system with orthogonal spreading codes is compared with that for the non-orthogonal spreading codes for different users. Impact of these channel imperfections on an orthogonal CDMA link is compared with the impact on the non-orthognal CDMA link. Chapter 5 focuses on interference rejection algorithms, and describes a digital CDMA system that may achieve improvements over the FM CDMA scheme. Concluding chapter summarizes the thesis research, and presents suggestions for the future work.

Chapter 2

System Description

WLL system development encompasses a broad range of design and implementation challenges. This chapter provides an introductory treatment of various FM CDMA WLL engineering issues such as cell and frequency planning, air and wireline interface protocols, and system evolution strategies. The base-station and user phone architectures of the FM CDMA WLL system are described, and a framework for the remainder of the thesis is built.

At this stage, it is necessary to present the simulation strategy adopted for performance evaluation of the FM CDMA WLL system. Simulated system block diagrams, along with the characteristics of the waveforms at input and output of various signal processing modules, are described for a better understanding of the operation of the FM CDMA system. Various challenges encountered during software implementation of the FM CDMA system are detailed in the concluding section of the chapter.

2.1 FM CDMA WLL Engineering Issues

The main components of the WLL system are shown in Figure 2.1. The system provides tetherless connection between the base-station and the user phone. The system does not support hand-off, and roaming user identification typically associated with cellular mobile radio networks.

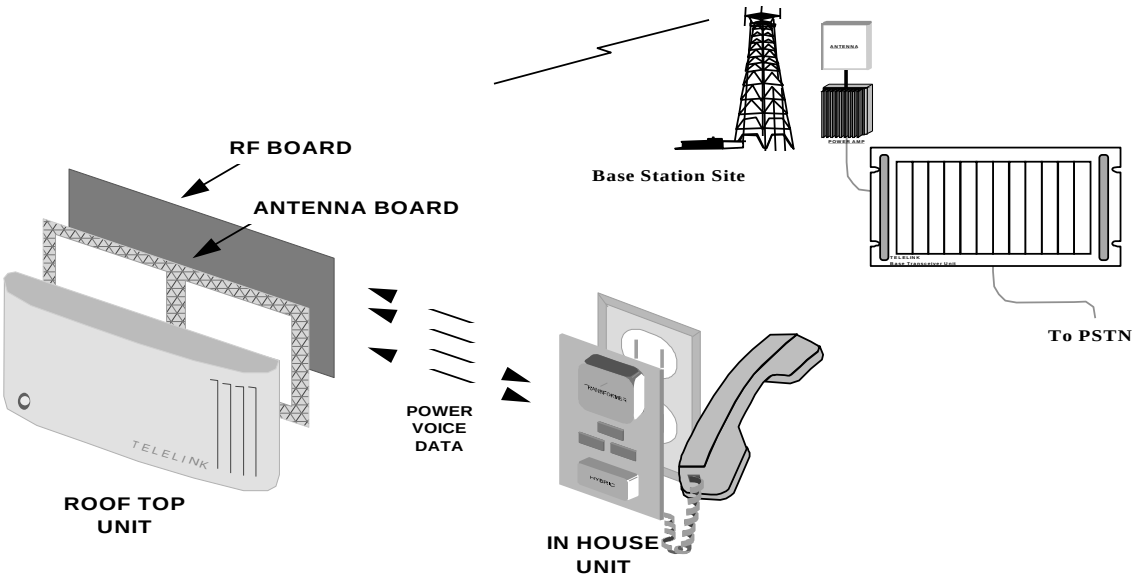

Figure 2.1: Elements of Wireless Local Loop System

2.1.1 System Planning

Ensuring a good quality of service is the primary challenge faced during the design and planning of WLL systems. For the FM CDMA system, this requirement translates to achieving a robust interference cancelation such that the FM demodulator operates above its threshold for severe multiple access interference (MAI). Thus, it becomes important to identify an FM demodulator which offers high output SNR values above the threshold region. Dynamic range of the operation of the FM demodulator determines the system capacity, and by lowering the demodulator threshold, an increase in the simultaneous channels served by the system can be achieved. Identifying a good set of spreading codes is even more important for CDMA systems, since in-cell interference is reduced if different user's spreading codes have very low cross-correlation values. Out of cell interference is reduced if the autocorrelation function for the spreading codes have a very sharp peak at the zero lag, and very small values for non-zero delays. By assigning different initial delays for the co-channel spreading codes in a cluster, the out-of-cell interference is reduced significantly [Whi94].

Achieving a good coverage, regardless of the terrain and user density variations, is yet another requirement of WLL engineering. Cell planning and frequency planning play crucial roles in removing coverage holes. This task is simplified for the FM CDMA system due to the universal frequency reuse capability of CDMA technique. It is still necessary to recognize the effects of large-scale and small-scale propagation phenomena in 1.9 GHz range on the system coverage. Due to large scale propagation effects, which include free-space distance dependent losses, and the losses due to reflections, refraction, and diffraction of the transmitted energy, the received power decays as a function of the T-R separation distance raised to some power, i.e. the loss follows a power-law function. Propagation effects are more precisely determined on the basis of empirical measurements. Due to time and energy intensive nature of empirical channel modeling, a more practical approach uses the documented propagation prediction models in varying channel conditions. Such propagation models include Okumura model, Hata model, Longley-Rice model etc [Pro88].

Since large-scale propagation effects cause very low signal to interference ratios for the WLL users at a large distance from the base-station, it is advantageous to employ power control. Power control plays a more important role for the CDMA technique. Link quality of a user in a CDMA system is greatly affected if the received power from an interfering user has a much higher value. Open loop power control adjusts the transmitted powers of different users based on the received signal strength at the user phone receiver, and attempts to drive the received power values at the base-station from different users to a constant value. However, open loop power control does not take into account small-scale variations in the received signal levels. Closed-loop power control mechanisms wherein the base-station controls the transmitted power of different user phones, are usually more effective in reducing the MAI levels for CDMA systems. Due to random nature of the channel attenuation, and an irreducible response time of power control schemes, it is impossible to achieve perfect power control at all times under practical conditions. Resulting mismatch in power levels causes degradation in terms of the received signal quality, and coverage regions [Lee91].

Power control schemes vary in different wireless CDMA system implementations. The proposed power control scheme for the FM CDMA WLL system uses a subaudible pilot tone multiplexed with the FM signal. The FM signal is 15 dB higher,

in terms of total power, than the pilot signal. The base-station controls the pilot tone amplitude to within ± 5 dB of the nominal value depending on the received power from the user phone. The user phone despreads the received signal, extracts the pilot tone, and changes its transmit power level depending on the detected pilot tone amplitude, thus, implementing a combined open and closed loop power control. Chapter 4 discusses the power control algorithm for the FM CDMA system in further details.

The pilot tone in the FM CDMA system also helps in deriving the timing information, and in achieving a very rapid synchronization of the spreading code at the receiver. The pilot tone is also used in detecting multipath delays [Sig95]. The performance of wideband CDMA systems can be improved by coherent combination of different resolvable multipath components.

Some of the functions performed by pilot tone, such as power control and timing information, are conventionally performed by dedicated control channels in most cellular/PCS standards. For the FM CDMA WLL system, the control channel is designed to aid in call-setup procedures, and hence requires low data rates up to 10 kbps. The control channel uses quadrature phase shift keying (QPSK) on the binary control data.

System Evolution

Initial design of the FM CDMA WLL system is aimed at simplicity and exploits a low expected user density. Each base-station covers a cell with radius of approximately 10 km. Omnidirectional antennas are used initially, and larger areas are covered using multiple base-stations. Each base-station supports 60 trunked channels, which translate to 500 to 1500 subscriber channels depending on the traffic intensity, and required grade of service.

Increasing capacity requirements may be handled by installing additional radio frequency (RF) hardware such that the number of trunked radio channels supported by each base-station increases. However, a more economical and elegant method is to employ cell-sectoring. With the CDMA approach, significant capacity improvement may be achieved by reducing the multiple access interference within a cell by means of sectorized antennas at the base-station. A sectored cell, using 60 degree antenna beam-width, is shown in Figure 2.2. A conservative estimate allows for three times

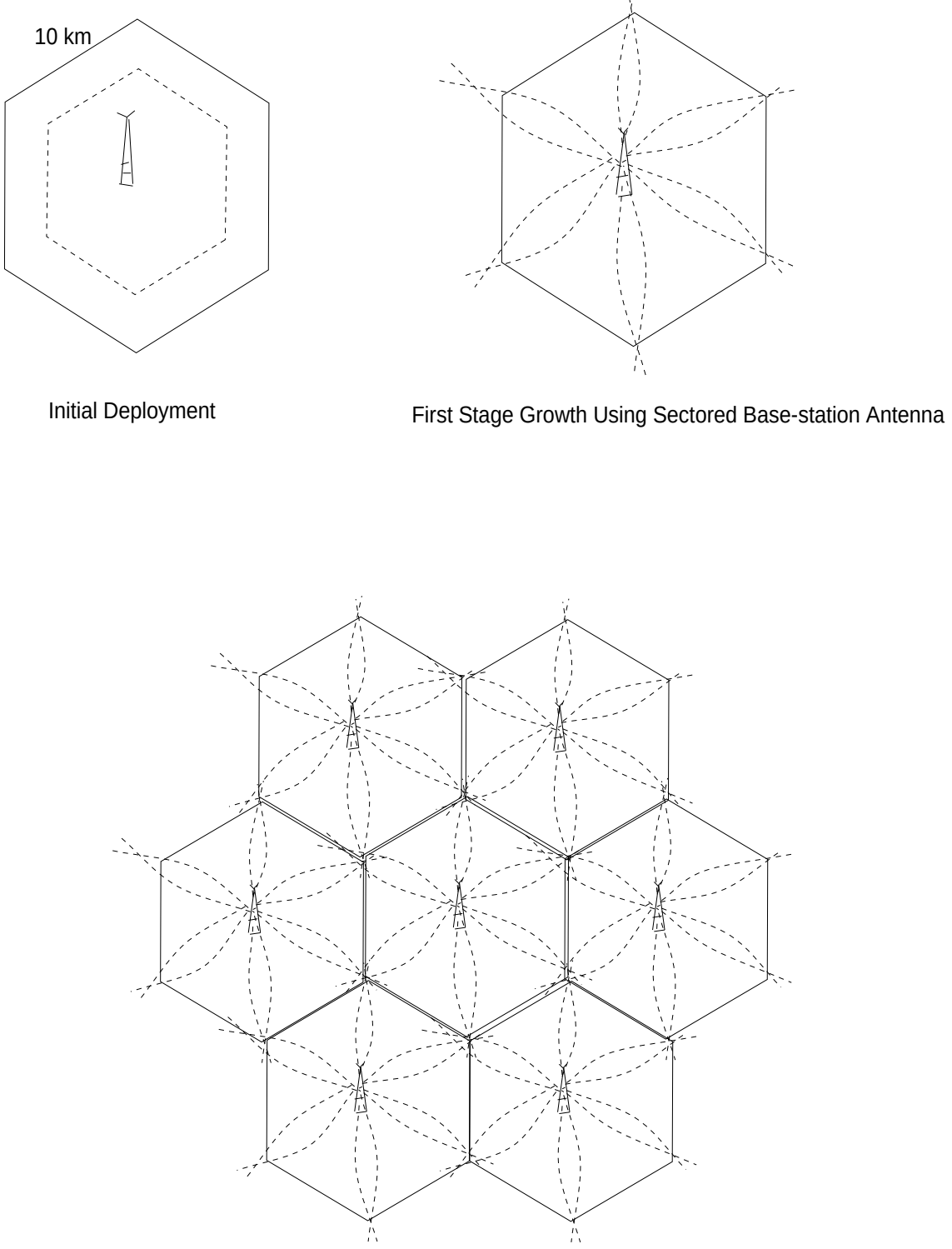

Figure 2.2: Different Phases of System Evolution

capacity increase with the same quality of the service. As the system evolves, it may become necessary to further increase the system capacity by cell-splitting. Universal frequency reuse supported by the CDMA scheme can be exploited by reducing the cell areas, and increasing the number of base-stations in the region of service. The final stage of the system growth may incorporate interference rejection processing at the base-station, or a digital modulation format with the CDMA scheme. Chapter 5 discusses these capacity improvement techniques in further details.

2.1.2 Air and Wireline Interface Protocols

As shown in Figure 2.1, the base station provides the wireless communication links to various user phones within its coverage area. Private Branch Exchange (PBX), or system switch, handles the traffic served by a group of base-stations, and acts as an interface to the digital telephone network. The system switch need not be collocated with any base-station. Typically, a digital wireline link connects the system switch with the base-stations. Complexity of the system switch, and the bandwidth of the wireline link determine number of the system switches required to serve deployed set of base-stations.

Each user of WLL system is first assigned to a specific system switch. The related registration, identification, and security issues are important for ensuring correct setup sequence for each call served by the system. Each user phone is assigned a public and a private ID number which are also registered at the system switch database. During operation of the WLL system, the base-station periodically interrogates the user phones using a control channel. The control channel, which carries digital data for user and channel identification, periodically establishes the link between the base-station and the user phone even during the periods of inactivity.

A protocol that may be adopted for the calls originated by an external party is shown in Figure 2.3 [Rap95]. The system switch informs the base-station public ID number of the desired phone. The base station broadcasts the public phone ID number on forward control channel. Each subscriber phone equipment continually tracks the forward received control channel, and if the broadcast public ID matches with the record of its own public ID, the user phone conveys its private ID to the base-station on the reverse control channel. The base-station informs the system switch of the private ID number of the user phone, and if the database record at the

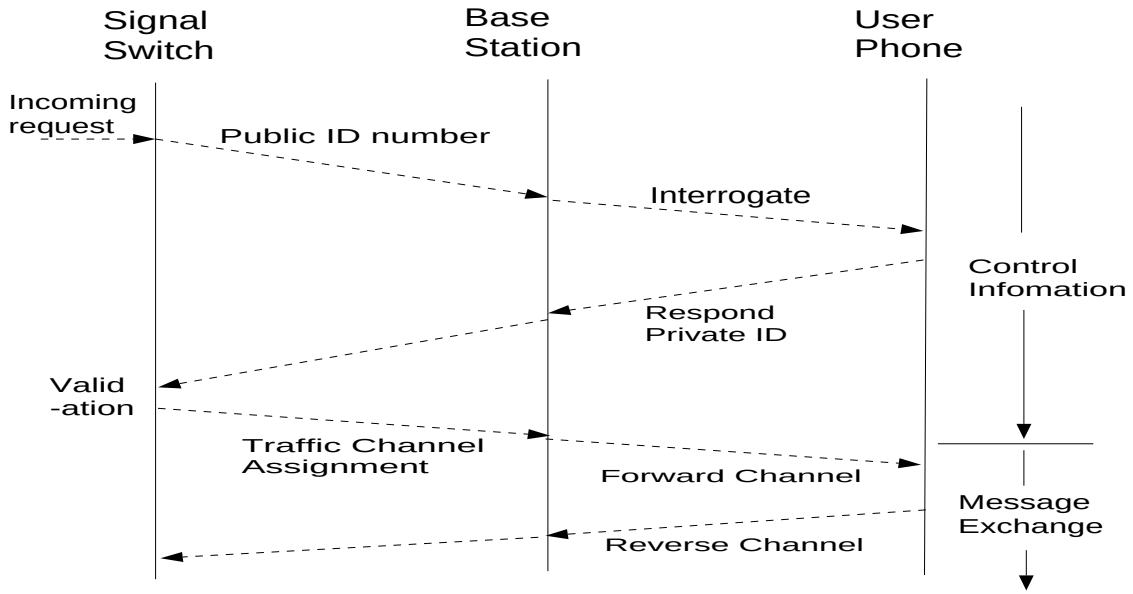

Figure 2.3: Call Setup Procedure: Initiated by the System Switch

system switch matches with the information received from the base-station, the call setup is completed, and the system switch instructs the base-station to assign a pair of forward and reverse link traffic channels to the user phone.

The calls initiated by the user phones are also processed in a similar manner. The user phone transmits an initial short request message on the reverse control link. The request contains the public and private user ID numbers and is received by the base-station as a random process. Usually, random access protocols, such as ALOHA, or slotted ALOHA, are suitable for handling the reverse link requests. When the base-station successfully receives the request message from the user phone, it passes the voice channel request, along with the user public and private ID numbers, to the system switch. The switch performs user validation checks, and informs the base-station the pair of forward and reverse voice link assignment to the user phone.

The above set of protocols require the system switch to handle all the processing related to the call setup. Variation of the above scheme may distribute the processing and database resources between the base-station and the system switch [Rap95].

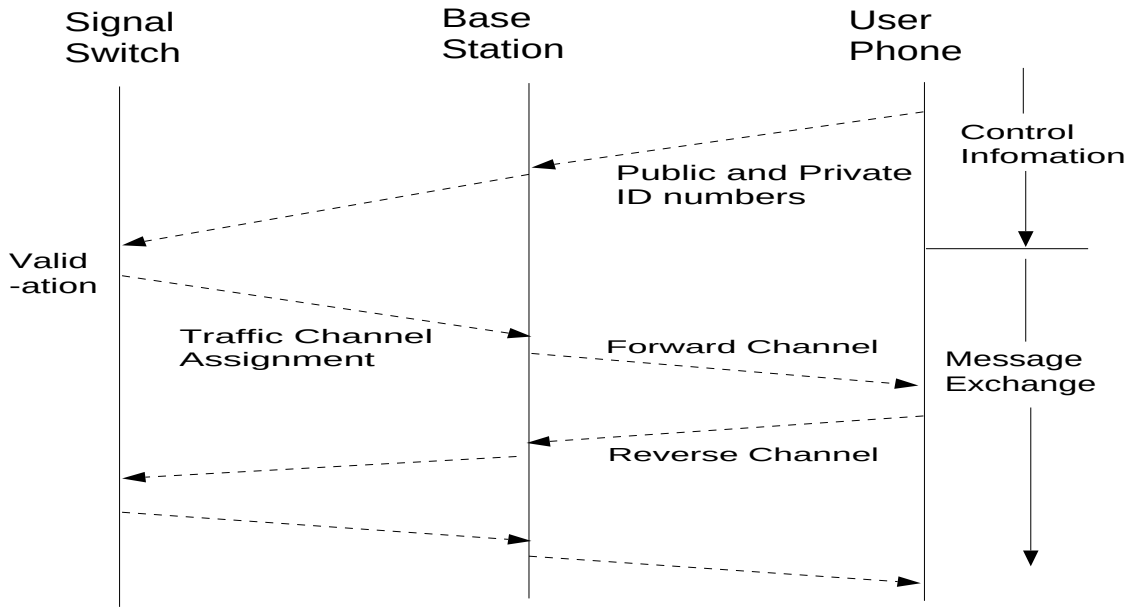

Figure 2.4: Call Setup Procedure: Initiated by the User Phone

2.2 System Architecture and Modeling

The hardware architectural block diagrams for the FM CDMA base-station and the user phone are shown in Figure 2.7, and Figure 2.5 respectively. Figure 2.6 shows a typical layout of the base-station equipment [Sig95].

2.2.1 FM CDMA Transmitter Configuration

The FM CDMA base-station and user phone transmitter architectures show many functional similarities, and certain implementation differences.

The user phone transmitter DSP unit converts analog output of the microphone to digital voice signal at sampling frequency of 64 KHz. At the base-station, the ADC unit is replaced by a transcoding unit which converts digital data received from the system switch to the digital voice signal.

Discrete time voice signal is passed through a pre-processor unit which performs 2:1 dB amplitude compression, and pre-emphasis filtering on the voice signal. Output of the pre-processor FM modulates a carrier at an intermediate frequency of 16 KHz. The pilot tone is generated at the baseband and added to the FM signal.

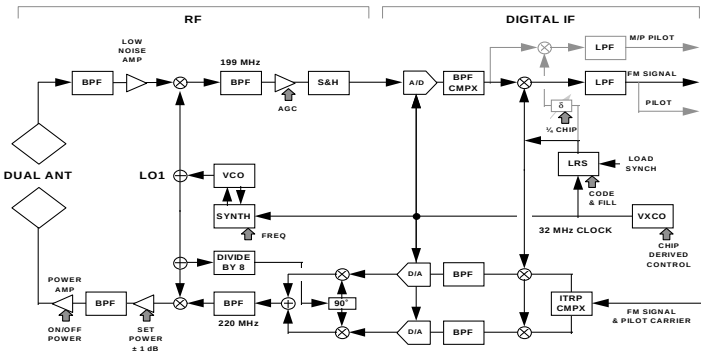

Figure 2.5: User Phone Hardware Architecture [Sig95]

An eleven bit linear feedback shift register (LFSR), initialized with the user-specific spreading code, operates at 8 MHz chip frequency. The length of the spreading code is 2048, and the code repeat frequency is approximately 4 KHz. Each rectangular pulse (chip) of the spreading code is sampled four times (at a sampling frequency of 32 MHz), and is filtered using square-root raised cosine characteristics. The resultant discrete time digital waveform is then multiplied with the combined FM and pilot signal at the sampling frequency of 32 MHz. The spread FM signal at the digital signal processor output is converted to an analog signal before upconversion to an IF frequency of 220 MHz.

The final RF unit at the user phone transmitter upconverts the IF signal to the transmission frequency of 1.9 GHz, and feeds the transmitter antenna after amplification and bandpass filtering.

Since each user's signal requires the signal processing functions prior to the transmission, a base-station transmitter supporting 64 trunked channels has an equal number of DSP units. Output signals for different DSP units at the base-station are combined after upconversion to the IF. A single IF unit combines four to eight DSP

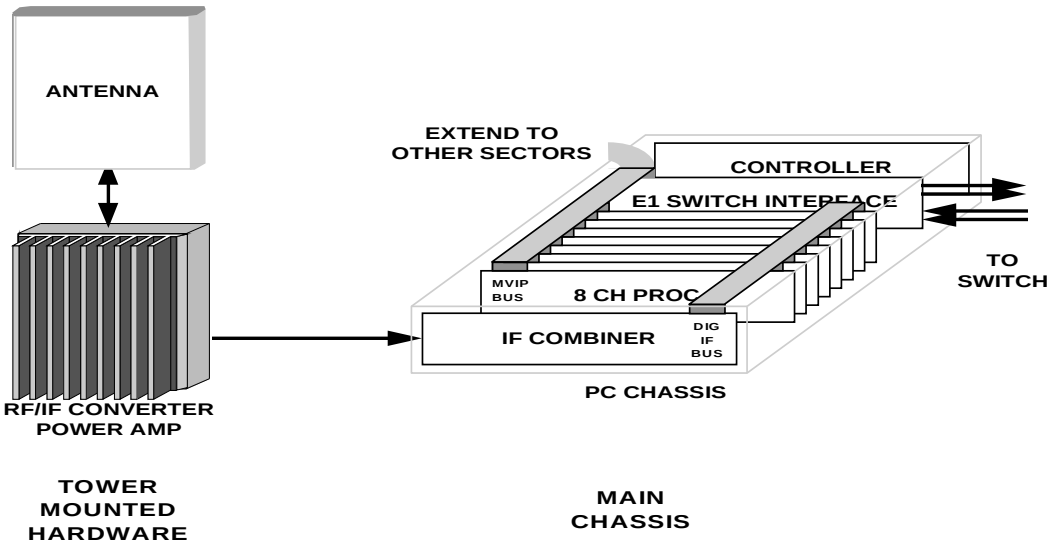

Figure 2.6: Base-station Block Diagram [Sig95]

module outputs. The RF unit at the base-station upconverts combined IF signals for all users, before amplification, bandpass filtering, and transmission. The base-station power amplifier handles a greater load compared to the user phone RF amplifier, and is affected by amplifier saturation effects particularly during the periods of peak traffic load [Sig95b].

Simulation model

Simulation approach for the base-station and the user phone transmitters is illustrated in Figures 2.8, and 2.9 respectively. The simulated transmitter model performs all DSP functions performed by a base-station or user-phone transmitter, except real-time ADC or DAC operations.

The transmitted signal for the forward link is the combined synchronous FM CDMA signals for different users. The simulation uses analytic FM signals at 16 KHz IF. The complex valued FM signal is spread by a real valued spreading code at 8 MHz. The sampling frequency of the FM signal and the spreading code is increased to 32

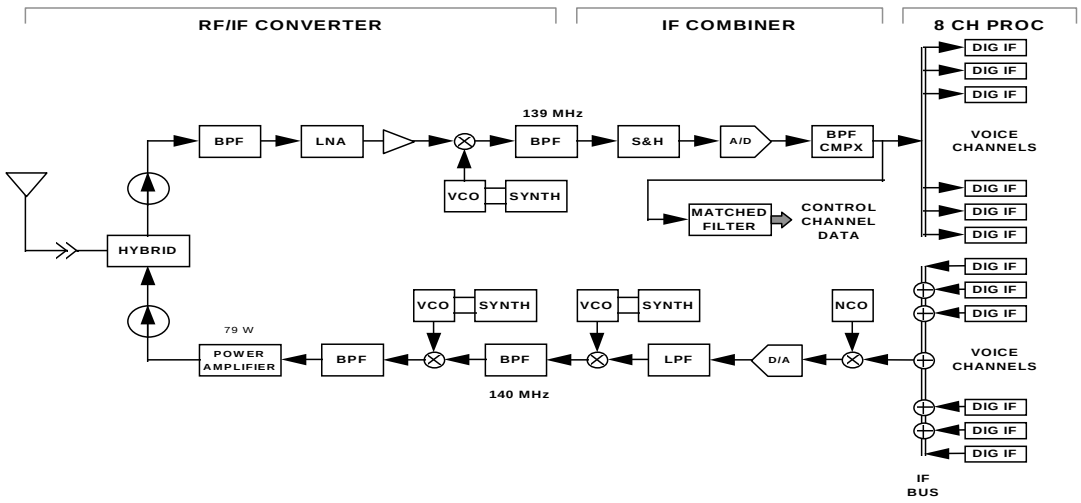

Figure 2.7: Base-station Hardware Architecture [Sig95]

MHz before the multiplication. Non-linear effects due to a saturated power amplifier driven by a large number of simultaneous users are accounted for in the simulation. The nonlinear model of the base-station power amplifier is based on the assumption of frequency and phase insensitive amplifier nonlinearity. The mathematical model for the nonlinearity is

$$y = \frac{Lsgn(x)}{[1 + (l/z)^s]^{1/s}}, \tag{2.1}$$

where y is the output of the nonlinearity, x is the input to the nonlinearity, z is the modulus of the input x, L is the asymptotic output level as $z \rightarrow \infty$, l is the input limit level, and s is the knee sharpness parameter [Jer92].

The graphical presentation of the relationship between input and output for different values of the input limit level l is shown in Figure 2.10. In this plot $L = 1$, $s = 4$, and the amplitude of the input signal x varies from -5 to 5.

The user phone transmitter model does not include synchronous addition of different users' FM CDMA signals. Random time and phase offsets are imparted to

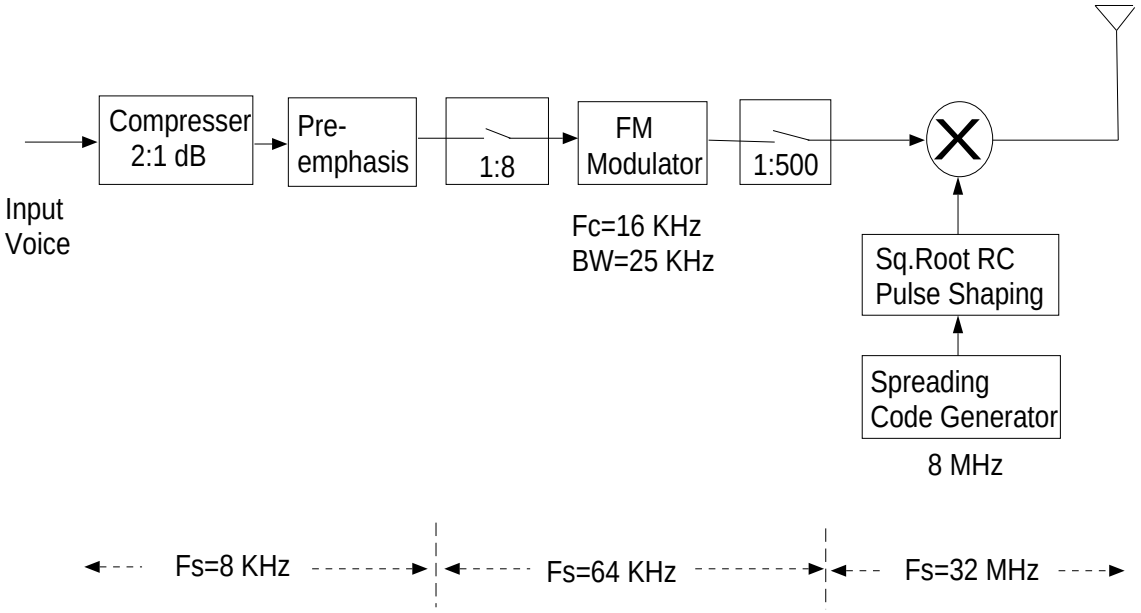

Figure 2.8: User Phone Transmitter Model

the signals transmitted by the user phone prior to the asynchronous addition at the base-station, thereby modeling the asynchronous reverse FM CDMA link. The non-linear amplification of the FM CDMA signal is also not included in the user phone transmitter model.

2.2.2 FM CDMA Receiver Configuration

The FM CDMA receiver bandpass filters, and amplifies the received RF signal before down-converting the signal to IF. At the base-station, the output of the IF unit feeds different DSP channel modules. The DSP modules at the base-station receiver are similar to the one at the user phone. The DSP units perform analog to digital conversion on the analog IF signal and despread the discrete time, discrete amplitude signal. A local spreading sequence generator is initialized with the individual user's spreading code. The tau-dither approach, described in [Pro95], is adopted to maintain code synchronization. The synchronization scheme searches for the spreading code phase value that maximizes the despread pilot tone amplitude. The LFSR at the receiver DSP module generates the spreading code waveform locked to the spreading signal at the transmitter within $\pm\ 1/4^{th}$ of the chip period [Sig95].

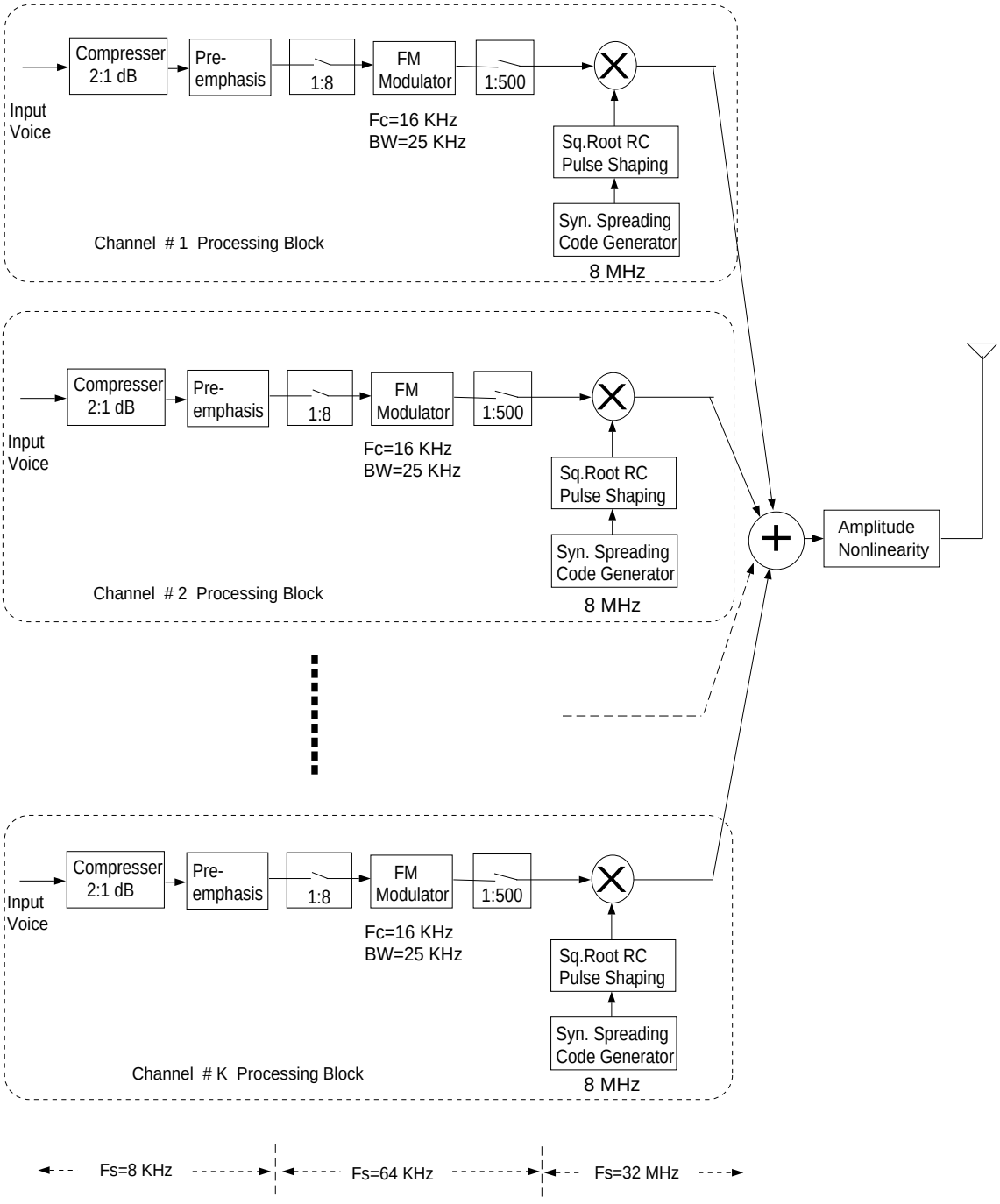

Figure 2.9: Base-station Transmitter Model

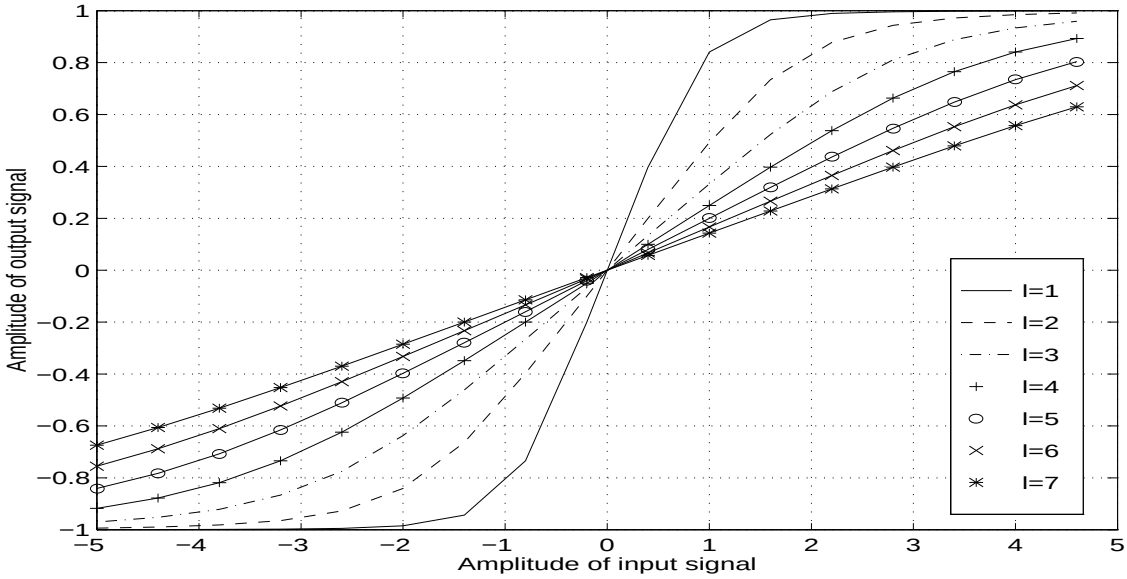

Figure 2.10: Example of Nonlinear Characteristics

The despread signal is bandpass filtered to realize the CDMA processing gain. The BPF output has the same bandwidth as that of the pre-spread FM signal at the receiver. Hilbert transformation of the filter output is then used to form analytic (complex) signal. The DSP based FM demodulator recovers the desired voice signal by taking time derivative of the phase of the analytic signal at its input.

At the user phone, the FM demodulator output is processed through a DAC unit interfaced to a pre-amplifier and speaker assembly. At the base station, the FM demodulator output is fed to the transcoder unit for landline transmission to the signal switch.

Simulation model

The simulation model of the forward link assumes synchronous transmission, whereas the revere link model assumes asynchronous transmission of the FM CDMA signals of different users. The received signal is multiplied with a synchronous copy of the spreading code of the desired user. The resulting signal is bandpass filtered to remove out of band interference and noise. The despread signal is FM demoduled using the quadrature FM demodulation algorithm explained in Chapter 3. The demodulator

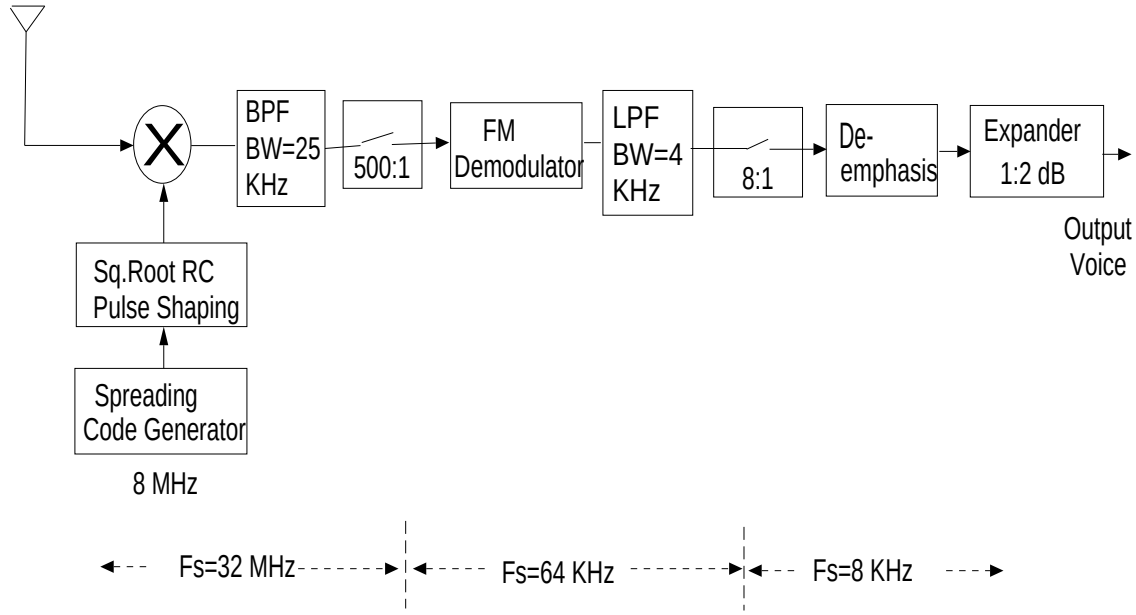

Figure 2.11: User Phone Receiver Model

output is lowpass filtered using a 6^{th} order elliptic filter, and is post-processed, i.e. de-emphasized and expanded. The simulation block diagram also includes decimator stages to reduce the 32 MHz sampling frequency of the received signal to the 8 KHz sampling frequency of the recovered voice signal.

2.2.3 Scope and Issues related to Simulation

The simulated FM CDMA system does not take into consideration real-time ADC and DAC operations, or transcoding operation performed at the base-station. The simulated system model does not consider the finite precision DSP effects, such as quantization noise, and overflow and round-off errors, which are significant particularly because of the disparate sample rates in the system.

The simulation of the FM CDMA system is affected by the high sampling frequency requirements. The subjective tests of the system performance require voice signals to be at least 2 seconds long, which translates to 16000 voice samples at the 8 KHz sample rate. The sampling frequency of the simulated CDMA signal is 4000 times greater. Hence, processing a 2 second long speech signal corresponds to processing 64 million samples of the FM CDMA signal. Generation and accumulation

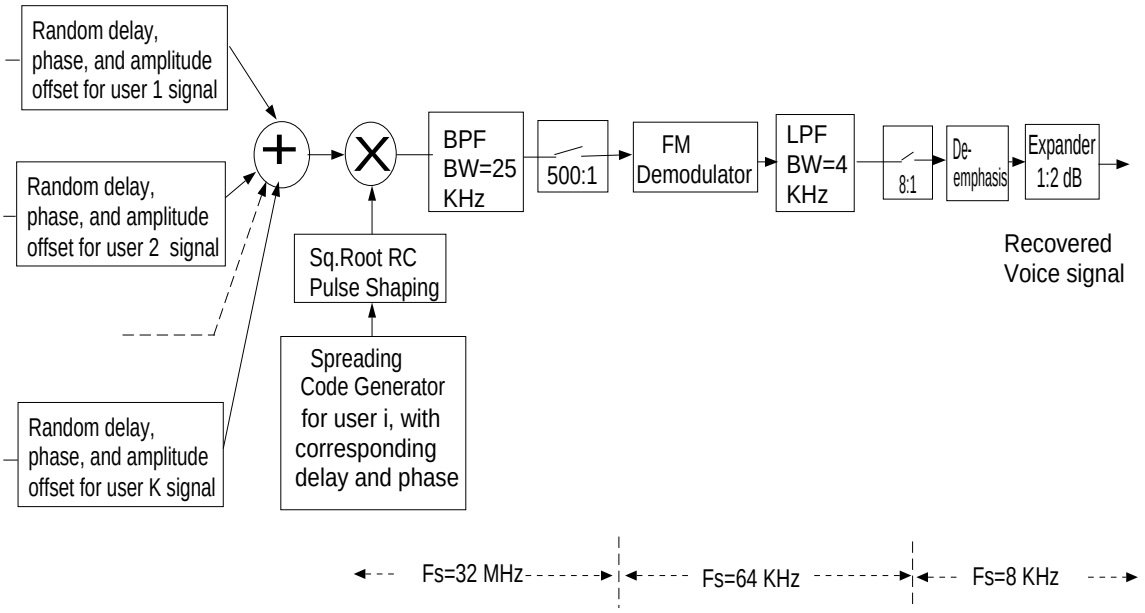

Figure 2.12: Base-station Receiver Model

of such large amount of data in a computer is a memory inefficient operation. The memory bottlenecks get more pronounced as the number of simultaneous users increases. Moreover, such large differences between sampling rates at different system stages cause very high interpolation and decimation factors. The interpolation and the decimation are not exactly inverse operations particularly when the change in the sample rate is very high, since an accurate design of the lowpass filter for a single stage interpolator (decimator) becomes very difficult. The complexities of the filter design can be reduced by breaking the interpolation (decimation) into a number of stages. However, with the multi-stage interpolation (decimation), the noise power at the output of the first interpolation (decimation) stage gets successively amplified in following stages. Thus, such an approach for simplifying the multi-rate signal processing system design is not an ideal solution in terms of minimizing system imperfections. Finally, the presence of the non-linearity in the base-station transmitter model requires further increase in the sampling rate in order to reduce the distortion effects caused by aliased intermodulation terms. However, the simulations are performed without incorporating such an increase of the sampling rate, since an additional interpolation stage can cause signal distortion comparable to that due to

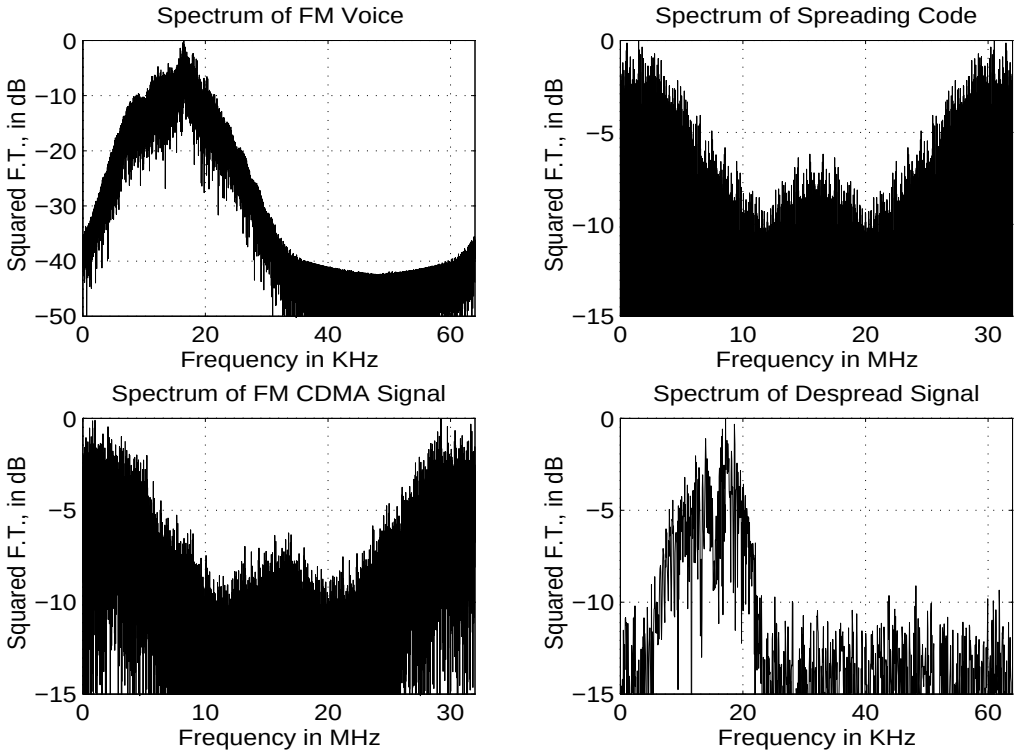

Figure 2.13: Spectra of Signals at Various Stages in the FM CDMA System

aliasing.

Another trade-off during the development of the simulation model involves the filtering operation required before the FM demodulation. A degradation of the phase sensitive FM signals results, if the IIR filters with nonlinear phase characteristics are used. The linear phase FIR filters may circumvent this problem, however such filters require a larger order to meet sharp transition band requirements. A long filter can cause the computational burden to increase drastically, and can render the linear phase implementations of the filters impractical. It is noted that a compromise between the sharp transition band requirements and computation costs is achieved in the simulation models by using a linear phase FIR filter of length 260.

Figure 2.13 shows the spectra of signals at various stages in the FM CDMA system. It is noticed that the FM signal spectrum does not show the pilot tone. The power control simulation were performed using a 2 KHz pilot tone. The spectral characteristics of the FM CDMA signal with the pilot tone are shown in Chapter 4,

where further details of power control scheme are presented.

2.3 Chapter Summary

In this chapter, the system level details of the FM CDMA wireless local loop were described. A brief overview of the system planning and a possible system evolution was provided with the emphasis on the propagation effects, and power control issues. The architectural and the functional descriptions of various system modules from the hardware and the simulation perspectives were presented. The final section of the chapter emphasized various issues related to the development of the simulation models for the FM CDMA system.

Chapter 3

DSP based FM Demodulators

Frequency modulation is an example of analog modulation scheme. Implementation of the analog FM demodulator using DSP algorithms is investigated in this chapter. Primary advantages of a DSP based FM demodulator are its simplicity, flexibility, and economy of implementation. Frequency modulation offers advantages of robust voice quality and bandwidth-SNR exchange. Besides, FM demodulators based on custom designed DSP algorithms facilitate the interface to CDMA DSP processing blocks of the WLL receiver, and are easier to upgrade.

All implementations of the DSP based FM demodulators investigated in this chapter perform signal processing operations, such as discrete time integration, differentiation, and phase angle extraction, relevant to the FM demodulation. It is to be noted that hardware issues related to DSP implementations are not the concern of this study. Bit level or assembly level programming for a DSP chip, developing and studying the operation of ADC/DAC under high sampling rates, or designing a Hilbert transformer for converting a real FM signal to its analytic complex form are the examples of issues not investigated in this study. Primary purpose of the research is to develop high level, algorithmic, descriptions of various DSP based FM demodulators, and to perform comparative analyses of different possible FM demodulation structures.

The output signal to noise ratio is a simple measure for the performance evaluations of analog modulation techniques. Determining output SNR is not a trivial task, and there exists many different approaches for the SNR calculations. Four different SNR calculation methods are summarized in this chapter. Final section of the chapter

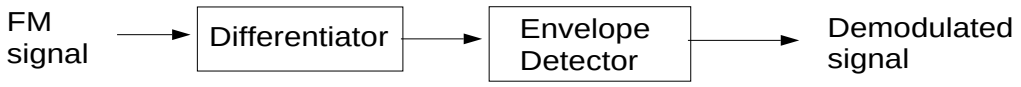

Figure 3.1: Differential FM Detection

presents results of an objective voice quality evaluation method that is more effective in conveying the short time voice quality variations, and provides a better handle for accessing the perceptual voice quality than the MSE based SNR calculations. A comprehensive summary of different objective voice quality measures is presented in Appendix A.

3.1 A Summary of FM Demodulation Techniques

This section investigates various digital signal processing implementations of the FM demodulator. In the following discussion, "t" denotes a continuous time variable, and "t_n" denotes a discrete time variable.

3.1.1 FM Differentiation Discrimination

An expression for the analytic FM signal is shown in Equation 1.1, and reproduced here.

$$\begin{aligned} s(t) &= A_c e^{(j2\pi f_c t + \theta(t))} \\ &= A_c e^{(jw_c t + D_f \int_{-\infty}^{t} m(\sigma)\ d\sigma)}. \end{aligned}$$

The task of demodulating the FM signal involves extracting the instantaneous frequency term from the received signal.

The slope discriminator for the FM demodulation is shown in Figure 3.1. The FM discriminator operates by taking time derivative of the received signal $s_r(t) = Re\{s(t)\}$.

$$\frac{d(s_r(t))}{dt} = \frac{d}{dt}[A_c cos(w_c t + D_f \int_{-\infty}^{t} m(\sigma)\, d\sigma)] \quad (3.1)$$

$$= A_c[w_c + D_f m(t)] sin[w_c t + D_f \int_{-\infty}^{t} m(\sigma)\, d\sigma]. \quad (3.2)$$

Thus, the differentiated FM signal is both amplitude and frequency modulated. If we assume constant envelope[1] of the received FM signal, the message signal $m(t)$ can be recovered by performing amplitude demodulation, usually by envelope detection, of the derivative of received signal [Tau86].

A DSP implementation of the slope discriminator extracts the phase of $s(t_n)$, and recovers the message signal $m(t_n)$ by differentiation operation. Since, signal $s(t_n)$ is a bandpass signal, the derivative of the phase of $s(t_n)$ has a dc value corresponding to the carrier frequency term. One approach for avoiding this effect is to convert the IF signal $s(t_n)$ to baseband signal. The message signal $m(t_n)$ is then recovered by following operation.

$$m(t_n) = \frac{d}{dt_n}[\angle\{s(t_n)e^{-w_c t_n}\}]. \tag{3.3}$$

For wideband FM signals, the extracted phase term is wrapped about 2π radians. It is necessary to unwrap the phase term before performing the differentiation operation.

DSP implementation of the FM demodulator does not require a constant envelope of the received signal. However, an analytic representation of the signal is required in order to extract the phase term. Analytic FM signal is derived by taking Hilbert transform of the received FM signal to obtain the imaginary part

$$s(t_n) = s_r(t_n) + j\hat{s_r}(t_n) = s_r(t_n) + js_i(t_n), \tag{3.4}$$

where $\hat{s_r}(t_n)$ represents the Hilbert transform of the signal $s_r(t_n)$.

3.1.2 Quadrature FM Demodulation

Quadrature detection is one of the more popular method of implementing the FM demodulation. The block diagram of the quadrature FM detector is shown in Figure 3.2.

The detector consists of a phase shift network that changes the phase of the received FM signal in proportion to the instantaneous frequency, and uses a product detector to determine the phase difference between the received FM signal, and the signal at the output of the phase shift network. The operation of quadrature detector is affected by the characteristics of phase shift network. Ideally, the network should introduce 90^o phase shift at the carrier frequency, and a very small shift, within range

[1] In practice, the received FM signal does not have a constant envelope. The signal is passed through a limiter stage before performing the differential demodulation.

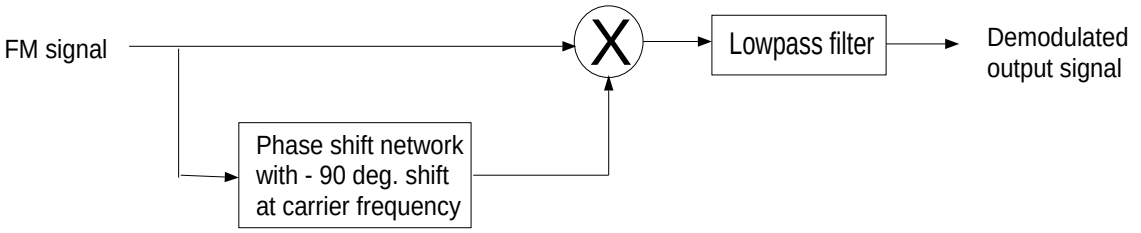

Figure 3.2: Quadrature FM Detection

of $\pm 5^o$, for the frequencies unequal to the carrier frequency [Rap95], i.e., the phase response of the network should be

$$\phi(f) = -\frac{\pi}{2} + 2\pi K(f - f_c), \tag{3.5}$$

where K is a proportionality constant. If the received FM signal $s_r(t)$ is passed through the phase shift network, the output signal is

$$\begin{aligned} s_\phi(t) &= K_1 A_c cos[w_c t + \theta(t) + \phi(f_i(t))] && (3.6)\\ &= K_1 A_c cos[w_c t + \theta(t) + \phi(f_c + D_f m(t))], && (3.7) \end{aligned}$$

where K_1 is a proportionality constant. The product detector output after lowpass filtering is

$$\begin{aligned} \hat{m}(t) &= K_1^2 A_c^2 cos(\phi(f_i(t))) && (3.8)\\ &= K_1^2 A_c^2 cos[-\frac{\pi}{2} + 2\pi K(f_i(t) - f_c)] && (3.9)\\ &= K_1^2 A_c^2 sin[2\pi K D_f m(t)] && (3.10)\\ &\approx K_1^2 A_c^2 2\pi K D_c m(t) && (3.11)\\ &= K_2 m(t). && (3.12) \end{aligned}$$

Hence for small values of the phase shift, the output of the quadrature detector is proportional to the desired message signal.

The simulated model of quadrature detector performs indirect differentiation of the phase term. Instead of extracting the phase term and then performing explicit differentiation operation, the phase term of the analytic signal is differentiated by multiplying the analytic signal $s(t)$ with its delayed and conjugate version $s_d(t_n) =$

$s(t_n - \tau_n)^* = A_c e^{-j[w_c(t_n-\tau_n)+\theta(t_n-\tau_n)]}$. The phase of the product $s_p(t_n) = s(t_n)s_d(t_n)$ is directly proportional to the desired message signal.

$$\begin{aligned} s_p(t_n) &= A_c^2 e^{j[w_c t_n+]} e^{-j[w_c(t_n-\tau_n)+\theta(t_n-\tau_n)]} && (3.13)\\ &= A_c^2 e^{j[w_c\tau_n+\theta(t_n)-\theta(t_n-\tau_n)]} && (3.14)\\ &= A_c^2 e^{j[w_c\tau_n+m(\sigma)]}. && (3.15) \end{aligned}$$

The message signal $m(t_n)$ is then recovered by following operation.

$$m(t_n) = \angle\{s_p(t_n)\} - w_c\tau_n. \quad (3.16)$$

The phase wrapping effect is less likely to occur in quadrature demodulation method, since the extracted phase term is the differentiated version of the received FM signal phase.

3.1.3 Arctangent FM Demodulation

A brief explanation of the arctangent FM demodulation method is provided in this section.

The theoretical background for this method is better understood by considering the real part of the analytic FM signal, given in Equation 1.1,

$$\begin{aligned} s_r(t) &= Re\{A_c e^{(j2\pi f_c t+\theta(t))}\} && (3.17)\\ &= A_c cos[\theta(t)]cos(w_c t) - sin[\theta(t)]sin(w_c t) && (3.18)\\ &= x(t)cos(w_c t) - y(t)sin(w_c t), && (3.19) \end{aligned}$$

where $x(t)$ and $y(t)$ are the real and the imaginary parts of the complex baseband FM envelope. Since $\frac{y(t)}{x(t)} = \frac{sin[\theta(t)]}{cos[\theta(t)]} = tan[\theta(t)]$, we can obtain the message signal by taking the time derivative of the arctangent of the ratio of the imaginary and real parts of the complex envelope of the FM signal [Jas95].

$$\begin{aligned} m(t) &= \frac{d}{dt}\theta(t) && (3.20)\\ &= \frac{d}{dt} tan^{-1}\left[\frac{y(t)}{x(t)}\right] && (3.21)\\ &= \frac{1}{1+\left[\frac{y(t)}{x(t)}\right]^2}\frac{d}{dt}\left[\frac{y(t)}{x(t)}\right] && (3.22) \end{aligned}$$

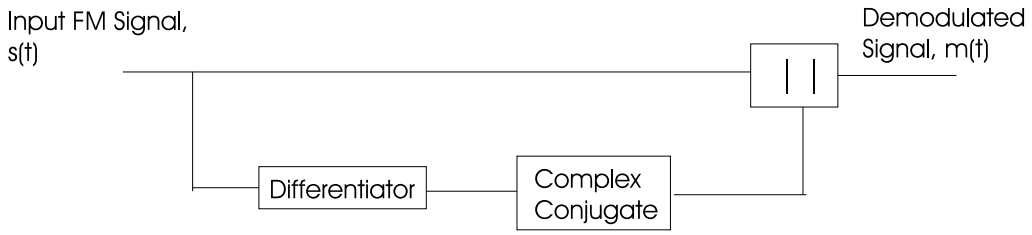

Figure 3.3: Arctangent FM Detection

$$= \frac{1}{1+\left[\frac{y(t)}{x(t)}\right]^2}\left[\frac{\dot{y(t)}}{x(t)} + (-1)\frac{y(t)}{x^2(t)}\dot{x(t)}\right] \tag{3.23}$$

$$= \frac{\dot{y(t)}x(t) - y(t)\dot{x(t)}}{y^2(t)+x^2(t)}. \tag{3.24}$$

The block diagram of the DSP implementation of arctangent FM demodulator is shown in Figure 3.3. The above block diagram implements Equation 3.24 in an indirect, but a simpler method. The analytic signal $s(t_n)$ is differentiated to obtain signal $s_d(t_n)$.

$$s_d(t_n) = \frac{d}{dt_n}A_c e^{j(w_c t_n + \theta(t_n))} \tag{3.25}$$

$$= \frac{d\theta(t_n)}{dt_n}A_c e^{j(w_c t_n + \theta(t_n))}. \tag{3.26}$$

Multiplying $s(t_n)$ with complex conjugate of $s_d(t_n)$, and taking the absolute value of the product, results in the desired signal.

$$\hat{m}(t_n) = |s(t_n)s_d^*(t_n) - w_c(dt_n)| \tag{3.27}$$

$$= \left|\left[A_c^2\frac{d\theta(t_n)}{dt}e^{j(w_c t_n+\theta(t_n))}e^{-j(w_c t_n+\theta(t_n))}\right] - w_c(dt_n)\right| \tag{3.28}$$

$$= K_3 m(t_n). \tag{3.29}$$

Thus, the message signal is obtained after the differentiation, and the conjugation operations on the analytic FM signal. Since, the phase extraction is not required, this method does not suffer from the phase wrapping effect, and the numerical imprecision in the phase detection. However, the performance of this method is very sensitive to the DSP differentiation algorithm.

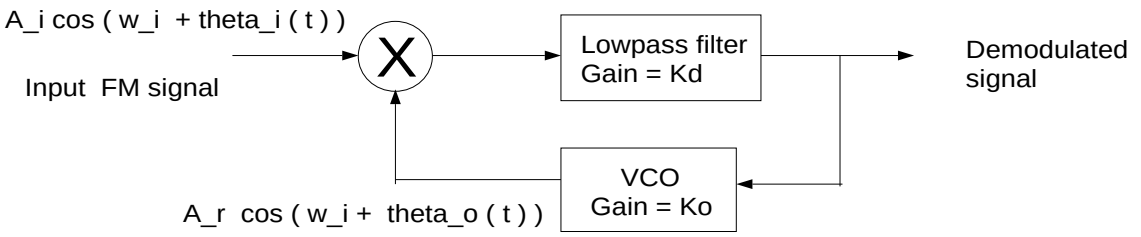

Figure 3.4: The Analog PLL for FM Detection

3.1.4 Phase Locked Loop

The phase locked loop (PLL) is a feedback system that extracts the baseband message signal from a frequency modulated carrier signal. The basic components of PLL are a phase comparator and a voltage controlled oscillator (VCO). PLL systems offer good performance even with high noise levels, and hence extend the dynamic range of the operation of the system. Primary purpose of this study was to implement a DSP algorithm for analog PLL, and study the threshold extension effects that can be achieved. An overview of the analog PLL principles is presented first, followed by the methodology for developing DSP simulation model.

Analog PLL as FM Demodulator

The block diagram of the analog PLL is shown in Figure 3.4.

The input and the output of the PLL are sinusoidal signals expressed as

$$s_i(t) = A_i cos(w_i t + \theta_i(t)) \tag{3.30}$$

$$s_r(t) = A_r sin(w_i t + \theta_o(t)), \tag{3.31}$$

where w_i is the VCO quiescent frequency [Tau86].

The input and the output signals of the PLL are fed to the phase detector. One model of the phase detector is a multiplier followed by a lowpass filter. The multiplier output $s_i(t)s_r(t)$ has spectral components at $[\theta_i(t) - \theta_o(t)]$ and at $[2w_i + \theta_i(t) + \theta_o(t)]$. The lowpass filter removes the high frequency components, and hence the phase detector output is a sinusoidal function of the phase difference between the PLL input, and the VCO output. As described subsequently, the linear model for the PLL simulations approximates the sinusoidal characteristics of the phase detector as linear

characteristics, which is an appropriate assumption for small phase differences.

$$e(t) = K_d sin[\theta_i(t) - \theta_o(t)] \tag{3.32}$$

$$\approx K_d[\theta_i(t) - \theta_o(t)], \tag{3.33}$$

where K_d is a gain constant for the phase detector. VCO output signal $s_r(t)$ is frequency modulated by the phase detector output signal $e(t)$,

$$s_r(t) = A_r sin(w_i t + K_o \int_{-\infty}^{t} e(\sigma)d\sigma), \tag{3.34}$$

where K_o is a gain constant for the VCO.

In steady-state condition, $\theta_i(t)$ and $\theta_o(t)$ are equal, and PLL input and output signals are in perfect phase quadrature. The output of the phase comparator, $e(t)$, is zero, and hence the VCO output frequency does not change [Bla76].

If the input signal frequency changes from w_i to $w_i + \Delta w$, the resulting phase difference causes non-zero error signal, $e(t)$, at the phase detector output, thereby changing the VCO output frequency. The steady-state condition is again reached when the VCO output frequency equals $w_i + \Delta w$. In the new steady-state condition, the phase difference between signals $s_i(t)$ and $s_r(t)$ has a constant non-zero value, and the amplitude of the phase comparator output signal $e(t)$ ceases to be time-varying.

For the case of a frequency modulated input signal, the PLL acquires and tracks the phase of the input signal. When the PLL is locked on to the input signal phase, the phase detector output is a time-varying signal proportional to the baseband FM modulating signal. Since the phase detector output frequency modulates the VCO signal, the VCO output frequency varies in the same manner as the input signal frequency. In such a condition, the error signal $e(t)$ driving the VCO represents the demodulated FM signal [Bla76].

There are many conditions required for the PLL to remain locked to the input signal. Such constraints are better understood by comparing the operation of the analog PLL to a mechanical device shown in Figure 3.5. The mechanical device is in form of a pendulum suspended from a shaft. The shaft is also the axis for a cylinder, and a weight platform hangs on the rope tied around the cylinder [Bes84].

When there is no weight on the platform, the pendulum remains in a vertical position. Such a condition is analogous to the steady-state condition of the PLL when the input signal frequency is same as the quiescent VCO frequency.

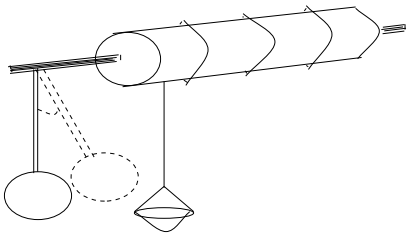

Figure 3.5: Mechanical Analogy to the PLL

A slow variation in the input signal frequency corresponds to a slow increase of the weight on the rope. Due to the increasing weight, the pendulum starts to deflect, representing a constant non-zero phase error at the phase comparator output. If the weight on the rope is increased such that the pendulum deflection increases beyond 90^o, it rotates forever around the shaft. Similarly, there is a maximum allowed input signal frequency deviation beyond which the PLL fails to acquire a steady-state condition, and the phase error increases infinitely. Such a value of the frequency deviation is known as *hold range*.

The mechanical pendulum may cross the 90^o angular shift momentarily, if there is a sudden increase of the weight on the rope. However, if the weight is small, the pendulum inertia drives it out of the instable condition. *Pull-out range* of the PLL is defined as the minimum value of the input frequency deviation for which the PLL momentarily stops tracking the input phase, and after skipping a number of cycles again reaches the steady-state condition. The pull-out range of the PLL is considerably smaller than the hold-in range.

Two other parameters associated with the PLL are *pull-in range*, and *lock range*. The pull-in range is defined as the maximum frequency deviation within which the PLL acquires the input phase (although the process may be a slow one). The lock range of the PLL represents the maximum frequency deviation for which the PLL acquires the input phase within one cycle of the input and output PLL frequency difference. The lock range of the PLL is usually considerably smaller than the pull-in range.

The FM demodulator based on the PLL must be designed such that the frequency deviation of the received signal remains smaller than the PLL hold range. A good design of the PLL based FM demodulator also ensures the peak input frequency

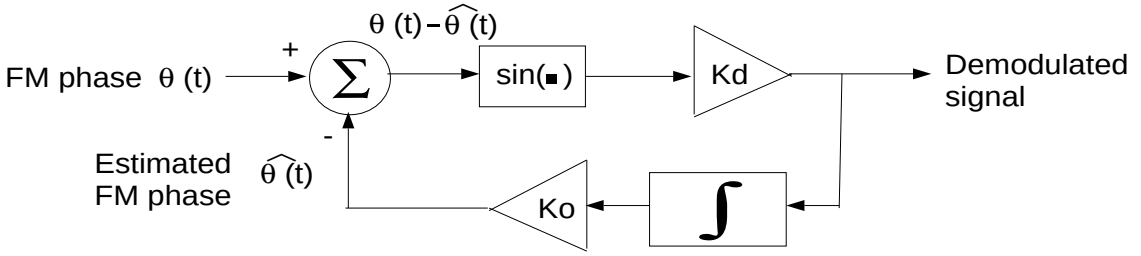

Figure 3.6: Nonlinear PLL Model

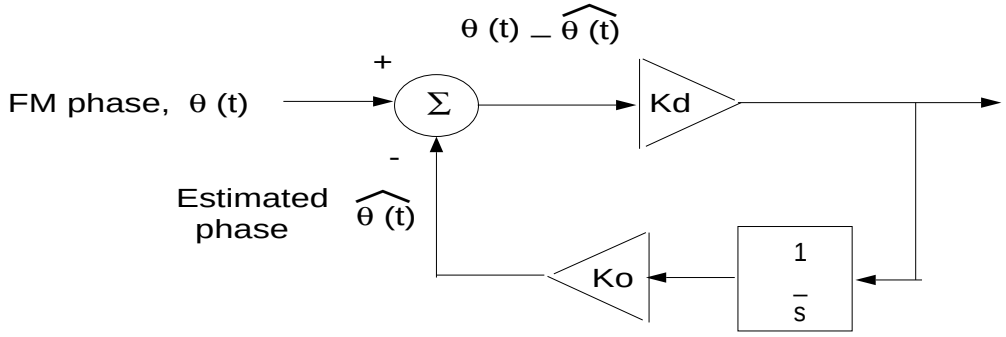

Figure 3.7: Linear PLL Model

deviation to fall within the lock range of the PLL.

Simulation Models of the Analog PLL

Figures 3.6, and 3.7 show nonlinear and linear models for the analog PLL[Dav86]. The linear model is valid for small phase errors, and when the input signal to noise ratio is higher than the FM demodulation threshold.

For a first order lowpass IIR filter, the transfer function of the loop filter is

$$F(s) = \frac{s\tau_1 + 1}{s\tau_2}. \tag{3.35}$$

The resulting closed loop transfer function for the linear model of the PLL is

$$H(s) = \frac{K_o K_d F(s)}{s + K_o K_d F(s)} \tag{3.36}$$

$$= \frac{K_o K_d (s\tau_2 + 1)/(\tau_1 + \tau_2)}{s^2 + \frac{1 + K_o K_d \tau_2}{\tau_1 + \tau_2} s + \frac{K_o K_d}{\tau_1 + \tau_2}}. \tag{3.37}$$

Comparing the denominator of the above equation with the standard form of an analog system transfer function $s^2 + 2\zeta w_n s + w_n^2$, we obtain following expression for loop natural frequency, and loop damping factor.

$$w_n = \left(\frac{K_o K_d}{\tau_1}\right)^{1/2} \tag{3.38}$$

$$\zeta = \frac{\tau_2}{2}\left(\frac{K_o K_d}{\tau_1}\right)^{1/2}. \tag{3.39}$$

Loop gain, $K_o K_d$, loop natural frequency, w_n, and loop damping factor, ζ, are the parameters affecting the operating ranges of the PLL, and should be determined carefully to ensure a stable FM demodulator.

DSP simulations of an analog PLL require a high sampling frequency. The error signal, $e(t)$, for the simulated PLL model can not be computed at the first sampling instant, or at n=1, since the simulation model cannot generate the estimated phase value at the output of the VCO when the input signal is not present. The first error signal sample, $e(1)$ will be, thus, $\theta_i(2) - \theta_o(1)$, instead of $\theta_i(1) - \theta_o(1)$. The effect of such one sample delay is to introduce instability in the simulated model of the PLL. The effect of the delay is reduced by increasing the sampling rate. A high value of the sampling rate for the nonlinear PLL simulations is also required since the nonlinear effects generate higher order frequency terms, and the resulting aliasing distortion can be reduced only by increasing the sampling frequency.

The loop filter for the simulated PLL model is in form of a 3rd order elliptic IIR filter. The VCO model is an implementation of the trapezoidal method for numerical integration, for which the output

$$y(n) = \frac{T_s}{2}[x(n) + x(n-1)] + y(n-1),$$

where T_s is the sampling interval, and $x(n)$ is the vector of the discrete time input signal. Other possible forms of the VCO model are the forward (or the backward) Euler integration method [Jer92].

3.1.5 Zero Crossing Detector

The block diagram of zero-crossing FM detector is shown in Figure 3.8. In the conventional approach, the message signal is recovered by measuring the instantaneous FM frequency from the zero-crossings of the FM modulated signal[Lat89]. As shown

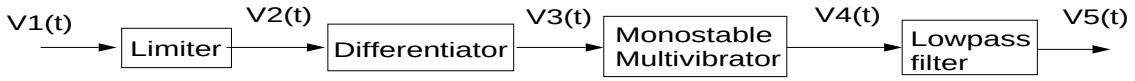

Figure 3.8: Zero-crossing FM Detection

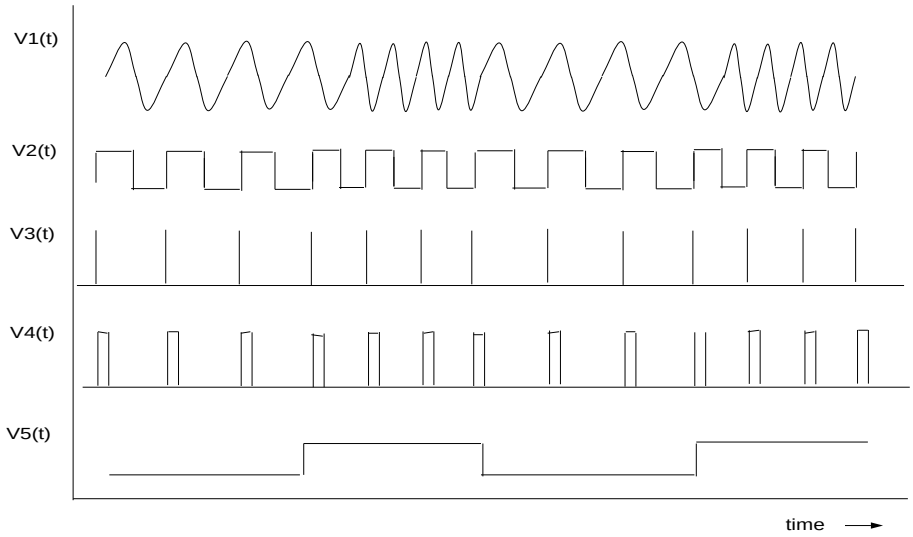

Figure 3.9: An Example of Zero-crossing FM Detection

in Figure 3.9, the hard-limiter converts the incoming FM signal into a square wave. A mono stable multivibrator is triggered at each positive edge of the square signal, and a rectangular pulse of fixed width is generated each time. The rate of such pulses is the rate of the zero-crossings, and represents the instantaneous FM frequency. A lowpass filter is then used to perform averaging operation to convert the mono-shot output to a slowly varying signal proportional to the desired message signal.

A DSP algorithmic implementation of above method failed to give a good result perhaps due to imperfect models of the mono-shot, and the lowpass filter. An alternate, successful, approach for the zero-crossing detector is illustrated in Figure 3.10. The straight line in the figure shows the zero-crossing instances of an unmodulated carrier signal. When the carrier is modulated by a message signal, the zero-crossing instances vary around the straight line as shown. The FM demodulation is achieved by transforming the zero-crossings of an unmodulated carrier signal to a constant zero amplitude [Voe72]. The same transformation maps the zero-crossings of the FM

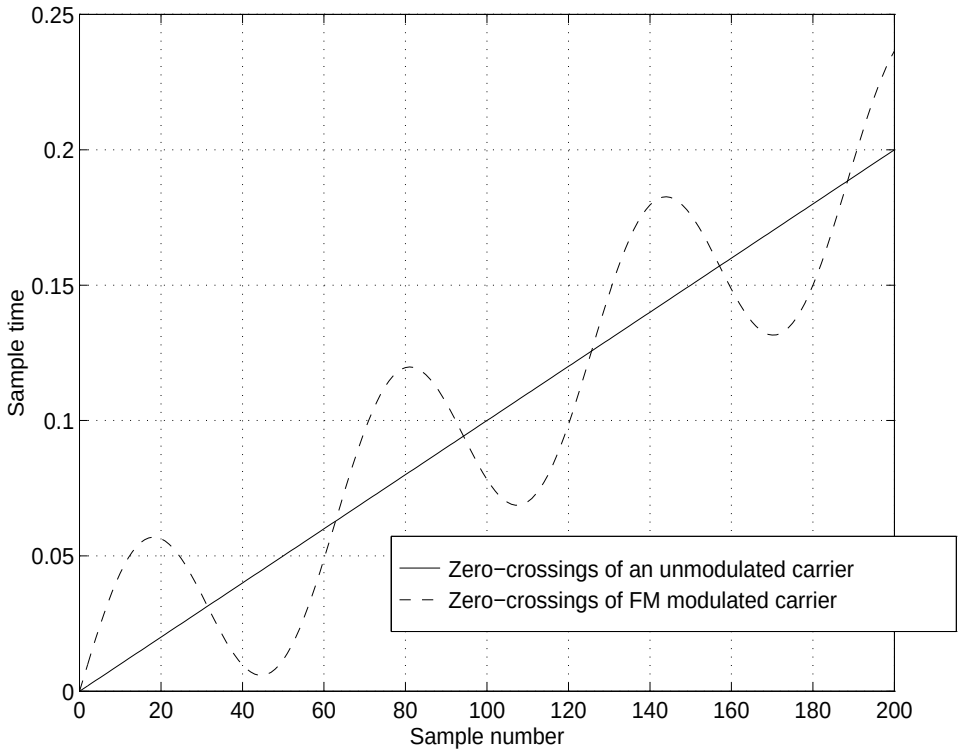

Figure 3.10: Simulation Philosophy for Zero-crossing FM Detection

modulated carrier to the sampled amplitudes of the modulating signal. The base-band message signal is then recovered by interpolating the amplitude samples. The performance of this algorithm is affected by the choice of the interpolation method. The*Lagrange's* interpolation method [Mar80] resulted in inferior results as compared to those for an ideal interpolator based on *sinc* rule.

3.1.6 Model based FM Demodulation

The model based frequency demodulation technique is an extension of the conventional quadrature FM detection technique, and has been successfully applied for the AMPS co-channel interference rejection problem [Wel96]. This method is based on modeling co-channel FM interference as a small number of sinusoids in noise (which is a valid assumption, if the time duration of the voice frames remains within a specific bound). The quadrature FM detector fails to identify different input signal frequencies, since it forms the desired signal's frequency estimate based only on two input signal samples. The parametric frequency estimation technique uses more than two input signal samples in each frame, and forms an L^{th} order prediction of the frequency content of the input signal. It has been shown that for sufficiently high Signal to Interference Ratio (SIR), the Signal of Interest (SOI) corresponds to the maximum modulus complex root of the polynomial representing the prediction filter. The lesser valued complex roots predict the interference signal frequencies, and hence are separated from the SOI.

The performance of this method is sensitive to the estimates of the input signal frame length N, and the prediction filter order L. If the frame length N is too high, the frequency variation of the FM signal dominates underlying sinusoidal carrier signal, and the assumption of sinusoidal interference does not remain valid. On the other extreme, very small values of the frame length N or the filter order L result in ambiguous frequency predictions.

The advantage of the model based FM detection is realized in an interference environment. In additive white Gaussian noise (AWGN) channel, the model based FM demodulation offers only a small gain compared to the quadrature detector, but requires significantly greater computational complexity.

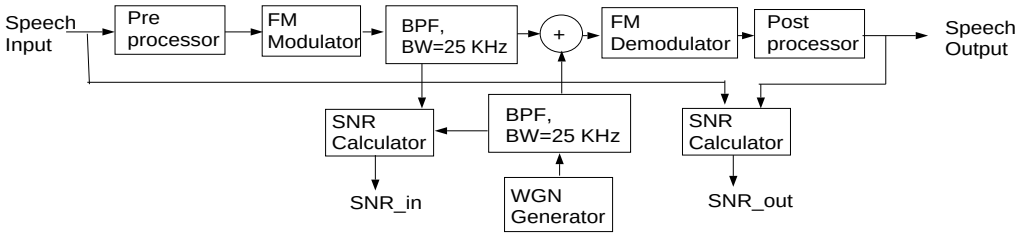

Figure 3.11: Simulation Approach for Performance Evaluation of FM Demodulators

3.2 Simulation Results

Figure 3.11 shows the block diagram of the simulation approach to evaluate the performance of different FM demodulators. The input speech is sampled at 8 KHz, and quantized. The resulting discrete time, discrete amplitude voice samples are passed through a pre-processor block. The pre-processor is comprised of *voice companding*, and *pre-emphasis* (these operations are detailed in the next section). The output signal of the pre-processor is upsampled to 64 KHz sample rate. The resulting signal modulates a carrier at 16 KHz to generate an FM signal with bandwidth of 25 KHz[2]. The FM signal is bandpass filtered to simulate the front-in filter at the receiver. A white Gaussian noise signal is also generated, and filtered using the same bandpass characteristics. The AWGN channel is simulated by adding the filtered noise signal to the noise-free FM signal at the input to the demodulator. The FM signal power and the power of the Gaussian noise signal are controlled before the addition to yield the desired input SNR. The output of the FM demodulator is post-processed, i.e. de-emphasized and expanded. The SNR at the input and the output of the FM receiver are calculated using *cross-correlation co-efficient method* described in Section 3.2.3.

3.2.1 Performance Comparisions

The SNR characteristics of different FM demodulators are shown in Figure 3.12. The three basic FM demodulation structures, namely the differentiator, the quadrature, and the arctangent FM demodulators, exhibit similar performance. Infact, the difference between the performance curves in Figure 3.12 for the differentiator, and the quadrature detector is indistinguishable. This similarity is expected since quadrature

[2]This follows the specifications of the FM CDMA system outlined in the previous chapter.

detection is just an alternate way of differentiating the phase of the FM signal. The arctangent demodulation, though based on the same principle, exhibits a slightly different behavior. This discrepancy is due to the fact that the arctangent method does not perform an explicit phase extraction, and it requires more than one differentiation operation in the demodulation process. Hence, the performance of this method is influenced by the accuracy of the differentiator. The result shown in Figure 3.12 pertain to a first order differentiator used in the arctangent method. As noted in [Sig95], the arctangent method with a higher order FIR (differentiator) filter achieves an improved performance characteristics.

Comparing the performance of the analog PLL, shown in Figure 3.4, with the differentiator detector or the quadrature detector, it is observed that the former two demodulation methods show a high output SNR values of 22-25 dB in the range above the threshold. However, the output SNR for the analog PLL saturates at 12-13 dB when the input SNR is above the threshold. This behavior of the analog PLL is better understood by studying the performance of the two other PLL simulation models, namely the nonlinear PLL model shown in Figure 3.6 and the linear PLL model shown in Figure 3.7. The linear PLL model exhibits 17-18 dB saturated SNR values above the threshold, whereas the nonlinear PLL model SNR characteristics saturates at values closer to that for the analog PLL model. Hence, we can conclude that the nonlinearity in the analog PLL model is the main cause behind its inferior performance[3]. Moreover, as mentioned in Section 3.1.4, the simulation models of the analog PLL require a very high sampling frequency. The results shown in Figure 3.12 pertain to the sampling frequency of 64 KHz which is not sufficient to offset the effects of the one-sample delay, and the aliasing distortion. Due to these inherent signal processing limitations, the analog PLL model fails to show a clear advantage in terms of the threshold extension over the differentiator, or the quadrature detector. However, the SNR characteristics for the linear and the nonlinear PLL models show a sharp knee near the threshold region unlike the other demodulation methods. Also, the perceptual voice quality with the PLL based demodulation is not inferior to that for the other demodulators.

The SNR characteristics of the zero-crossing detector is shown in Figure 3.12. The

[3]Infact, as shown in the next section, similar performance degradation (in terms of the output SNR characteristics above the threshold) is observed with the introduction of the nonlinear companding process.

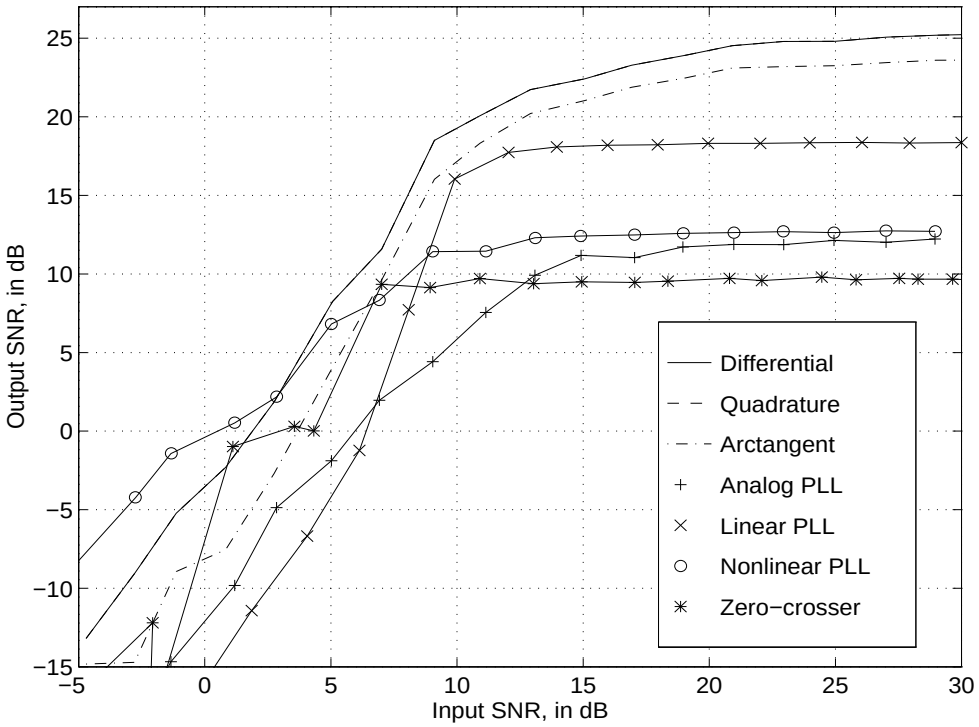

Figure 3.12: Performance Comparison of FM Demodulators

performance of the zero-crossing detector is observed to be inferior compared to the previous four FM demodulation structures due to the signal processing imperfections discussed previously. The zero-crossing detection requires IF processing, and a high sampling rate. These requirements cause computational difficulties during the simulation. However, the DSP hardware implementation of the zero-crossing demodulator does not face these limitations, and hence is a feasible option. Also, the threshold for the zero-crossing detection is the lowest among all the demodulation methods, which may serve as a motivating factor behind its choice.

We observe that the DSP based simulations show saturated output SNR for all the FM demodulation algorithms. Distortions introduced by non-ideal interpolation/decimation, and filtering processes are the main cause of this effect. Such inherent imperfections of the DSP models cause nonzero noise signal to appear at the output without any introduction of the noise at the input to the FM demodulator.

3.2.2 Performance Improvement Techniques

The performance of the frequency modulated systems can be improved by means of pre-deemphasis (PDE), companding, and threshold extension. The PLL based demodulation for the threshold extension has been explained previously. The former two techniques are discussed next.

Companding

The United States' analog cellular standard, Advanced Mobile Phone System (AMPS), specifies 2:1 dB compression of the voice signals prior to the FM modulation, and 1:2 dB expansion of the demodulated signal at the receiver. The signal compression and the expansion processes are jointly referred to as *companding*. The companding confines the FM modulated speech to the specified bandwidth, and improves perceptually pleasant quieting effect during the periods of silence [Rap95].

The effect of the companding process on the differential FM demodulator is shown in Figure 3.13. The compression of the speech signal increases its power during the intervals of very low speech amplitude, thereby increases the output SNR. Thus, an improvement due to the companding is observed with low values of input SNR. However, with high values of the input SNR, the nonlinearity introduced by the

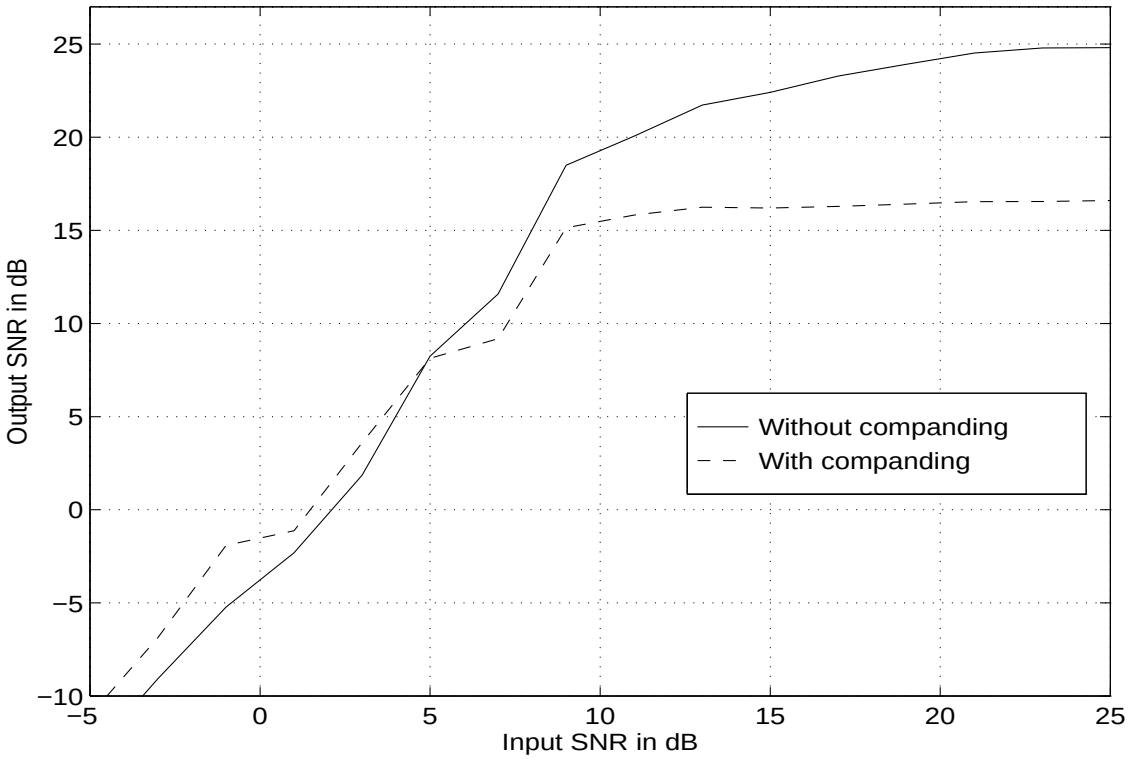

Figure 3.13: Effect of Companding on Differential FM Detector

companding process causes the output SNR curve to saturate at 6-8 dB lower values compared to the case without the companding.

Pre-deemphasis

The differentiation operation performed by the FM demodulator amplifies the high frequency noise components, and leads to a parabolic noise spectrum at the output of the FM demodulator [Cou93]. This phenomena is observed in Figure 3.14 which shows a flat input noise spectrum, and a parabolically increasing output noise spectrum.

The pre-deemphasis (PDE) approach combats this characteristics of the FM demodulators by attenuating, or *deemphasizing*, the high frequency components at the demodulated signal. The high frequency components of the baseband message signal are *preemphasized* before the modulation process using an inverse law, hence the recovered message signal at the receiver does not experience significant distortion.

The amplitude response for the PDE approach is shown in Figure 3.15. The design

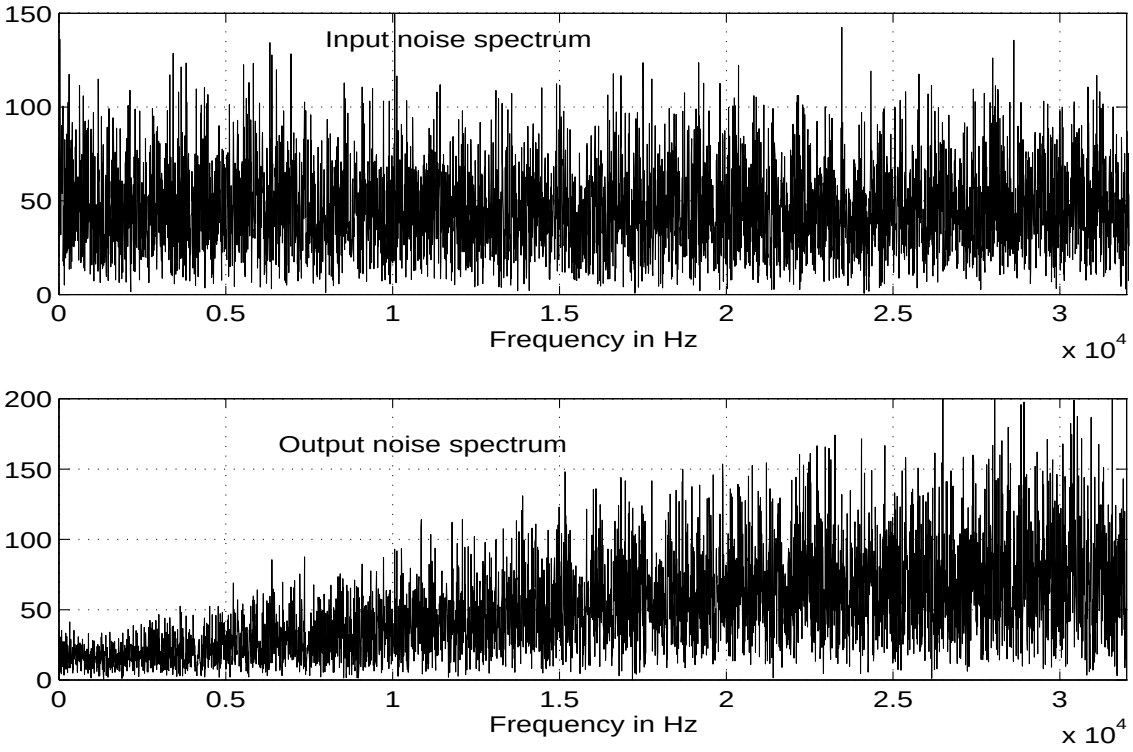

Figure 3.14: Noise Spectrum at Input and Output of Differential FM Detector

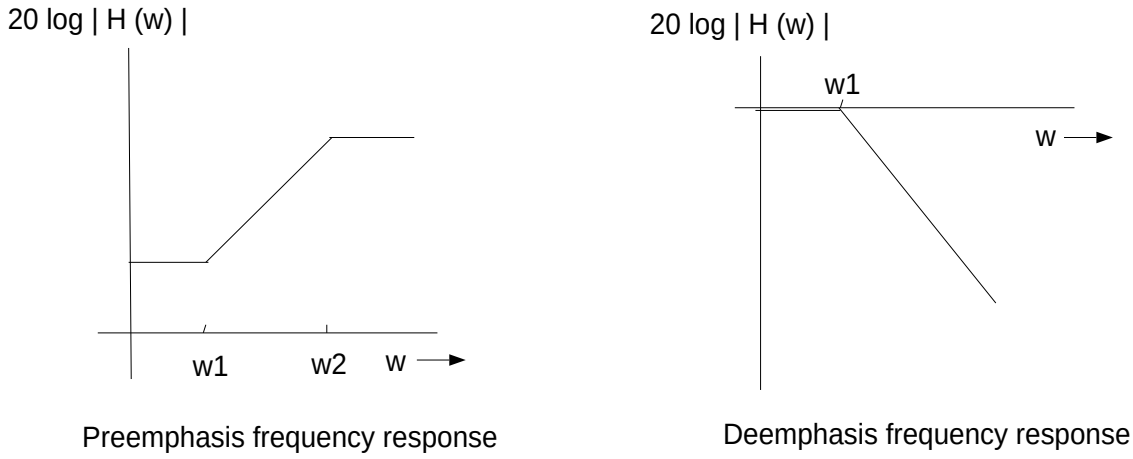

Figure 3.15: Characteristics of PDE Filters

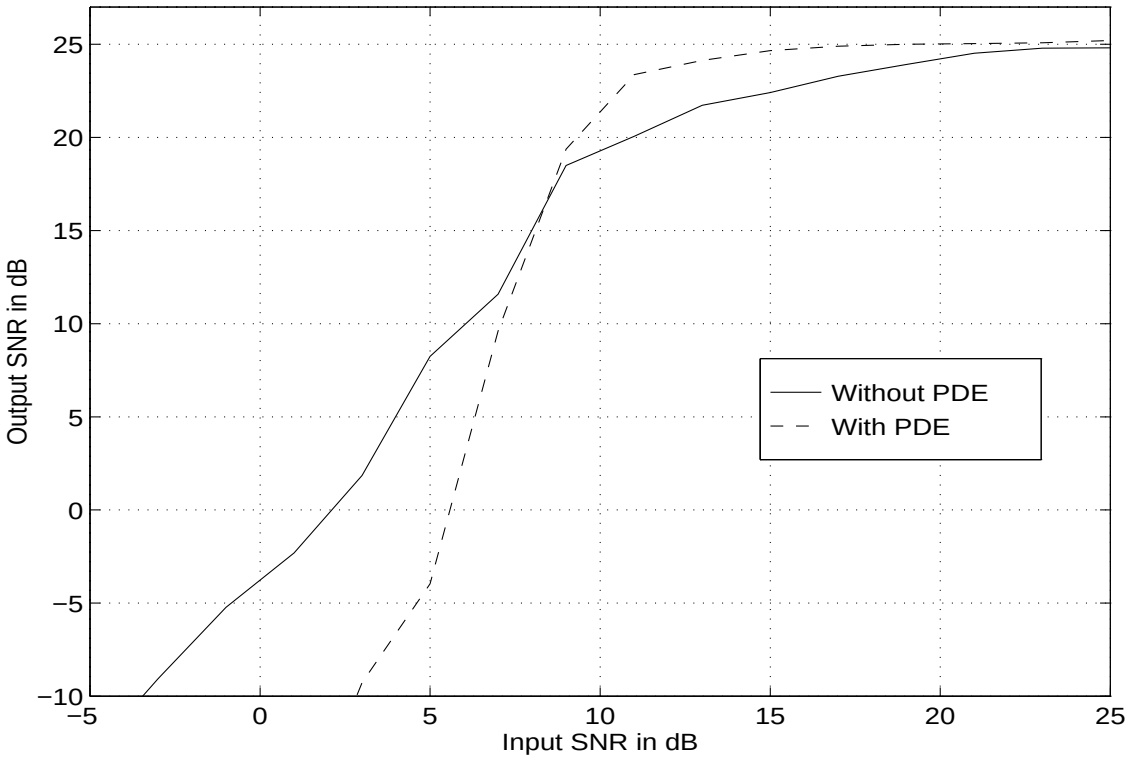

Figure 3.16: Effect of PDE on Differential FM Detection

of a computationally efficient model for implementing the PDE characteristics is not a trivial task. The Inverse Discrete Fourier transform (IDFT) of the filter characteristics in Figure 3.15 results in a poor filter design for short filter lengths. A more accurate design is obtained by providing more data in the IDFT operation. However, resulting long filter causes an unreasonable computational burden. An alternate method for implementing PDE characteristics is based on amplifying or attenuating the Discrete Fourier Transform (DFT) components of the speech signal, and is a more suitable simulation approach.

Typical values of the cutoff frequencies, f_1 and f_2, of the PDE characteristics are 2 KHz, and 30 KHz respectively. With these values of the cut-off frequencies, the simulation model of the PDE technique does not improve the performance of the FM demodulator. The errors introduced by interpolation and decimation stages disturb the (emphasized) speech spectrum. The resulting distortion in the recovered signal outweighs the improvement due to the PDE. Instead of pre-emphasizing (de-emphasizing) only a part of the input speech spectrum, if we emphasize (de-emphasize) entire speech spectrum, the impact of the signal processing imperfections on the PDE reduces significantly. With the cut-off frequency f_1 value of 0 Hz (instead of the conventional value of 2 KHz), it is possible to achieve pre-emphasis and de-emphasis operations that more closely follow an inverse relationship (inspite of the intermediate signal processing distortions). Figure 3.16 shows a slight performance improvement achieved by the PDE with the cut-off frequencies f_1, and f_2 set to 0 Hz, and 4 KHz respectively. It is observed that the PDE accomplishes a noticeble threshold extension, however the performance degrades drastically below the threshold.

3.2.3 A Summary of SNR Calculation Methods

The output SNR is a simple objective indicator of the analog FM receiver performance. The performance curves of the FM demodulators, shown in Figures 3.12, 3.13, and 3.16, employ the output SNR as the parameter for comparitive evaluations. The subsequent results (shown in Chapters 4, and 5) demonstrating the capacity of the FM CDMA system are also based on the output SNR. The simplicity in calculations and the performance comparisions offered by this parameter is the main reason behind its choice.

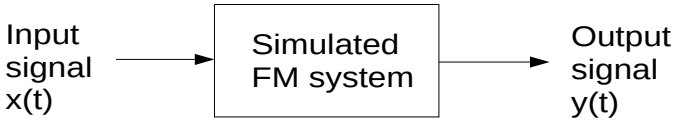

Figure 3.17: Reference Model for SNR Calculations

At this stage, it is necessary to investigate the reliability, and the accuracy of the method used for the SNR calculations. Relative merits and de-merits of different SNR calculation techniques are studied next. The subsequent system evaluations are performed on the basis of the understanding of the SNR calculation techniques developed in this section.

A reference system model for study of different SNR calculation techniques is shown in Figure 3.17.

Mean Squared Error Method

This method is based on determining the SNR value from the following formula.

$$SNR_{out} = 10log_{10}\left[\frac{P_x}{P_{x-y}},\right] \tag{3.40}$$

where $P_x = \overline{x^2}$ is the mean of the squared reference signal, and $P_{x-y} = \overline{(x-y)^2}$ is the mean squared error at the output.

This method is simple to understand, and computationally less intensive. However, a proper scaling of the signals $x(t)$ and $y(t)$ is necessary to avoid the errors due to amplitude mismatch. One approach is based on matching the peak amplitudes of the signals $x(t)$ and $y(t)$, however if the output noise is impulsive, resulting spikes can cause incorrect scaling of the signal $y(t)$.

Cross-correlation Coefficient Method

This method is based on determining the value of cross-correlation coefficient between signal $x(t)$ and $y(t)$ [Lee85].

$$\rho_{xy} = \frac{max[R_{xy}(\tau)]}{P_x P_y}, \tag{3.41}$$

where $R_{xy}(\tau) = \overline{x(t)y(t+\tau)}$ is the cross-correlation function between the signals $x(t)$ and $y(t)$, $P_x = \overline{x^2}$ and $P_y = \overline{y^2}$ denote the normalized powers of signals $x(t)$ and $y(t)$ respectively.

SNR_{out} is calculated as a function of ρ_{xy}.

$$SNR_{out} = 10log_{10}\left[\frac{\rho_{xy}^2}{1-\rho_{xy}^2}\right]. \tag{3.42}$$

This method has improved accuracy and reliability compared to those of the previous method. The cross-correlation coefficient method does not rely on a proper amplitude scaling of the input and the output signals. However, it is a complex, and a computationally expensive method. The accuracy of this method depends on the resolution in detecting the peak of the cross-correlation function $R_{xy}(\tau)$. A better resolution is achieved with a high sampling rate, thus the accuracy of the SNR calcuation improves as the sampling rate increases. Since, higher sampling rates lead to greater computational loads, the choice of this method involves a trade-off in terms of accuracy and computational intensity.

Gain-Delay Method

This method combines the above two approaches for the SNR calculations. The mean-squared error measure is again used to determine the noise power level. However, now the error signal is computed by subtracting the output signal from an amplitude scaled, time delayed version of the input. This new reference signal is the output of an ideal system[4] that most closely resembles the actual system under consideration [Lee85]. Thus,

$$SNR_{out} = 10\log_{10}\left[\frac{P_{x_d}}{P_{x_d-y}}\right], \tag{3.43}$$

where,

$$x_d(t) = A_{opt}x(t-t_{opt}), \tag{3.44}$$

and the values of the optimum gain A_{opt}, and the time-delay t_{opt} are calculated as

$$A_{opt} = \frac{max(R_{xy}(\tau))}{P_x}, \tag{3.45}$$

$$t_{opt} = \tau|_{max\{R_{xy}(\tau)\}}. \tag{3.46}$$

[4] An ideal system introduces an amplitude scale factor, and a time delay on its input. The output of such a system does not have any orthogonal noise components.

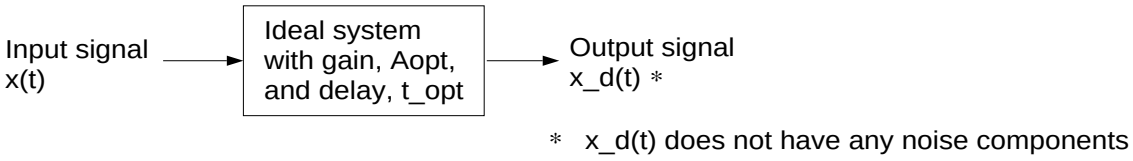

Figure 3.18: Reference Model for the Gain-delay Method

This method is an offshoot of the previous method. Hence, the merits and the demerits of the cross-correlation coefficient method apply to this method as well.

Noise Power Ratio Method

Noise Power Ratio (NPR) method calculates signal *plus* noise to noise ratio from the frequency domain representations of the signals $x(t)$, and $y(t)$.

In this approach for the SNR calculations, a narrow notch is, first, created in a specific frequency band of the input signal. The noise power at the system output is, then, calculated by integrating over the specified frequency band. Since, the input signal power over the specified frequency band is zero, the power observed at the output in the same frequency band represents the noise power introduced by the system.

Specifically, let $X(w)$ be the Fourier Transform (F.T.) of the input signal $x(t)$,

$$X(w) = \mathcal{F}[x(t)], \qquad 0 \leq w \leq w_p, \tag{3.47}$$

and $X_n(w)$ be the F.T. of the input signal $x(t)$ with a notch in frequency band $[w_n, w_n + \Delta w]$,

$$\begin{aligned} X_n(w) &= X(w), \quad 0 < w < w_n, \quad w_n + \Delta w < w < w_p & (3.48) \\ &= 0, \qquad w_n < w < w_n + \Delta w. & (3.49) \end{aligned}$$

The output signal *plus* noise to noise ratio is then determined using following equation.

$$SNNR_{out} = \frac{\Delta w}{w_p - w_n} \left[\frac{\int_0^{w_n} Y(w)^2 dw + \int_{w_n+\Delta w}^{w_p} Y(w)^2 dw}{\int_{w_n}^{w_n+\Delta w} Y(w)^2 dw} \right], \tag{3.50}$$

where $Y_n(w) = \mathcal{F}[y(t)]$ is the F.T. of the output signal $y(t)$. For the DSP implemntation of this method, the F.T. is replaced by DFT (or FFT) of the signals $x(t_n)$,

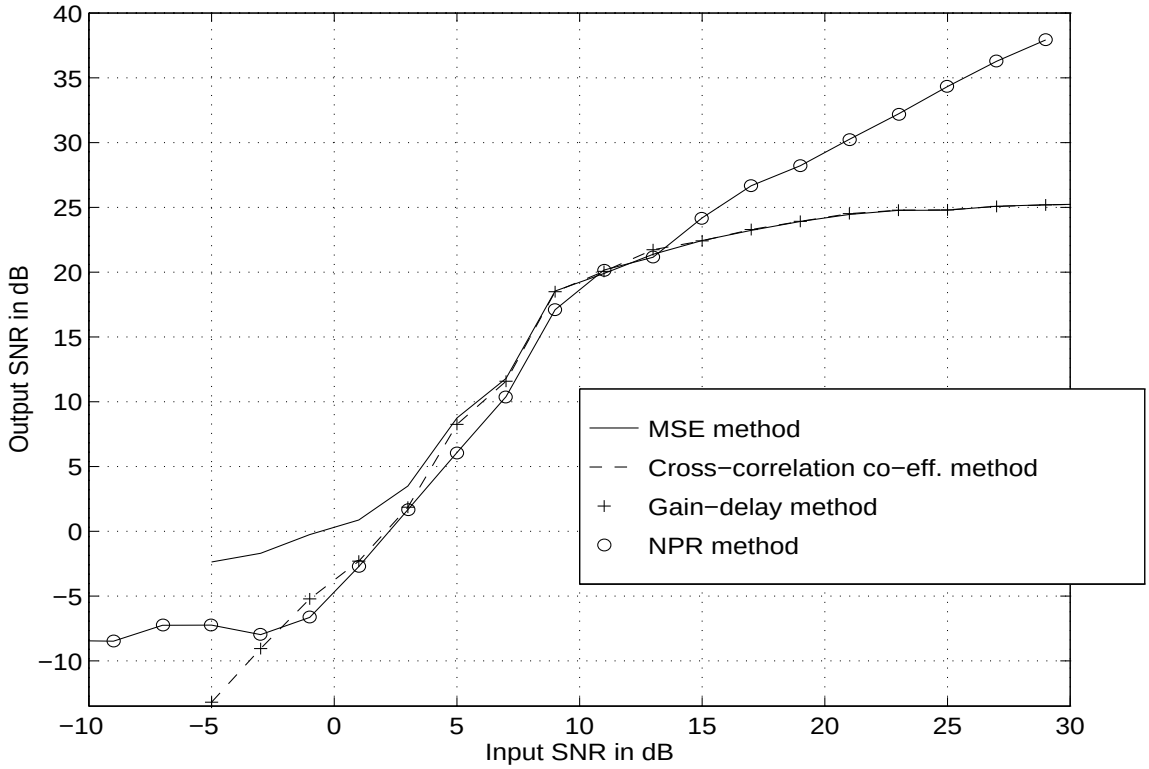

Figure 3.19: Comparison of SNR Calculation Methods

and $y(t_n)$. It is important to normalize the DFT of the signals before applying this method.

Following the Parseval's identity, the numerator of Equation 3.50 is proportional to the energy of the desired signal plus noise, and the denominator is proportional to the energy of the noise floor introduced by the system in the frequency band $[w_n, w_n+\Delta w]$. The multiplication factor $\frac{\Delta w}{w_p - w_n}$ normalizes the energy levels calculated for different bandwidths in order to obtain the ratio of the signal *plus* noise power to the noise power.

Figure 3.19 compares the above four SNR calculation methods for the differential FM detection. It is observed that the first three methods, namely the MSE method, the cross-correlation coefficient method, and the gain-delay method, show very similar results for high output SNR values. However, when the FM receiver operates below its threshold, the results of the MSE method differ from the other two methods. This difference gets increasingly pronounced as the input SNR decreases, however a

close match is observed, for the entire range of the input SNR, between the results of the cross-correlation coefficient method, and the gain-delay method. This is to be expected, since both the method employ the same essential principle for the SNR determination. The SNR values based on the NPR method do not match with that of previous methods. The first three methods consider time domain characteristics of the output signal, and hence are sensitive to the linear distortion effects introduced by non-ideal interpolation and decimation, and imperfect phase response of the filters as well as various other non-linear effects. The NPR method is less affected by these effects, since it forms the signal and the noise power estimates using frequency domain signal representations. Moreover, the SNNR parameter determined by the NPR method is greater by a factor of 1 (on linear scale) than the SNR parameter, which is another small factor causing the discrepancy.

3.2.4 An Objective Voice Quality Measure

SNR based objective voice quality measure fails to convey the perceptual voice quality, particularly for relatively high output SNR values. Improvements on the simple SNR based objective speech quality evaluations are possible, and form a very active research area. Different techniques for objective voice quality evaluations are summarized in Appendix I.

Figure 3.20 shows the result of one such method based on the segmented SNR calculations explained in Appendix I. A cumulative distribution function (CDF) of the segmented SNR values provides information regarding the number of frames with very high distortion, and serves as a magnifying glass for examining the recovered speech waveform.

3.3 Chapter Summary

The primary emphasis of this chapter is the study of different FM demodulators suitable for the DSP implementation in the FM CDMA receiver. Five DSP algorithms for the FM demodulation are discussed in this chapter. These algorithms are evaluated using the SNR based objective speech quality measure. The simulation results indicate that either the differential detector, or the quadrature detector has the best performance characteristics. It is observed that the performance of the PLL

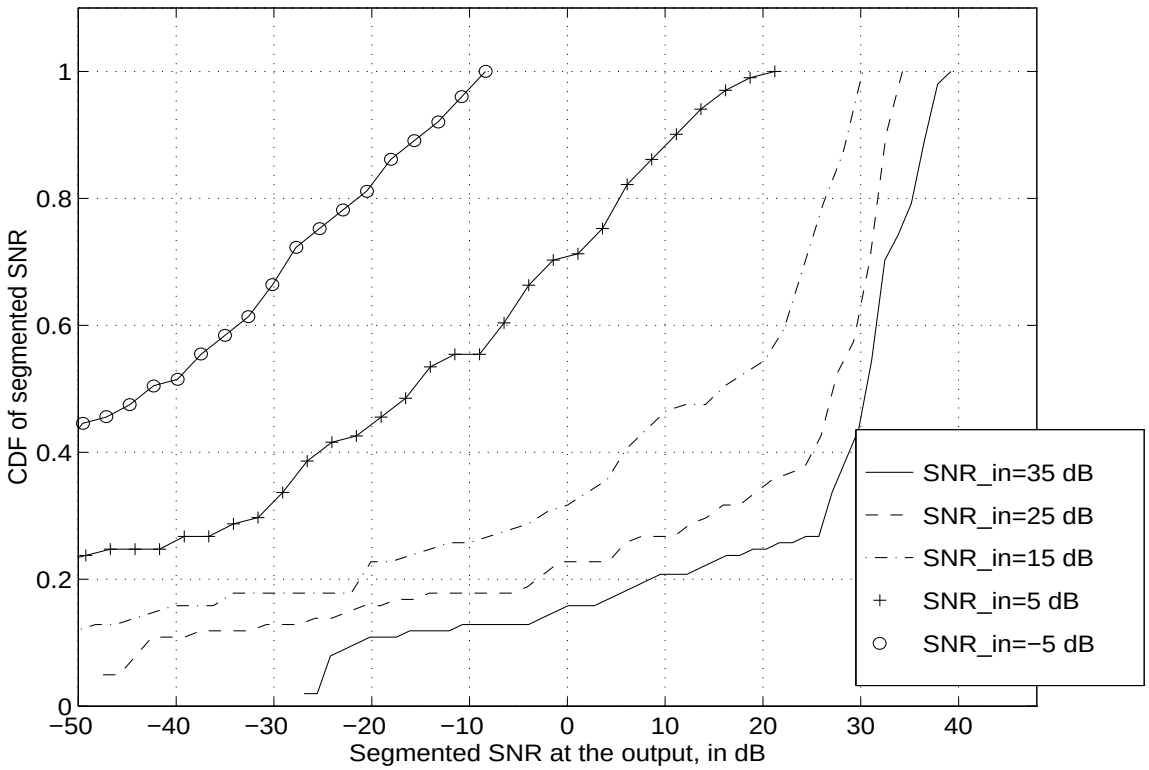

Figure 3.20: CDF of Segmented SNR for Differential Detector: An Objective Voice Quality Measure

based detector, and of the zero-crossing detector (and also, to a lesser extent, of the arctangent detector) is affected by the signal processing imperfections faced during the simulations. Many sources of the distortion, such as imperfect interpolator and decimator, are specific to the simulation model, and are likely to disappear, possibly with a slight increase in the computation complexity, with the DSP hardware implementation of the FM receivers.

The performance comparisions of the FM demodulators can be summarized as follows. The differential and the quadrature detectors are robust and simple FM demodulation methods, the arctangent demodulation is free of the phase extraction errors but requires more accurate differentiator, and the PLL based demodulation and the zero-crossing method may achieve a threshold extension of approximately 1-3 dB with an increase in the computation cost. The companding and the pre-deemphasis techniques may be used to achieve improvement near the threshold region, however they may cause a slight degradation in the output SNR with the input SNR above the threshold.

This chapter also summarizes the SNR calculation methods for speech quality evaluations. For the input SNR near or above the threshold, the results of the MSE method, the cross-correlation coefficient method, and the gain-delay method exhibit a close match. For very low SNR values, discrepancies are observed in the results of all the four methods. However, since we are interested in evaluating the system performance near or above the threshold, it is advantageous to employ the MSE method for the SNR calculations, since it offers accurate results with the least computation load.

Chapter 4

Systems Engineering

In this chapter, we investigate the performance of the FM CDMA system proposed in Chapter 2. The emphasis is on studying the system behavior with a variety of channel distortion effects. The results in this chapter are based on the MSE based SNR measure for the objective evaluations of the FM CDMA system performance. The system capacity is estimated with AWGN channel effects, as well as with time and frequency dispesive channel effects. As discussed in Chapter 2, the FM CDMA system design specifies a non-linear power amplifier at the base-station whose limiting effects become pronounced for high system loads. The effects of such nonlinear processing of the FM CDMA signal are also studied in this chapter. The final section of the chapter describes a hybrid power control scheme developed for the FM CDMA system, and presents the simulation results showing the effects of the power level variations at the base-station due such a scheme.

The system performance, for all the cases described above, is evaluated with the orthogonal, as well as with the non-orthogonal spreading codes for different users. The system capacity offered by the orthogonal link is compared with that of a non-orthogonal link. The multipath channel effects, and the nonlinear signal processing effects are also compared for the orthogonal and the non-orthogonal FM CDMA links.

4.1 Development of Simulation Test-bed

The simulation test-bed for the FM CDMA system followes the system specifications described in Chapter 2. The FM CDMA system simulations are performed at 16 KHz

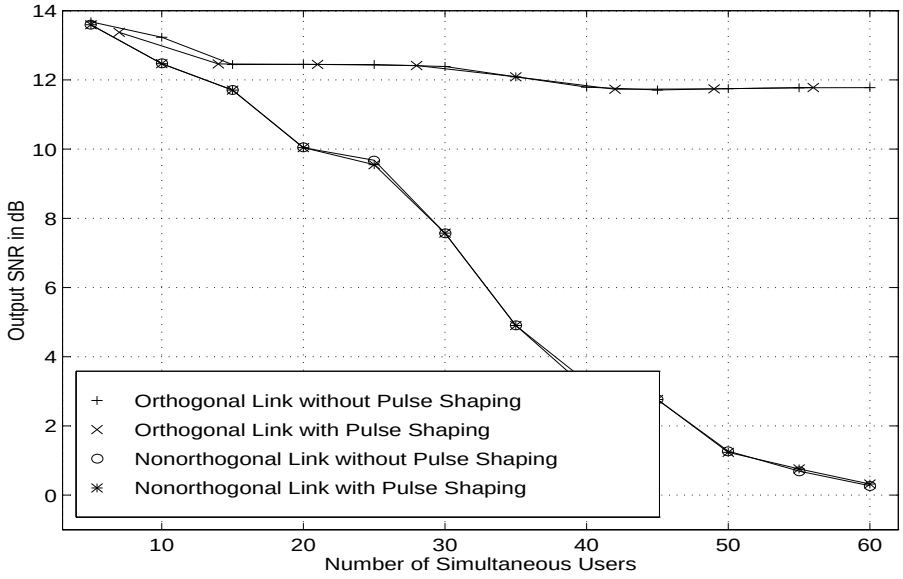

Figure 4.1: Effect of Square Root Raised-Cosine Pulse Shaping

IF, and use analytic (complex) signal representations. One of the major challenges in developing the simulation test-bed stems from a high sampling rate required for the CDMA signals. The solution to this problem lies in developing a block processing structure for the FM CDMA signals. Using the block processing method, a single discrete time-discrete amplitude voice signal, sampled at 8 KHz, is used to generate the desired levels of MAI. The FM modulated voice signal is divided into independent sub-frames. Each of the FM sub-frames corresponds to one system user, and meets the specified 25 KHz bandwidth. A very small number (between 15 to 30) of the samples of each of the FM sub-frames are processed through the transmitter, the channel, and the receiver in one processing step. By simulatneous processing only a very small number of the FM samples, we can avoid the memory inefficiencies resulting due to the high interpolation factor required for the FM signal before the spreading process. At the receiver, the processed samples are accumulated at the input to the bandpass filter before the FM demodulation. The FM demodulation is performed after combining all individual FM sub-frames, and a single speech signal at the output of the FM CDMA system is recovered.

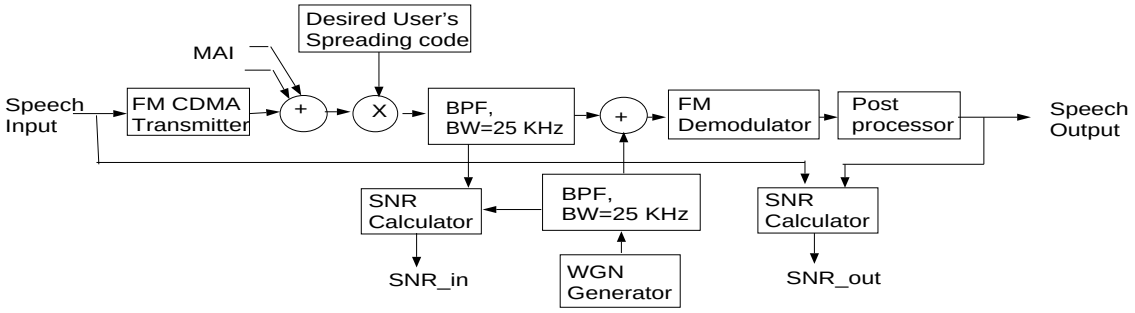

Figure 4.2: Simulation Model of the FM CDMA System Operating in AWGN Channel

The simulation test-bed uses the *Walsh-Hadamard* matrix for generating the orthogonal spreading codes [Jer92] and a Gaussian random process for generating the random spreading codes. As shown in Figure 2.9, the chip waveform of the spreading codes is shaped using the square-root raised cosine characteristics. Generating the *correct* square-root raised cosine characteristics is not a trivial task. The square-root raised cosine impulse response specified in [Kor85] fails to produce the desired pulse shape. An alternative method for generating the square-root raised cosine impulse response is based on taking the square root of the DFT of the raised cosine impulse response specified in [Jer92]. However, if the impulse response obtained using this method is passed through an identical filter, a very slight ISI effect is observed at the output. The distortion due to this imperfection is not significant enough to cause appreciable performance degradation. This observation is validated in Figure 4.1 in which the output SNR curves with and without pulse shaping are hardly distinguishable.

4.2 System Performance in AWGN Channel

Figure 4.2 shows block diagram of the approach used to evaluate the FM CDMA system performance in the AWGN channel. The bandpass filtered noise is added to the bandpass filtered despread signal at the input of the FM demodulator. The noise floor introduced by the channel remains unaffected by the despreading operation. Hence, adding the white Gaussian noise signal after the despreading process is equivalent to introducing the channel noise effects at the input to the FM CDMA receiver. Precise control of the input SNR is achieved by varying the powers of the

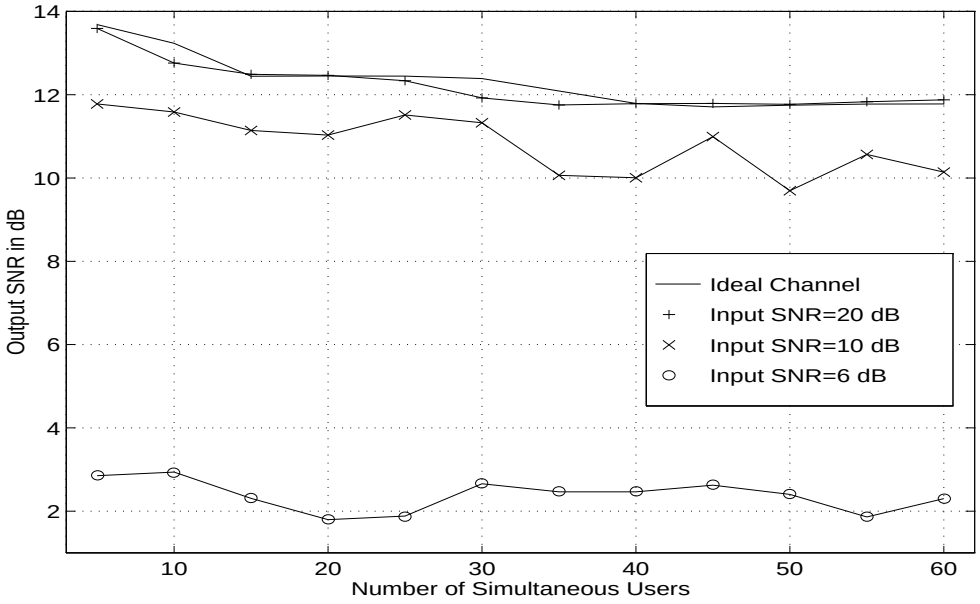

Figure 4.3: Performance of the FM CDMA System in AWGN: Orthogonal Spreading Codes

bandpass filtered signal, and the noise. Moreover, the input SNR for the simulation model of the FM CDMA system is same as the input SNR for the FM system shown in Figure 3.11, hence it is a common base for comparing the performance of both the systems.

4.2.1 Orthogonal Link Performance

Figure 4.3 shows the output SNR for a synchronous systems with orthogonal spreading codes for different users. It is observed that the system supports the desired capacity of 60 simultaneous users, if the input SNR remains above 10 dB.

4.2.2 Non-orthogonal Link Performance

Figure 4.4 shows the system performance in AWGN with the random spreading codes for different users. It is observed that the performance of the system degrades rapidly with increasing number of users. With 40 or more simultaneous system users, the FM CDMA receiver is driven below the threshold.

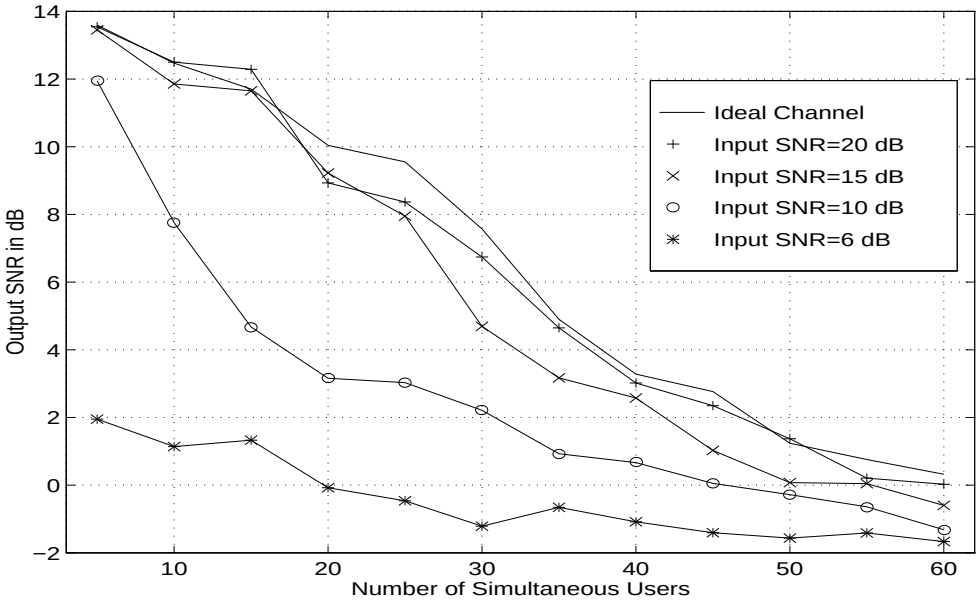

Figure 4.4: Performance of the FM CDMA System in AWGN: Random Synchronous Spreading Codes

Figure 4.5 depicts the system performance with the asynchronous random spreading codes. Such a scenario is typical for the reverse link of the CDMA systems, since different users' signals experience different time offsets, and are not aligned at the receiver with respect to their respective spreading codes. With a large spreading code length of 2048, average cross-correlation for a synchronous set of random codes does not differ significantly from the same for asynchronous random codes. Hence, the performance results in Figures 4.5, and 4.4 exhibit a close match.

Figure 4.6 shows the output SNR of the FM CDMA system as a function of the input SNR. The result shown in this figure corresponds to 30 simultaneous users. It is observed that the threshold of the FM CDMA receiver with orthogonal spreading codes is similar to the threshold of the FM receiver in Figure 3.12. This is not surprizing, since with orthogonal MAI, we can achieve *almost* perfect[1] interference cancellation. However, the high sampling rates required for the CDMA simulations

[1]Note that even with the orthogonal codes, it is not possible to achieve perfect interference cancellation. This is be due to non-ideal BPF used to perform the averaging operation on the despread signal. The orthogonal FM CDMA link performance remains same up to 150 simultaneous users. However, with greater than 200 simulataneous users, the FM CDMA receiver starts operating below the threshold even in ideal channel conditions.

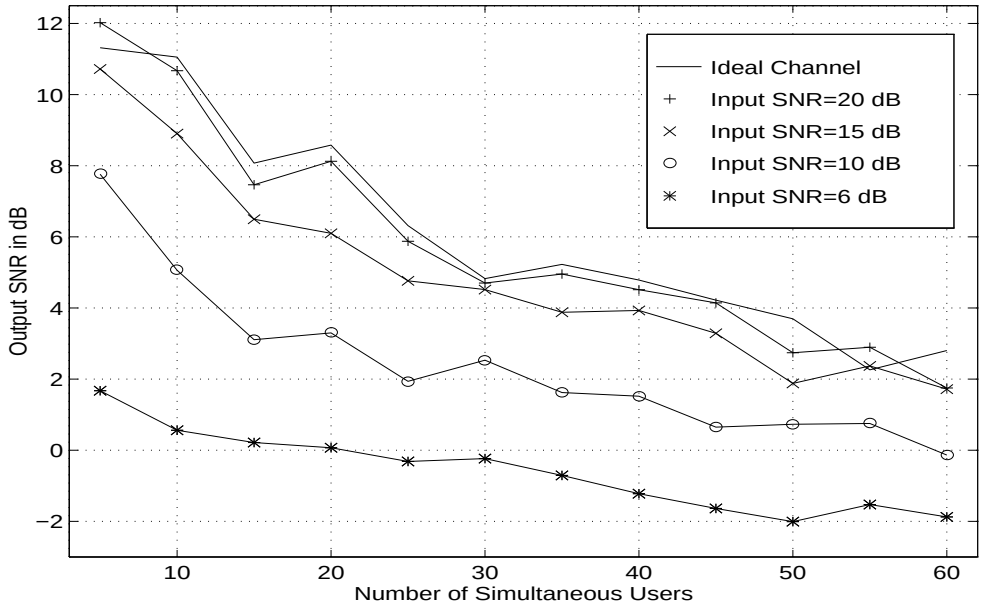

Figure 4.5: Performance of the FM CDMA System in AWGN: Random Asynchronous Spreading Codes

lead to the distortion effects. These effects cause the orthogonal FM CDMA link characteristics to saturate at 8-10 dB lower values above the threshold as compared to saturation level for the FM receiver discussed in Chapter 3.

With the random spreading codes, the FM CDMA receiver input threshold rises to 14-16 dB. The interference cancellation achieved by a non-orthogonal CDMA link falls far below the ideal performance. Hence, the noise floor contributed by the MAI at the input to the FM demodulator increases, and leads to a higher value of the input SNR threshold. The performance of the receiver above the threshold is also inferior compared to the performance achieved by the orthogonal spreading codes.

4.3 Time and Frequency Dispersive Channel Effects

The FM CDMA based WLL system is likely to face multiple channel degradation effects besides the thermal noise effects investigated in the previous section. Random time and frequency dispersion effects are the major sources of the distortion in the

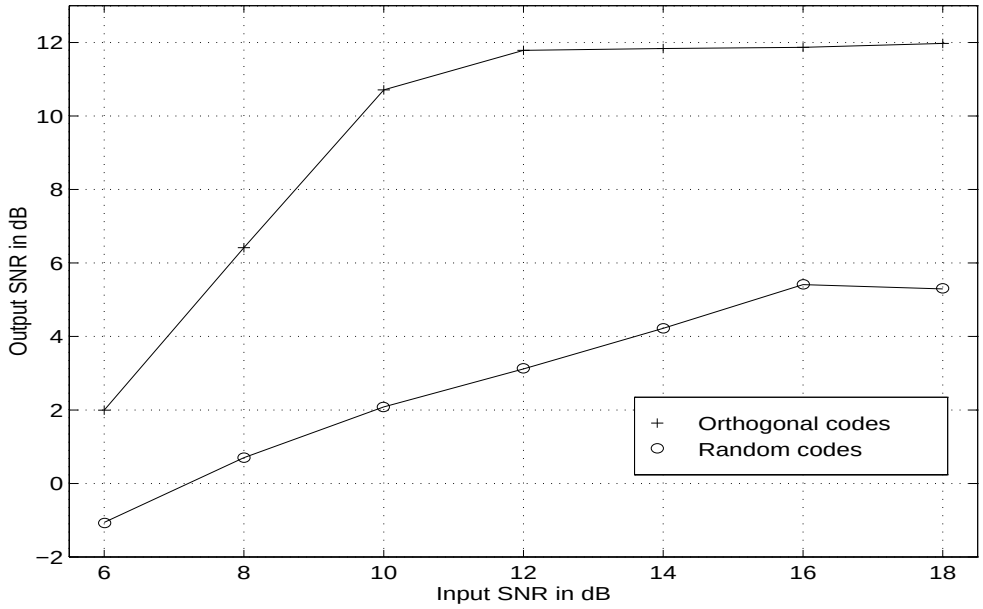

Figure 4.6: Performance of the FM CDMA System as a Function of Input SNR: Number of Simultaneous Users = 30

transmitted RF signal. A proper modeling of such channel effects is essential to gauge the system performance in the practical environments.

European commission for scientific and technical research (EURO-COST) has defined a standard, known as COST 207, for the multipath delays, and the Doppler fading effects for different regions such as urban, suburban, hilly and non-hilly terrains [Cos89]. The time-dispersive channel effects are specified by different channel

Multipath	Rural, non-hilly, region		Rural, hilly, region		Urban, hilly, area		Hilly terrain	
Component	$\tau(n)$	$a(n)$	$\tau(n)$	$a(n)$	$\tau(n)$	$a(n)$	$\tau(n)$	$a(n)$
1	0.0	1.0000	0.0	0.7071	0.0	0.7071	0.0	1.0000
2	0.2	0.7937	0.2	1.0000	0.4	1.0000	0.2	0.7931
3	0.4	0.3162	0.6	0.7937	1.0	0.7071	0.4	0.6525
4	0.6	0.1000	1.6	0.5000	1.6	0.5657	0.6	0.4472
5	-		2.4	0.4000	5.0	0.7937	15.0	0.5000
6	-		5.0	0.3166	6.6	0.6325	17.2	0.2449

Table 4.1: COST 207 Channel Specifications

Channel Parameter	Rural hilly	Rural non-hilly	Urban hilly	Hilly terrain
Mean Excess Delay. μs	0.098	0.705	2.14	2.06
RMS Delay Spread, μs	0.12	1.06	2.39	4.98
Coherence BW, KHz	1580	187	83.6	40.1

Table 4.2: COST 207 Channel Parameters

impulse response models. Each of these models has a typical multipath component distribution, or the power delay profile, along the incremental time-axis. Typical power delay profiles associated with different regions in COST 207 empirical standard are shown in Table 4.1, where delay values $\tau(n)$ are in μ-seconds, and the $a(n)$ specify the relative amplitude levels of different multipath components.

Table 4.2 shows values of *mean excess delay*, *rms delay spread*, and *coherence bandwidth* for different channel models. These parameters are defined in the reference [Rap95] as,

$$\overline{\tau} = \frac{\sum_n a(n)^2 \tau(n)}{\sum_n a(n)^2}, \tag{4.1}$$

$$\sigma_\tau = \sqrt{\overline{\tau^2} - (\overline{\tau})^2}, \tag{4.2}$$

$$B_c \approx \frac{1}{5\sigma_\tau}. \tag{4.3}$$

It is observed that the coherence bandwidth of all the channel models is significantly less than the FM CDMA signal bandwidth of approximately 10 MHz. Thus, the COST 207 specifications cause *frequency selective* fading on the FM CDMA signal. In order to determine the effect of *flat fading* channel on the system performance, a different model is used. The values of $\tau(n)$ for this flat fading channel model are chosen as 0, 31.2, and 62.4 nano-seconds. Corresponding amplitude levels $a(n)$ are 1, 0.1, and 0.05 respectively. The coherence bandwidth for this channel model is approximately 45 MHz, which is larger than the FM CDMA signal bandwidth. Thus, a flat fading environment is simulated by this channel model.

The WLL system is characterized by a stationary transmitter and a receiver. This characteristic greatly reduces the frequency dispersion experienced by the received signal. A small Doppler spread f_d still is still introduced in the transmitted signal due to the movement of the surrounding objects that cause random scattering and reflection effects. Frequency dispersion effects are considered in the COST 207 model

by different fading spectrums. The multipath components with time-delays, $\tau(n) \leq 0.5\ \mu s$ are modeled with Rayleigh distributed envelope variations. Rayleigh envelope distribution is appropriate for flat fading effects typical for small multipath delay values. The simulation model for generating the Rayleigh fading signal, based on the procedure explained in [Smi75], uses the Doppler channel spectrum defined as

$$s(f) = \frac{A}{\sqrt{1-(f/f_d)^2}}, \tag{4.4}$$

where A is the channel attenuation factor.

For multipath delays $\tau(n) > 0.5\ \mu s$, COST 207 model uses Gaussian channel function,

$$G(A, f_1, f_2) = Ae^{-\frac{(f-f_1)^2}{2f_2^2}}, \tag{4.5}$$

in the channel transfer function

$$\begin{aligned} s(f) &= G(A, -0.8f_d, 0.05f_d) + G(A_1, 0.4f_d, 0.1f_d), \quad 0.5\mu s < \tau(n) \leq 2\mu s, & (4.6)\\ &= G(B, 0.7f_d, 0.1f_d) + G(B_1, -0.4f_d, 0.15f_d), \quad 2\mu s < \tau(n), & (4.7) \end{aligned}$$

where A_1 is 10 dB below A, and B_1 is 15 dB below B. The frequency selective nature of the channels for greater values of multipath dispersion is simulated by decreasing the bandwidth of the Gaussian model.

The Line of Sight (LOS) propagation effects are modeled in the rural non-hilly area channel model by Ricean distributed envelope variations. The transfer function of such a channel is

$$s(f) = \frac{0.41}{2\pi f_d\sqrt{1-(f/f_d)^2}} + 0.91\delta(f-0.7f_d). \tag{4.8}$$

Figure 4.7 shows a generic block diagram for implementing flat or frequency selective channel models [Rap95]. The same block diagram is used to implement the COST 207 channel models by choosing values of $\tau(n)$, and $a(n)$ from Table 4.1. The fading simulator is then selected on the basis of the factors discussed above.

4.3.1 Impact on Orthogonal Link

The effect on flat fading channel on the output SNR of the orthogonal link is shown in Figure 4.8. The orthogonal link performance with specular flat fading multipath effects exhibits negligible degradation compared to the performance of the ideal channel. However, diffuse multipath components cause appreciable performance degradation.

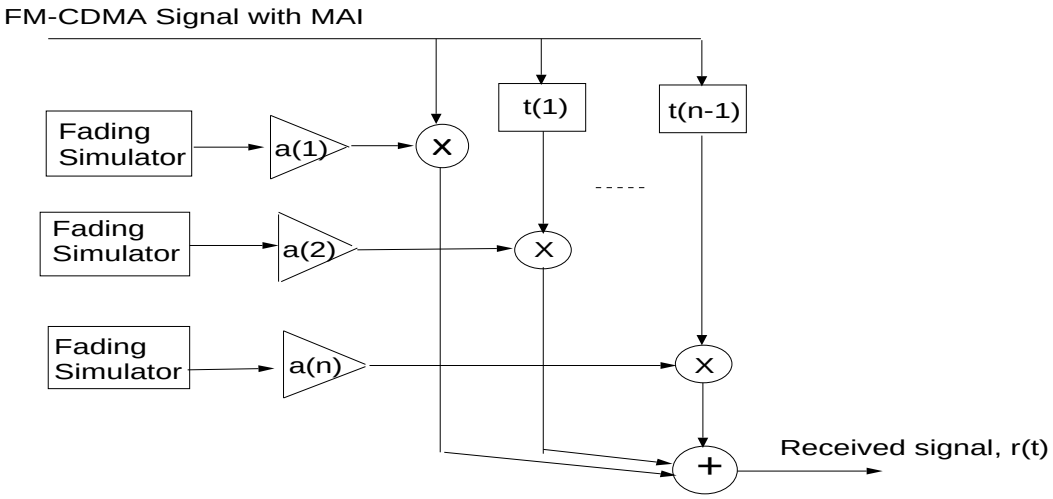

Figure 4.7: A Generic Channel Model

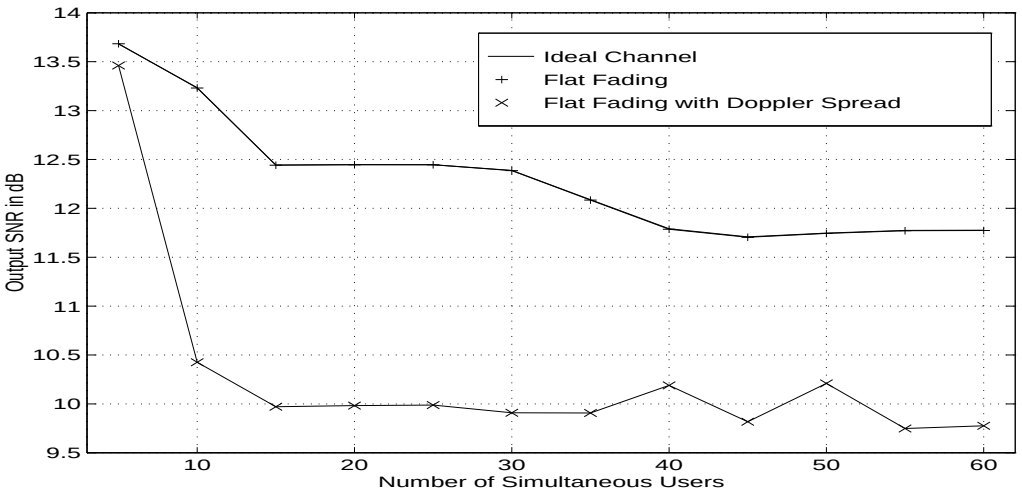

Figure 4.8: Orthogonal Link Performance in Flat Fading Environment

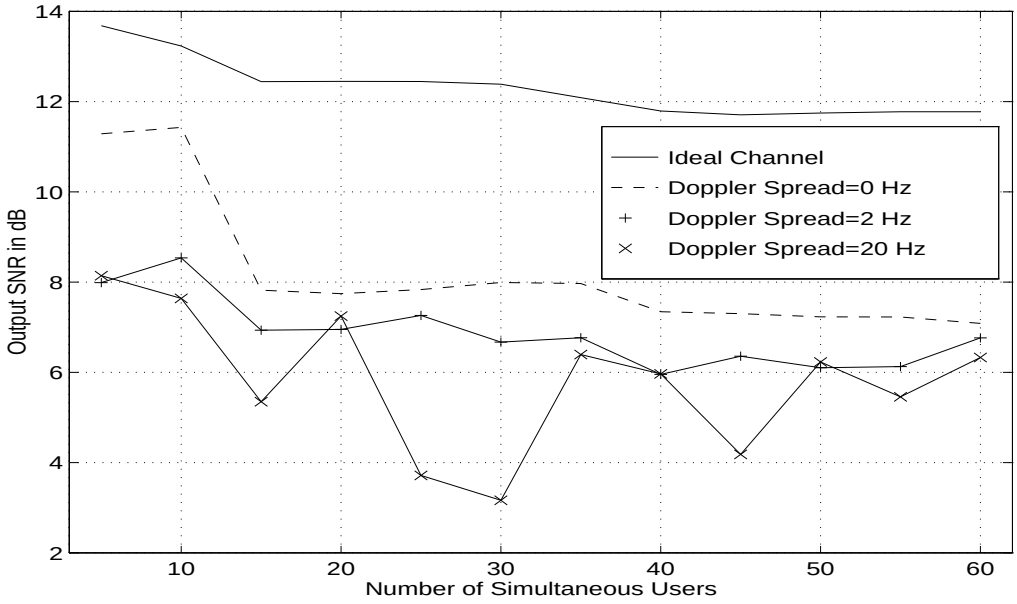

Figure 4.9: Orthogonal Link Performance in Rural Non-hilly Area Channel with Varying Degrees of Doppler Spread

The effect of frequency selective channel on the performance of the FM CDMA system is shown in Figure 4.9. The channel model follows the rural non-hilly area power delay profile specified in COST 207 standard. The coherence bandwidth for this channel model is 1.58 MHz, which results in the frequency selective fading on the FM CDMA signal. The FM CDMA receiver operates above the threshold with up to 60 simultaneous orthogonal users in such a channel environment. However, a very small Doppler spread of 2 Hz (corresponding to 1.2 km/hr velocity at 1.9 GHz RF frequency) affects the system performance significantly. Infact, the system performance does not degrade further, even if the Doppler spread increases to 20 Hz (corresponding to 11.5 km/hr velocity).

Figure 4.10 shows the output SNR curves obtained for an orthogonal link with the different channel models specified in COST 207 standard. The figure shows the system performance with the urban hilly area channel model whose coherence bandwidth is approximately 185 KHz. The performance in such a channel degrades rapidly with greater than 5 simultaneous users. The hilly urban area model and the hilly terrain model, whose coherence bandwidths are 85 KHz and 40 KHz respectively, have a very severe impact on the system performance. The FM CDMA receiver operates below

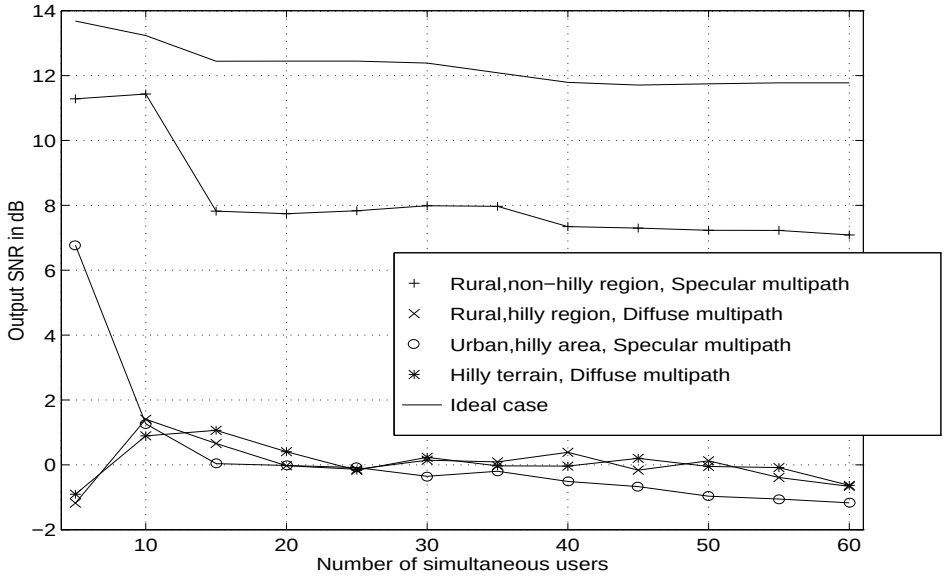

Figure 4.10: Orthogonal Link Performance in different COST 207 Channel Models

the threshold even with very low MAI. The COST 207 standard describes the above two models as the examples of very bad channel conditions, hence the poor system performance with such channel models is not very discomfiting.

4.3.2 Impact on Non-orthogonal Link

The effect of the flat fading channel model on the performance of the non-orthogonal link is shown in Figure 4.11. It is observed that the flat fading channel without the Doppler spread does not have any significant impact on the system performance. However, diffuse multipath components cause appreciable performance degradation.

The effect of frequency selective channel model on the non-orthogonal FM CDMA link is shown in Figure 4.12. The frequency selective multipath fading is simulated by the rural non-hilly area channel model specified in COST 207 standard. It is observed that without any Doppler spread effects, the frequency selective fading does not impact the system performance significantly. However, with a small Doppler spread of 2 Hz on each of the multipath components, the system capacity reduces drastically. Infact, further capacity reduction is not observed even if the Doppler spread increases to 20 Hz.

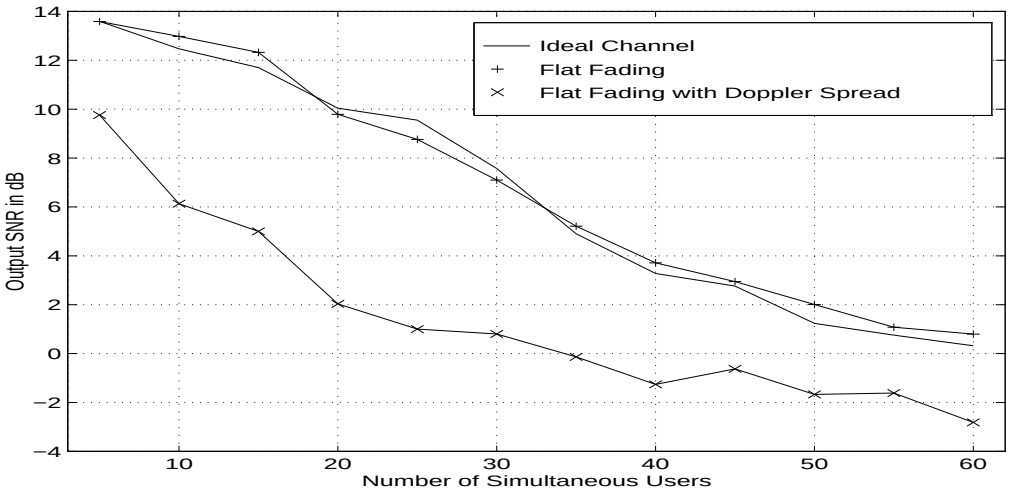

Figure 4.11: Non-orthogonal Link Performance in Flat Fading Environment

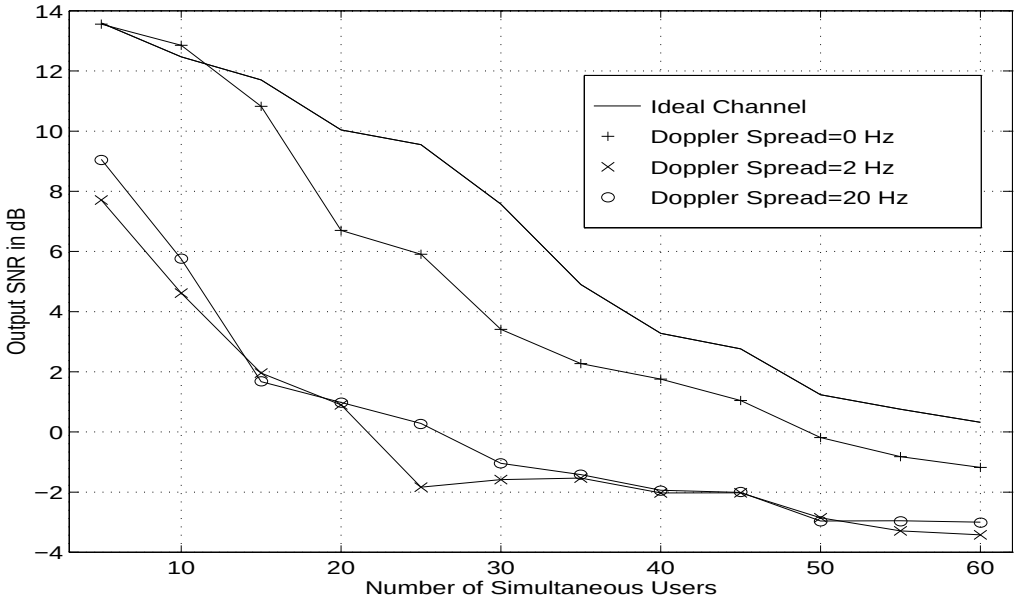

Figure 4.12: Non-orthogonal Synchronous Link Performance in Rural Non-hilly Channel with Varying Degrees of Doppler Spread

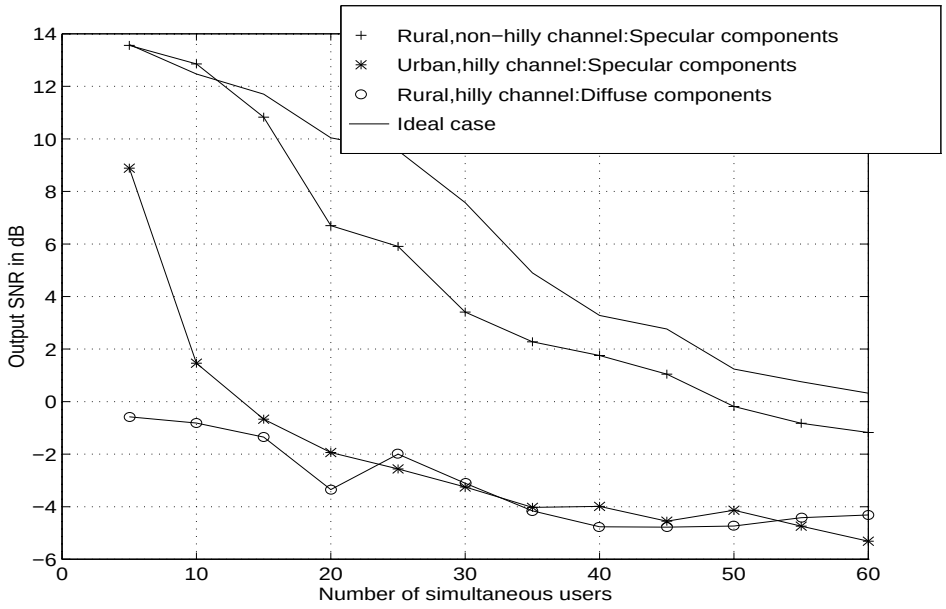

Figure 4.13: Non-orthogonal Synchronous Link Performance in Multipath Effects

Figure 4.13 shows the effects of COST 207 channel models with the synchronous random spreading codes for different users. The FM CDMA receiver fails to operate above the threshold for the channel models with small coherent bandwidth and many multipath components, such as in the bad case hilly urban channel model, or in the bad case rural hilly region. The system performance is unacceptable even with the minimum system loads.

Figure 4.14 shows the effects of channel models on asynchronous random spreading codes. The multipath channel effects on such a link are very similar to the previous example of synchronous random link.

Comparing the performance of orthogonal link in multipath fading effects (refer to Figures 4.8, and 4.9) with the system capacity obtained using random spreading codes (refer to Figures 4.11, and 4.12), we observe that the orthogonal codes do not show capacity improvments over the random non-orthogonal spreading codes. This is to be expected, since orthogonality among different users is not preserved with time-dispersive effects.

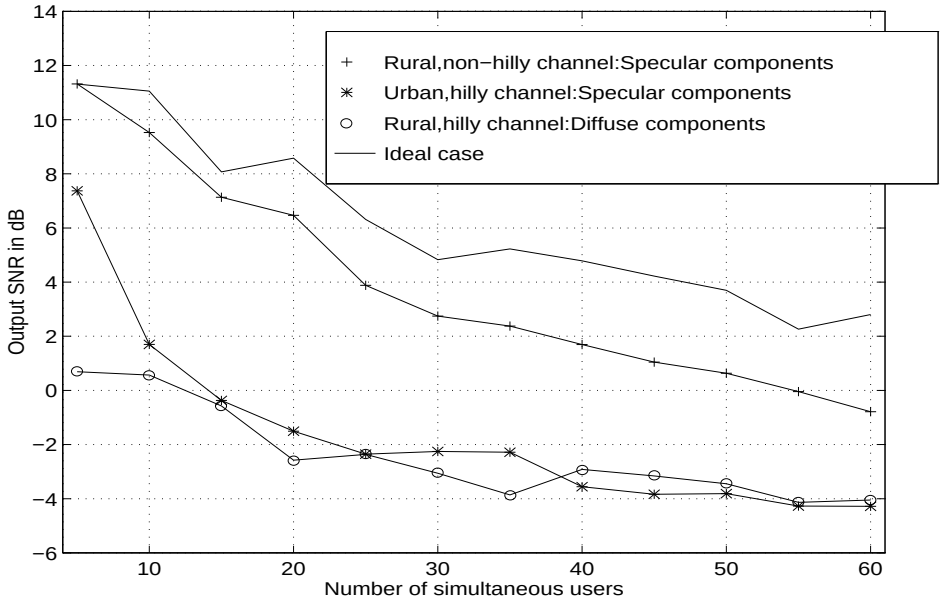

Figure 4.14: Non-orthogonal Asynchronous Link Performance in Multipath Fading

4.4 Effects of Non-linearity

Using the nonlinear model specified in Equation 2.1, the capacity of the FM CDMA system is estimated for the orthogonal spreading codes as well as for the random spreading codes. Figure 4.15 shows the effect of variations in the input limit level l. The results pertain to a case of 30 equal power simultaneous users. For 30 simultaneous users, the FM CDMA signal envelope varies between $5A_c$ to $6A_c$, where A_c denotes the amplitude of the FM signal. Assuming $A_c = 1$ (without any loss of generality), we can conclude that the effects of the nonlinearity are significantly less pronounced if $l > 4$. The results shown in Figure 4.15 match this conclusion. It is also observed that with 30 simultaneous users, the performance of random spreading codes is noticeably poor compared to the orthogonal system performance. This matches with the capacity curves in Figure 4.4 where the non-orghogonal link shows approximately 6 dB output SNR with 30 simultaneous users.

Figures 4.16 and 4.17 further illustrate the impact of nonlinearity on the FM CDMA system capacity. Figure 4.16 pertains to the orthogonal spreading codes. It is observed that if the input limit level l is 5.5, the system performance is almost similar to the ideal case. This is to be expected, since with a high value of the

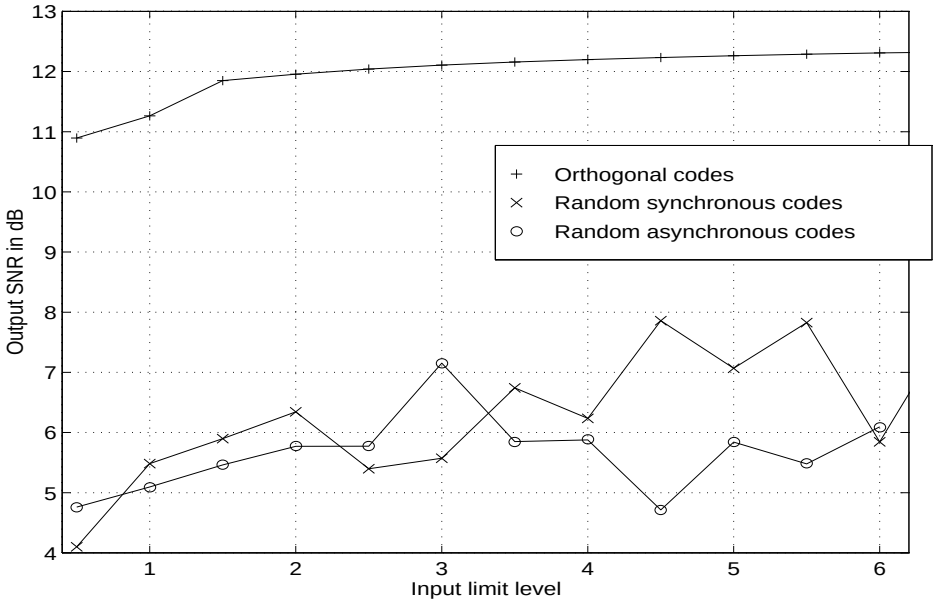

Figure 4.15: Effect of Input Limit Level Variation: Number of Simultaneous Users = 30

input limit level, the saturation effects due to the nonlinearity occur less frequently. However, even with a very low value of 1.5 of the input limit level l, the orthogonal link performance does not degrade drastically. This phenomena occurs, since the cross-product terms generated due to the non-lineary also have a near orthogonality. Figure 4.17 shows the effect of the input limit level variations on the capacity of the non-orthogonal FM CDMA link. It is observed that the performance of the non-orthogonal link is also not significantly affected, even if the nonlinear characteristics are very severe.

4.5 Power Control Algorithm

The FM CDMA system uses a low level pilot tone to implement a hybrid, closed and open loop, power control. The pilot tone is generated at 2 KHz IF[2] for each forward and reverse user channel along with the user specific FM signal. Both the pilot tone and the FM signal are spread before the transmission.

[2]An alternate approach uses a baseband pilot tone.

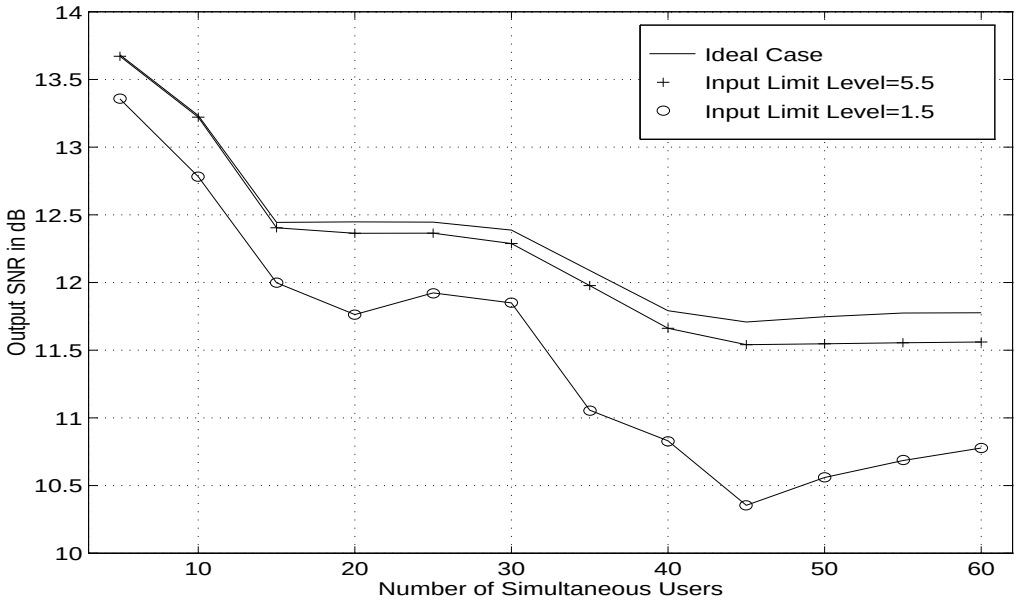

Figure 4.16: Orthogonal Link Capacity for Two Values of Input Limit Level

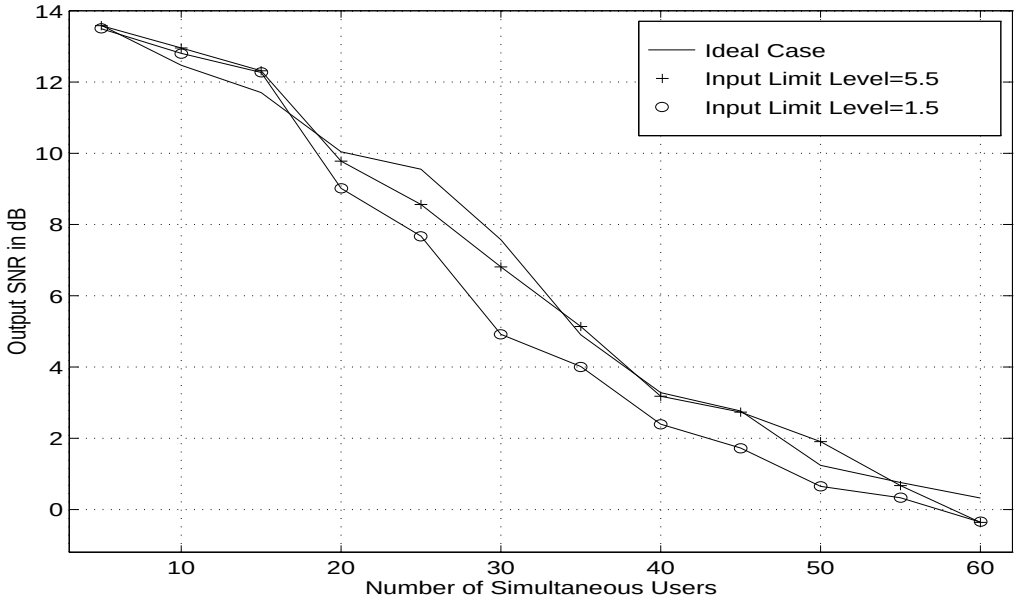

Figure 4.17: Non-orthogonal Link Capacity for Two Values of Input Limit Level

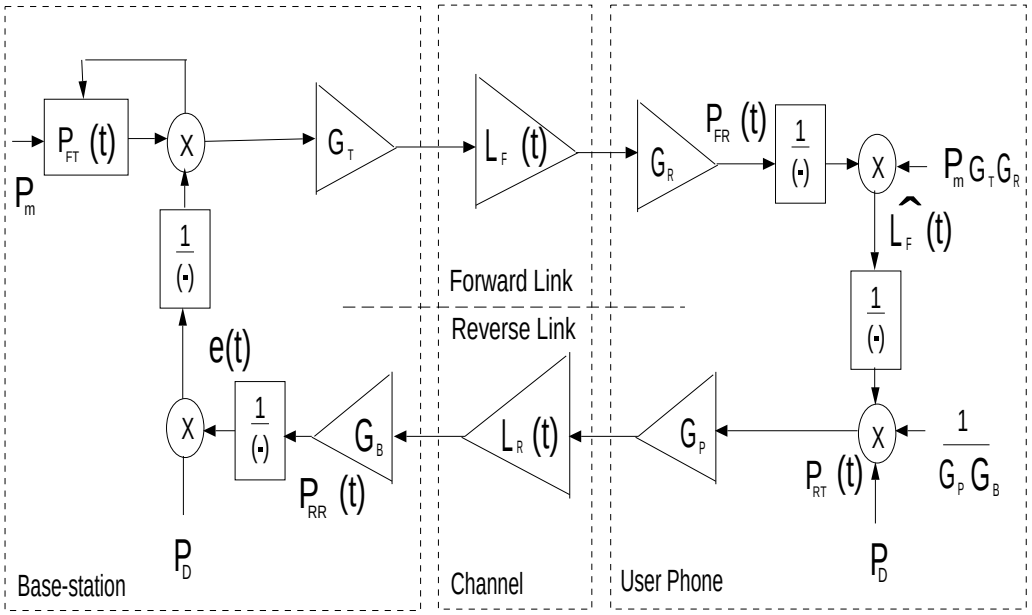

Figure 4.18: Block Diagram of Power Control Algorithm

4.5.1 Description of the Approach

The block diagram of the power control algorithm is shown in Figure 4.18.

On the forward link, the base-station transmits the pilot tone at a power level $P_{FT}(t)$. The time varying transmit level, $P_{FT}(t)$, has a mean value P_m which is approximately 15 dB below the FM signal power. The base-station varies $P_{FT}(t)$ in small incremental steps (with a maximum of approximately ± 5 dB deviation about the mean value P_m) to convey the closed loop power control information. The user phone receives the pilot tone on the forward channel at a level of $P_{FR}(t) = G_T G_R P_{FT}(t) L_F(t)$, where $L_F(t)$ is the forward link path-loss, and G_T and G_R are the base-station transmitter and the user phone receiver gain-levels.

The user phone forms an estimate of the forward link path-loss value from the received power $P_{FR}(t)$.

$$\hat{L_F}(t) = \frac{P_m G_T G_R}{P_{FR}(t)}. \tag{4.9}$$

Using the estimated link loss value $\hat{L_F}(t)$, the user phone calculates the reverse link pilot transmit level $P_{RT}(t)$ required to achieve a desired received power level P_D at

the base-station.

$$P_{RT}(t) = \frac{P_D}{\hat{L_F}(t) G_P G_B}, \tag{4.10}$$

where G_P and G_B denote the user phone transmitter and the base-station receiver gain-levels.

The received power at the base-station is $P_{RR}(t) = P_{RT}(t) L_R(t) G_P G_B$, where $L_R(t)$ denotes the reverse link time-varying path-loss. Due to the small-scale fading effects, the forward link path-loss estimate $\hat{L_F}(t)$ formed by the users phone is not accurate. Moreover, the forward link path loss $L_F(t)$ does not match exactly with the reverse link path-loss $L_R(t)$. Hence, $P_{RR}(t) \neq P_D$ at the base-station receiver, which leads to an error

$$e(t) = \frac{P_D}{P_{RR}(t)} \neq 1.$$

The small variations in the transmitter and the receiver gain-levels G_T, G_R, G_P and G_B caused due to component aging and imperfections form another source of the error.

The power control algorithm attempts to minimize the impact of these sources of errors by modifying the forward link transmit power level. The new value of $P_{FT}(t)$ is calculated as

$$P_{FT}(t + \Delta t) = \frac{P_{FT}(t)}{e(t)}.$$

Thus, the closed-loop control exercised by the base-station drives the errors $e(t)$ for all the users towards unity.

4.5.2 Implementation

The above hybrid power control algorithm is implemented using large scale and small scale propagation models. The power control algorithm assigns each user a distance from the base-station. The user-distances are uniformly distributed in the range of 0 m to 10,000 m.

The long-term average forward and reverse link path-loss values, $L_F(t)$ and $L_R(t)$, are estimated using either a power-law function, two-ray ground reflection model, or Hata model. Small scale fading effects are simulated in the power control algorithm by imposing a short term random variation on the long term average path-loss values. The short term random variation due to small scale fading follows either Rayleigh or Ricean distribution. It is to be noted that Ricean distribution is a good choice for

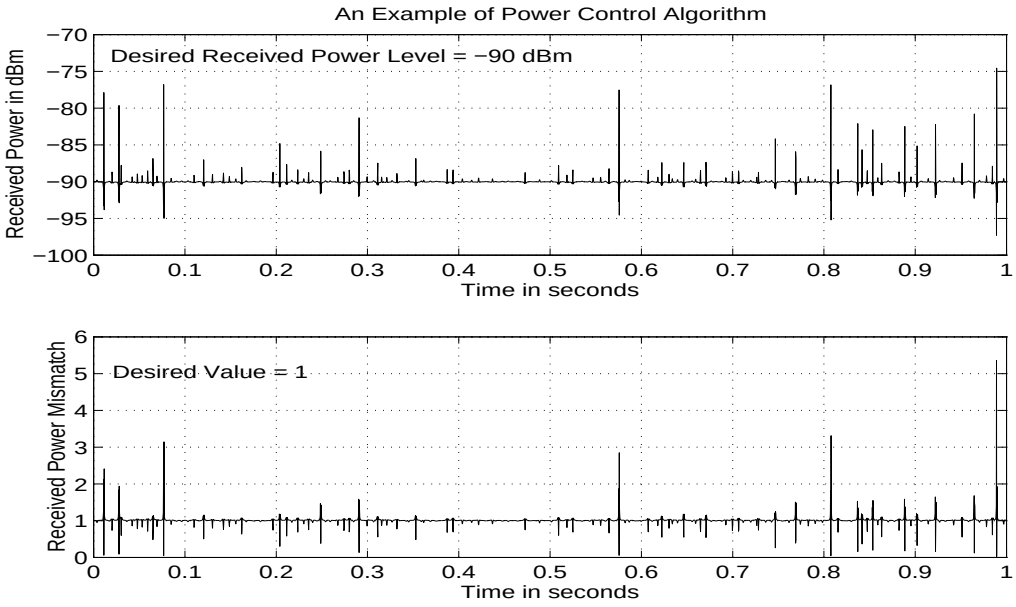

Figure 4.19: Power Control Algorithm: A Performance Example

the line of sight (LOS) small scale fading effects. Additional statistical variations are introduced by randomly varying the transmit and receive gain levels.

The power control algorithm assumes a constant time period between successive power control information exchanges between the base-station and the user phone. The short term power level variations are smoothed over this time interval. The power mismatch at the base-station receiver increases, if this time interval of the power control exchanges increase. If this time interval is less than 0.1 $m\,s$, almost perfect power control is realized. However, if its values increases to 1 $m\,s$, a variance of approximately 1 dB is observed in the mean power levels of different users. This power level variance is also a function of the Doppler spread, and hence the severity of the small scale fading effect. The results shown in this section pertain to a Doppler spread of 50 Hz, which is the worst case condition for the fixed wireless systems.

Figure 4.19 shows the received power levels $P_{RR}(t)$ at the base-station as a function of time, with the specified desired power level P_D = - 90 dBm. It is observed that the power control algorithm enables the mean value of $P_{RR}(t)$ to converge to the desired received power P_D. The short term error statistics $e(t)$ between P_D, and $P_{RR}(t)$ is also indicated in the Figure. It is noticed that the error $e(t)$ does not always remain

unity due to the random effects experienced by the forward and the reverse links, however its value does not stray significantly away from the unity for a long duration.

The result shown pertains to a user-distance of 5 km, forward link large scale propagation model with power-law exponent $n = 4$, reverse link pathloss exponent $n = 3.5$, and Ricean distributed short term fading statistics. The similar results are obtained with the other values of the user-distance, and different forward and reverse link path-loss models.

4.5.3 Simulation Results

Figure 4.20 shows the output SNR for the FM CDMA system with the power control variations determined using the above power control algorithm. The results pertain to the power control information exchange rate of 1.5 $m\,s$. We observe that the performance of the asynchronous non-orthogonal link is not greatly affected with the introduction of the power control scheme. The results for the non-orthogonal link with such non-ideal power control are similar to those shown in Figure 4.5 where we assumed ideal power control. The performance of asynchronous link with the orthogonal spreading codes is observed to be inferior. This is to be expected since with asynchronous reception, the orthogonality between different users is not maintained.

The power control algorithm explained in the previous section assumes unambiguous power level information exchanges between the base-station and the user phone. Hence, it is necessary to determine the effectiveness of the detected pilot tone at the receiver in conveying the power control related information. Figure 4.21 shows that the despread pilot tone provides a reliable power information with the orthogonal spreading codes. In the figure, the envelope of the despread pilot tone remains almost constant, and reaches the transmitted pilot tone amplitude level of 0.1. However, with the random spreading codes, the pilot tone envelope does not attain a constant value after the despreading. This effect is partially understood by studying Figure 4.22 which shows the spectra of the despread FM CDMA signal plus pilot tone. With 30 orthogonal users, the despread signal spectrum does not show any distinguishable noise floor outside the FM bandwidth. Hence a noise-free pilot tone recovery is possible. However, with 30 non-orthogonal users, the despread signal spectra exhibits a significant noise floor. The imperfect MAI cancellation gives rise to

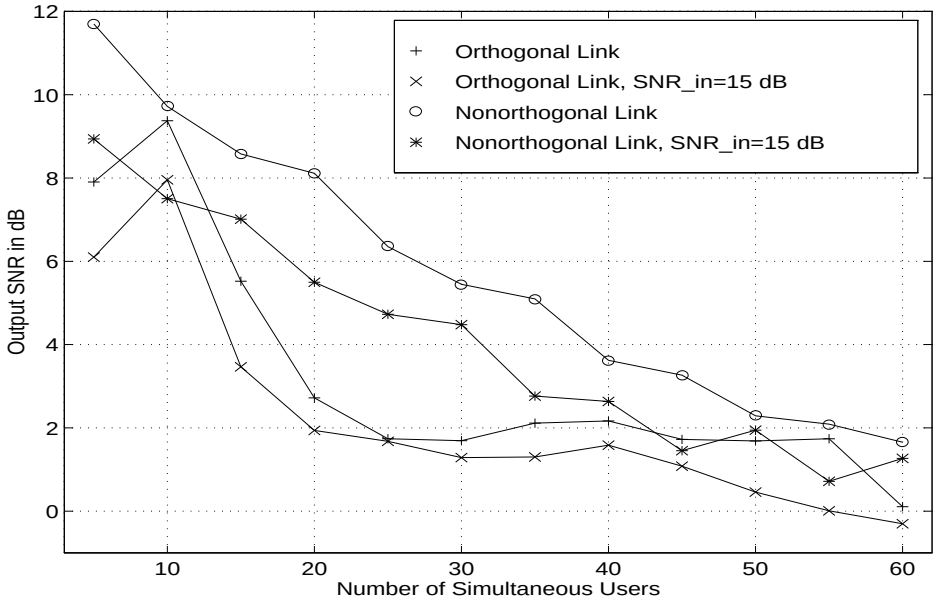

Figure 4.20: Effect of Power Control Imperfections

spectral components that fall within the narrow bandwidth of lowpass filter. These lowpass filtered noise components affect the reliability of the recovered pilot tone in conveying the power related information.

It is possible to improve the power estimates with the non-orthogonal spreading codes by averaging the power of the despread pilot tone over a large interval, and by carefully determining the decision threshold. Another approach may lie in integrating the energies at the harmonics of the pilot tone, since Figure 4.22 shows significant despread pilot tone harmonic components with non-orthogonal spreading codes.

4.6 Chapter Summary

In this chapter, we arrived at the estimations of the FM CDMA system capacity under different channel conditions.

With the assumption of a benign channel that allows reception of perfectly orthogoal equal power user signals, the FM CDMA performance is very similar to the performance of the FM system, and the FM CDMA receiver shows the same input SNR threshold as exhibited by different FM demodulators in Chapter 3. However,

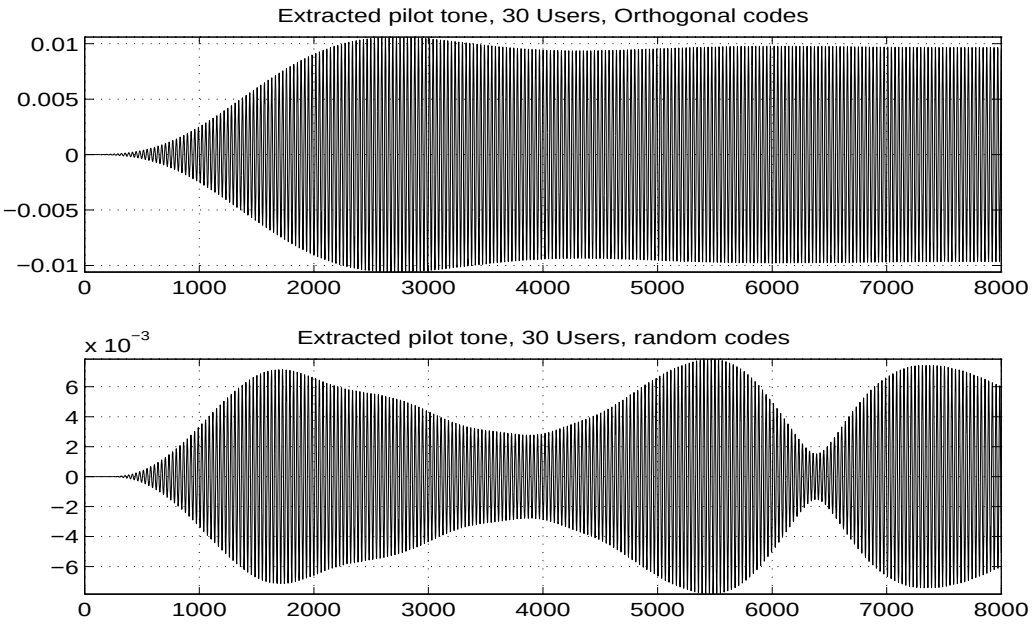

Figure 4.21: Pilot Tone Recovery for Power Control (X-axis shows the number of samples)

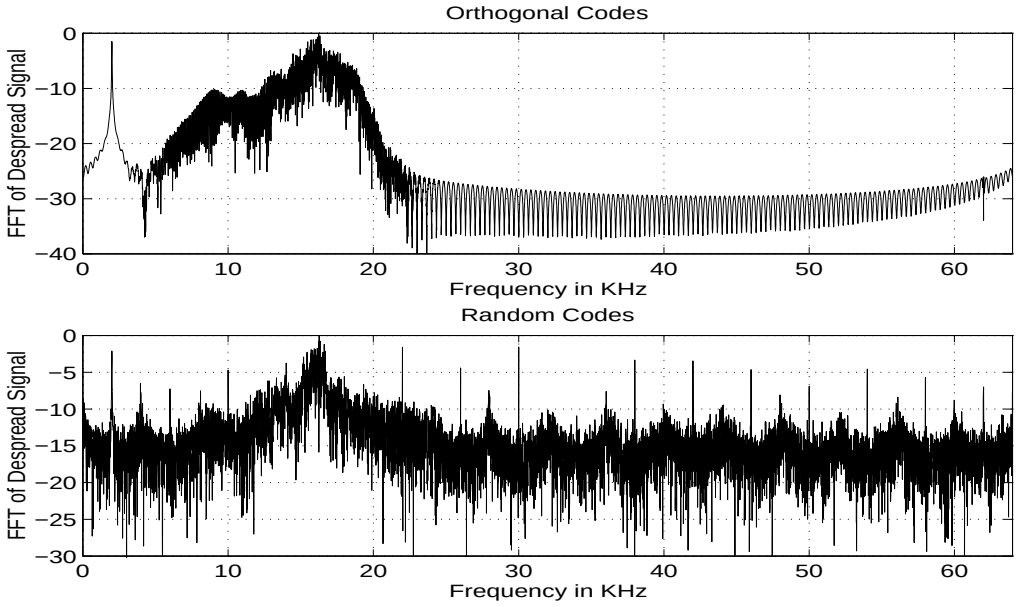

Figure 4.22: Spectra of Despread FM CDMA Signal With Pilot Tone

if the multiple FM CDMA signals are not orthogonal, the threshold of the receiver raises by approximately 2-4 dB. The system simulations indicate that the capacity of the orthogonal link is at least 150 simultaneous users, whereas with non-orthogonal signals, the capacity drops to a maximum of 40 simultaneous users.

The effects of flat fading channel and frequency selective fading channel are investigated in this chapter. The flat fading channel model (with the coherence bandwidth approximately two times greater than the FM CDMA bandwidth) does not cause noticeble capacity reduction. The frequency selective channel model (with the coherence bandwidth approximately $1/10^{th}$ of the FM CDMA bandwidth) shows a slight, 1-3 dB, performance degradation. A very small Doppler spread on the received multipath signal, however, worsens the perfromance significantly. Infact, higher values of the Doppler spread do not inflict further capacity reduction. Under bad channel cases specified in COST 207 standard, the FM CDMA receiver operates below the threshold regarless of the MAI level.

The non-linear processing of the FM CDMA signal does not significantly affect the system capacity. The performance of the reverse FM CDMA link with the hybrid, open and closed loop, controled received power levels is also encouraging. The power control algorithm drives the received power levels from different users to fall within a specific bound, regardless of the user-distances and the small-scale fading effects. However, the implemented power control algorithm assumes a perfect power related information conveyed by the pilot tone. With random spreading codes, the pilot tone reliability in the power information exchanges needs further investigation.

Chapter 5

Design Improvements

The choice of the frequency modulation for the CDMA based WLL system involves a compromise in terms of the system capacity. As the results of the previous chapter indicate, the CDMA with FM modulation enables the desired user capacity. However, with the random codes and with severe interference and fading effects, the system performance degrades significantly . Moreover, as the WLL system continues to evolve, the subscriber load may exceed the designed system capacity, thereby further necessitating modifications in the system architecture.

This chapter investigates two approaches for improving the FM CDMA system capacity. The first section of the chapter describes an adaptive receiver structure that exploits cyclostationarity property of the received FM CDMA signal. The second possibility for future system modifications is to adopt digital modulation with the CDMA technique. The capacity advantages of the digital CDMA system are investigated in the second section of the chapter.

5.1 Single User Adaptive Receivers

The conventional receiver for the FM-CDMA system correlates the received signal with the desired user's spreading code and performs the FM demodulation on the despread signal. In the presence of multiple access interference (MAI) and multipath fading effects, improvements on conventional FM-CDMA receiver are possible, since the conventional CDMA receiver structure is an elementary approach to the CDMA signal detection and it disregards the structure of the MAI.

Multi-user CDMA receiver structures have been proposed as one approach for exploiting the MAI structure, and achieving performance improvements. The optimum multiuser detector for the digital CDMA systems has been shown to be the maximum likelihood sequence detector [Ver86]. The complexity of the maximum likelihood sequence detector grows exponentially with the number of users, and hence such a receiver is impractical even with a small number of users. The suboptimum multiuser detectors for the digital CDMA are decorrelating receiver, multi-stage receiver, decorrelating decision feedback multi-stage receiver etc. [Lup89], [Var90], [Due93]. These multi-user CDMA receiver structures have demonstrated significant capacity gains over the conventional CDMA receiver, with a considerable complexity reduction as compared to the maximum likelihood detector.

Multi-user detectors require the knowledge of the spreading codes, the timings, and the received powers of all the users. Hence, even the sub-optimum multi-user CDMA structures have a very high complexity. In contrast, the single user adaptive receivers require only the knowledge of the desired user's spreading code and the timing. Their complexity is less than that of the multiuser receivers and is independent of the number of the users. Infact, the structure of a single user detector is very similar to that of a conventional receiver, the difference being that the despreading is now achieved by a transversal filter whose weights are adaptive.

Adaptive receivers have many advantages over the conventional receiver. They perform despreading, MAI rejection, ISI rejection and in some cases act as RAKE receivers, coherently combining multipath signals. They also provide near-far resistance making power control requirements less stringent [Maj96]. Such receiver structures, however, require a relatively small spreading code due to increased computational burden associated with a large transversal adaptive filter.

This thesis investigates the performance improvements offered by the fractionally spaced adaptive receivers. The structure of the fractionally spaced FM CDMA adaptive receiver is very similar to that of the fractionally spaced equalizer [Pro95]. It has been shown that significant performance improvements are possible by the use of a fractionally spaced equalizer instead of a symbol spaced equalizer [Git81]. This provides motivation for the use of the fractionally spaced adaptive receivers as opposed to the chip spaced adaptive receiver structures for the FM-CDMA system.

Fractionally spaced adaptive receivers exploit the spectral correlation of the direct sequence spread FM signals and act as time-dependent adaptive filters [Aue94]. There are variety of fractionally spaced equalizer-like structures suitable for the single user CDMA detection. They can be broadly classified as the fractionally spaced linear adaptive receivers and the nonlinear decision feedback fractionally spaced adaptive receivers [Maj96]. The study on the FM CDMA system improvements has focused on the linear fractionally spaced receivers.

5.1.1 Theoretical Background

Traditionally, random real world signals have been modeled as stationary random processes. Gardner emphasized that random data signals are more appropriately modeled as cyclostationary process rather than stationary process [Gar87]. For acyclostationary signal, the statistics vary periodically with time and there is significant correlation between sprectral components. A time dependent adaptive filter (TDAF) can exploit this spectral correlation by combining frequency shifted and weighted versions of the received signal, and gives a better estimate of the signal compared to the signal estimate formed by a time-independent filter or a conventional FM-CDMA receiver.

Figure 5.1 shows the FREquency SHift (FRESH) version of the TDAF. The filter operates on different frequency shifted versions of the signals according to the set of harmonics, $\overline{\alpha}$, for which cyclic autocorrelation function is non-zero [Aue94].

A complex weight fractionally spaced linear adaptive FM CDMA receiver can be derived from above FRESH TDAF. The received FM CDMA signal is sampled $p = 4$ times per chip, or at the sampling frequency of $F_{ss} = pF_{ch}$, where chip frequency F_{ch} is 8 MHz. The adaptive filter is at least Np taps long, where $N = 128$ is the length of the spreading code. The filter output is sampled at the FM signal sampling rate $F_s = 64$ KHz to obtain an estimate of the desired user's FM signal.

The adaptation algorithm is chosen to minimize the mean squared error (MSE), and it operates either in blind mode which does not require the knowledge of the desired signal at the receiver, or in learning mode which assumes atleast a partial knowledge of the desired signal, which is used for training the filter weights, at the receiver. The blind algorithm for filter weight adaptation exploits constant envelope property of the FM signals [Age83]. The block diagram of such a constant modulus

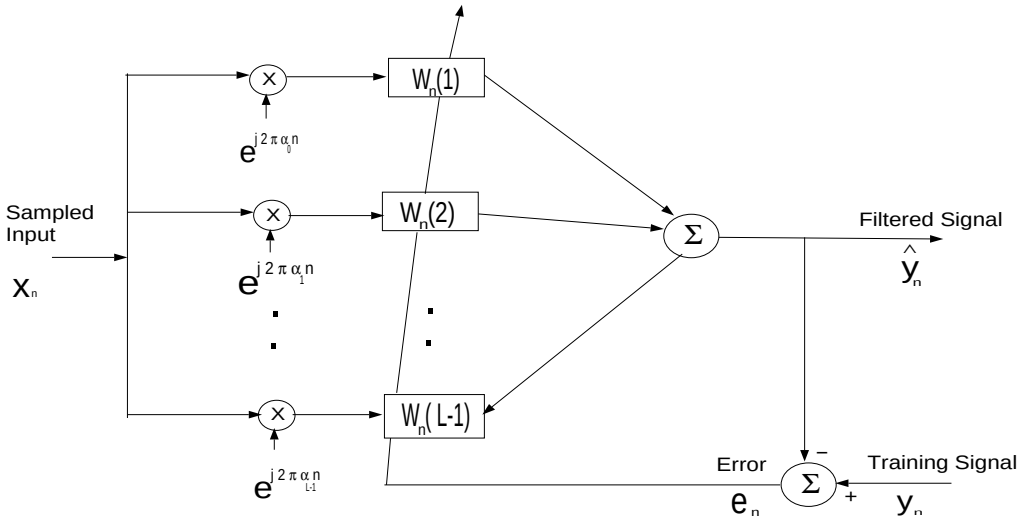

Figure 5.1: Frequecy Shift Version of TDAF

algorithm (CMA) based fractionally spaced adaptive receiver is shown in Figure 5.2. CMA can be described as

$$y(n) = \mathbf{w}_n^H \mathbf{x}_n, \tag{5.1}$$

$$e(n) = sgn[|y(n)|^2 - \delta(n)], \tag{5.2}$$

$$\mathbf{w_{n+1}} = \mathbf{w}_n + \mu_w e(n) y^*(n) \mathbf{x}_n, \tag{5.3}$$

$$\delta(n+1) = \delta(n) + \mu_\delta e(n), \tag{5.4}$$

where $y(n)$ is the sample of output signal, $\mathbf{x_n}$ is the vector of the received signal at n-th instant, and $e(n)$ is the error sample. It is to be noted that the CMA recursion shown here assumes uncoupled weight vector, $\mathbf{w}_n$ at the n-th instant, in relation with the modulus factor $\delta(n)$, and hence convergence coefficients μ_w and μ_δ are chosen independently, and a much faster convergence is possible by using a value of μ_δ an order of magnitude higher than μ_w.

In scenarios with multiple co-channel CM signals, such as in FM CDMA environment, the CMA suffers from an ambiguity problem, since each undistorted signal is a valid output of the CMA, and it is difficult to guarantee that that the signal selected by CMA will be the signal of interest (SOI). This issue has been addressed either by specifying the filter weight coefficients for a specific application, or by imposing a set of linear constraints on the filter coefficients through *a priori* knowledge of the desired

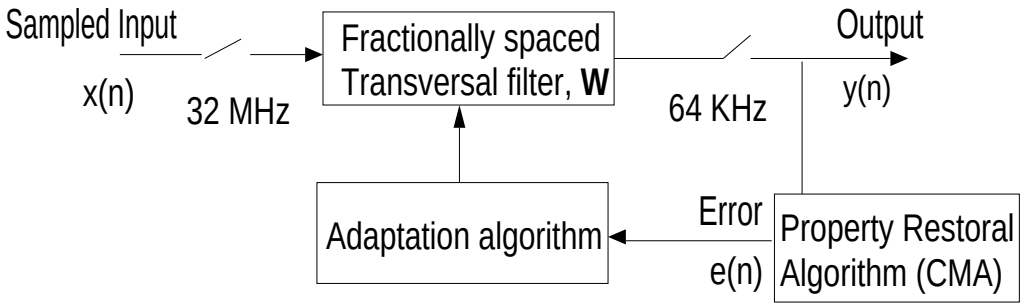

Figure 5.2: Blind fractionally Spaced FM CDMA Adaptive Receiver

signal [Rud90]. The later approach results in a linearly constrained CMA algorithm. The results indicated in this chapter follow the former approach where each user's transversal filter is initialized with the corresponding spreading code.

The learning mode for the filter weight adaptation requires knowledge of the desired user's uncorrupted FM signal, acting as a training signal $x_{tr}(n)$, at the receiver to calculate the error signal. The filter weights are adapted using a training sequence based on the *normalized least means squares* (NLMS) algorithm. The NLMS algorithm is shown here.

$$\hat{y}(n) = \mathbf{w}_n^H \mathbf{x}_n, \tag{5.5}$$

$$e(n) = |y(n) - \hat{y}(n)|, \tag{5.6}$$

$$\mathbf{w}_{n+1} = \mathbf{w}_n + \frac{\mu_w e^*(n)\mathbf{x}_n}{[a + \|\mathbf{x}_n\|^2]}, \tag{5.7}$$

where a is a small constant required to prevent singularities when input signal power tends towards zero, $y(n)$ is the training sequence, and $\hat{y}(n)$ is the output signal. The normalized LMS algorithm reduces the impact of the eigen-value spread of the auto-correlation function of the input signal $x(n)$, and achieves an improved convergence rate [Hay91]. The learning mode adaptation does not require a priori knowledge of the desired user's spreading code; however, it is based on the assumption of the availability of the training sequence at the receiver.

5.1.2 Simulation Results

The simulation results for the complex weight fractionally spaced adaptive receivers are presented in this section. All results pertain to random spreading codes for

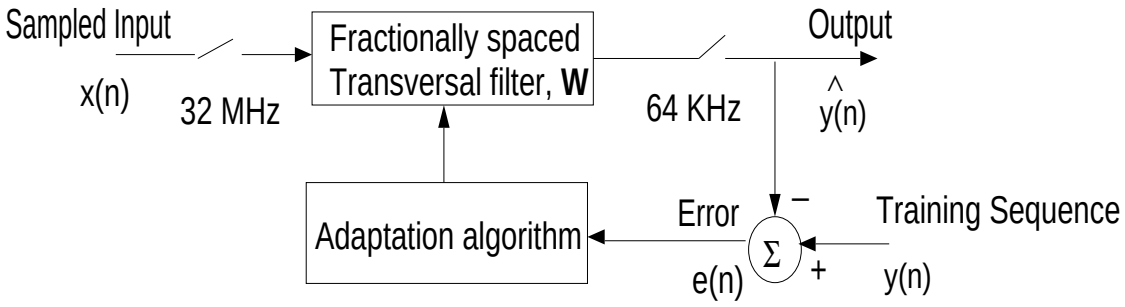

Figure 5.3: Nonblind Fractionally Spaced FM CDMA Adaptive Receiver

different users. For the conventional FM CDMA receiver, the length of the spreading codes is 2048, whereas the adaptive techniques use the spreading codes of length 128.

Figure 5.4 compares the performance of the conventional FM-CDMA receiver with that of the adaptive receivers in presence of ISI. As intuitively expected, the fractionally spaced, equalizer-like, filter structure not only rejects ISI, but also achieves MAI rejection, and shows significant performance improvement over the conventional receiver. Specifically, the non-blind adaptive receiver shows 1-2 dB gain in terms of output SNR with small number of simultaneous users, and 3-5 dB gain with highly loaded system. Blind adaptive receiver performs even better in ISI, and exhibits 5-8 dB gain at any given system load.

The reason behind the better performance of the blind algorithm compared to the performance of the nonblind technique is not fully understood. However, it may be worth noting that if the non-blind technique is implemented using a real-weight fractionally spaced equalizer structure [Maj96], it shows even further performance degradation. Similarly, the complex weight fractionally spaced equalizer-like structure may also not be the optimum non-blind receiver structure for the FM CDMA signals. However, a search of the optimum non-blind adaptive algorithm is not attempted, since, in general, the non-blind receiver structure is a less practical choice for the FM CDMA system upgrades.

Figure 5.5 shows the improvement in output SNR obtained by the adaptive receiver operating in multipath environment. The channel model used for this comparison is based on COST 207 specifications for a typical rural, non-hilly, area. As shown in Tables 4.1, and 4.2, the specified channel model has four multipath components

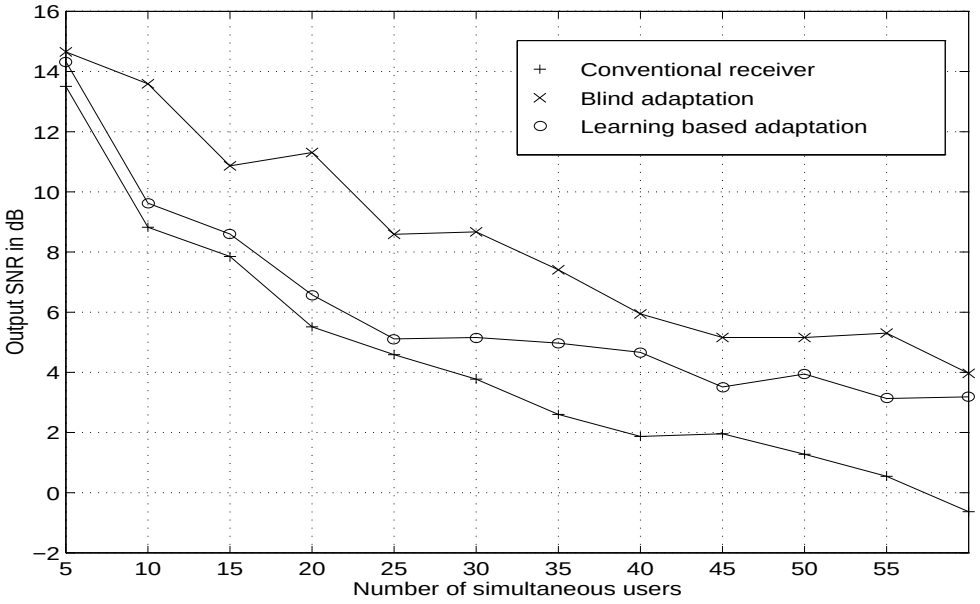

Figure 5.4: Performance Improvement due to Fractionally Spaced Adaptive Receiver: Non-orghogonal Link

with a mean excess delay of 0.098 μ-seconds, and a coherence bandwidth of 1.58 MHz. The results shown here do not account for the Doppler fading effects on individual specular multipath component. The blind adaptive receiver outperforms the conventional receiver by 5-8 dB in terms of output SNR. The non-blind adaptive receiver also shows good improvement in output SNR particularly with very high number of users. These results suggest that the fractionally spaced adaptive structures perform like the RAKE structures for the FM CDMA system.

The ability of adaptive receivers for resisting degrading effects of imperfect power control are demonstrated in Figure 5.6. The blind adaptive receiver shows improved output SNR values when the power levels of different users follow the profile obtained by the power control algorithm explained in previous chapter. Non-blind technique fails to exhibit a clear advantage over the conventional technique in power level mismatches. These results correspond to a variance of approximately 3.5 dB in the received power levels from different users.

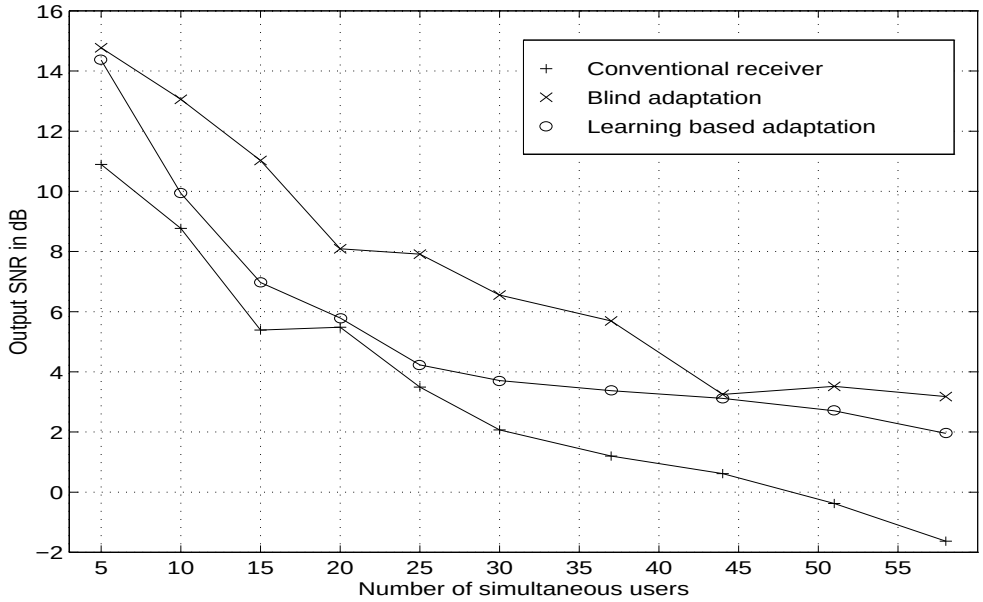

Figure 5.5: Performance of Fractionally Spaced Adaptive Receiver in Multipath Fading

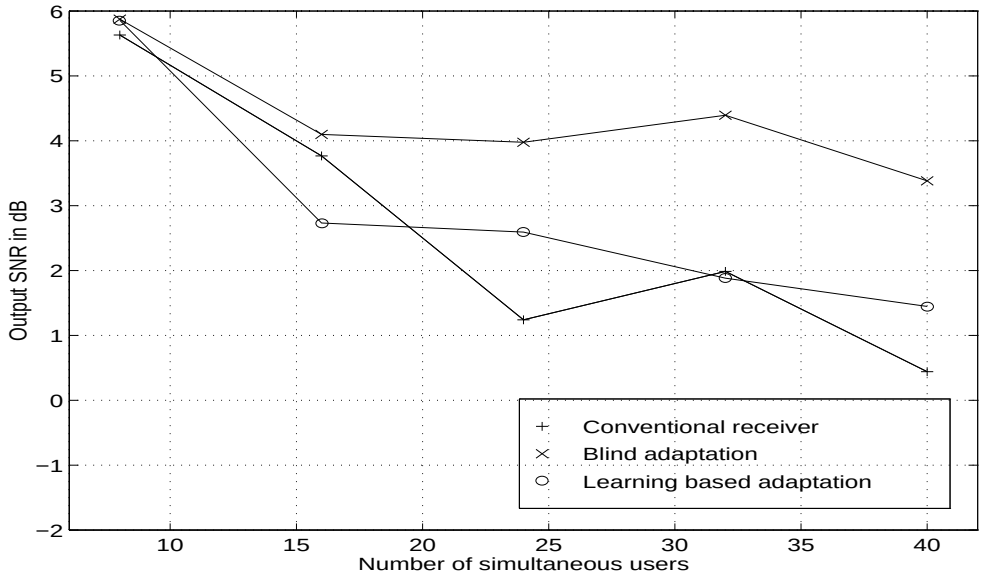

Figure 5.6: Performance of Fractionally Spaced Adaptive Receiver in an Imperfect Power Control Scenario

5.2 Digital CDMA for Capacity Improvements

As mentioned in Chapter 1, digital systems have inherent advantages over analog systems. This section employs analytical tools to estimate the capacity improvements possible in case of a future migration to the digital CDMA system. The proposed digital CDMA system is based on binary phase shift keying (BPSK) modulation with adaptive differential pulse coded modulation (ADPCM) speech coder . Such a simple digital system is suitable from economical perspectives, and also facilitates the comparisons with the FM CDMA system. The analytical comparisons indicate that a significant capacity improvement is possible by the digital CDMA approach. A channel coding scheme for the proposed digital system is also suggested, and further improvements possible at an expense of the system complexity are predicted. The capacity supported by the digital CDMA system is estimated using Gaussian approximation for the DS-SS CDMA systems [Pur77]. In order to form a common base for the comparison, an analytic expression for the FM CDMA system capacity is derived in the next section.

5.2.1 Analytical Performance Estimations for the FM CDMA System

Couch [Cou93] shows that the output SNR for the FM demodulator is,

$$SNR_{out} = \frac{P_s}{P_n} \tag{5.8}$$

$$= \frac{\left(\frac{kD_f}{2\pi}\right)^2 \overline{m^2(t)}}{\int_{-B}^{B} P_{no}(f)df}, \tag{5.9}$$

where P_s is the signal power, P_n is the noise power, and k is the FM demodulator proportionality constant. D_f, $m(t)$, and B are previously defined as the FM frequency deviation constant, the message signal, and the message signal bandwidth. $P_{no}(f)$ is the power spectral density at the output of the FM demodulator, which can be expressed as

$$P_{no}(f) = (\frac{k}{A_c})^2[N_o + 2I(f)]f^2, \qquad |f| \leq B_T/2, \tag{5.10}$$

where $N_o/2$ is the double sided Gaussian noise power spectral density (PSD) at the input to the FM demodulator, A_c is the peak carrier amplitude, and $I(f)$ is the PSD

of the multiple access interference. The received signal is multiplied at the receiver with the desired user's spreading code. The expression for multiple access interference $i(t)$ after this multiplication process is

$$i(t) = \sum_{k=2}^{N_u} a_1(t)a_k(t)A_c\cos(w_c t + D_f \int_{-\infty}^{t} m_k(t)dt), \tag{5.11}$$

where N_u is the number of simultaneous users, $a_1(t)$ is the desired user's spreading code, and $a_k(t)$ is the k-th user's spreading code. The term $A_c\cos(w_c t+D_f \int_{-\infty}^{t} m_k(t)dt)$ represents the k-th user pre-spread FM signal. If we assume synchronous reception of different users' signals at the input to the FM demodulator with polar NRZ spreading code waveform, the above expression simplifies to

$$\begin{aligned} i(t) &= \sum_{k=2}^{N_u} i_k(t) && (5.12)\\ &= \sum_{k=2}^{N_u} i_{1,k}(t)i_{2,k}(t), && (5.13) \end{aligned}$$

where

$$\begin{aligned} i_{1,k}(t) &= a_1(t)a_k(t) && (5.14)\\ &= \sum_{n=0}^{L_c-1} a_{1,n}a_{k,n}p(t-nT_c) && (5.15)\\ &= \sum_{n=0}^{L_c-1} a_{1k,n}p(t-nT_c). && (5.16) \end{aligned}$$

Here, L_c is the length of the spreading codes, and $p(t)$ is rectangular chip waveform (assuming, for the sake of simplicity, no pulse shaping). Also, assuming random spreading code for each user, we can substitute the product $a_{1,n}a_{k,n}$ with $a_{1k,n}$, where $\text{Prob}\{a_{1k,n}=1\} = \text{Prob}\{a_{1k,n}=-1\} = 1/2$. Power spectral density (PSD) of $i_{1,k}(t)$ is, then, given as [Cou93],

$$I_{1,k}(f) = T_c sinc^2(T_c f), \tag{5.17}$$

where T_c denotes the chip period. A closed form expression for the PSD of the k-th user's FM signal, $i_{2,k}(t)$, is not tractable, though it can be approximated as the probability distribution function (pdf) of the message signal. Since the message signal is the voice signal with an exponential distribution function, the PSD of $i_{2,k}(t)$ can be approximated as

$$I_{2,k}(f) = K_c e^{-\frac{2|f-f_c|}{B_T}}, \tag{5.18}$$

where K_c is a proportionality constant, and f_c is the carrier frequency. The PSD of the product $i_{1,k}(t)i_{2,k}(t)$ is the convolution of individual PSD's $I_{1,k}(f)$, and $I_{2,k}(f)$. The determination of the convolution of the expressions of PSD's in Equations 5.17, and 5.18 is simplified, if we assume a high value of processing gain,

$$N = \frac{B_s}{B_t} \approx \frac{1}{T_c B_t} \gg 1$$

, With this assumption, the PSD of the FM signal, $I_{2,k}(f)$, can be approximated as an impulse with a height equal to the power of the k-th user FM signal, i.e.

$$I_{2,k}(f) \approx \frac{A_c^2}{2}\delta(f - f_c), \tag{5.19}$$

The resulting expression for the PSD for the k-th interfering user $I_k(f)$ is

$$\begin{aligned} I_k(f) &= I_{1,k}(f) * I_{2,k}(f) && (5.20)\\ &\approx [T_c sinc^2(T_c f)] * \frac{A_c^2}{2}\delta(f - f_c) && (5.21)\\ &= \frac{A_c^2}{2} T_c sinc^2[T_c(f - f_c)]. && (5.22) \end{aligned}$$

Using Equation 5.22, and referring to Equation 5.10, we can approximate the PSD of MAI $i(t)$ at the input to the FM demodulator as,

$$\begin{aligned} I(f) &\approx \sum_{k=2}^{N_u} I_k(f), \qquad |f - f_c| \le B_t/2 && (5.23)\\ &= \sum_{k=2}^{N_u} \frac{A_c^2}{2} T_c sinc^2[T_c(f - f_c)], \qquad |f - f_c| \le B_t/2 && (5.24)\\ &= \frac{(N_u - 1)A_c^2 T_c sinc^2[T_c(f - f_c)]}{2}, \qquad |f - f_c| \le B_t/2 && (5.25)\\ &\approx \frac{(N_u - 1)A_c^2 T_c}{2}, \qquad |f - f_c| \le B_t/2, && (5.26) \end{aligned}$$

where we have assumed equal received powers from all users. Using Equation 5.26 in Equation 5.9, we obtain the noise power at the output of the FM demodulator as

$$\begin{aligned} P_n &= \int_{-B}^{B} \left(\frac{k}{A_c}\right)^2 (N_o + (N_u - 1)T_c A_c^2) f^2 df && (5.27)\\ &= \frac{2}{3}\left(\frac{k}{A_c}\right)^2 [N_o + (N_u - 1)T_c A_c^2] B^3. && (5.28) \end{aligned}$$

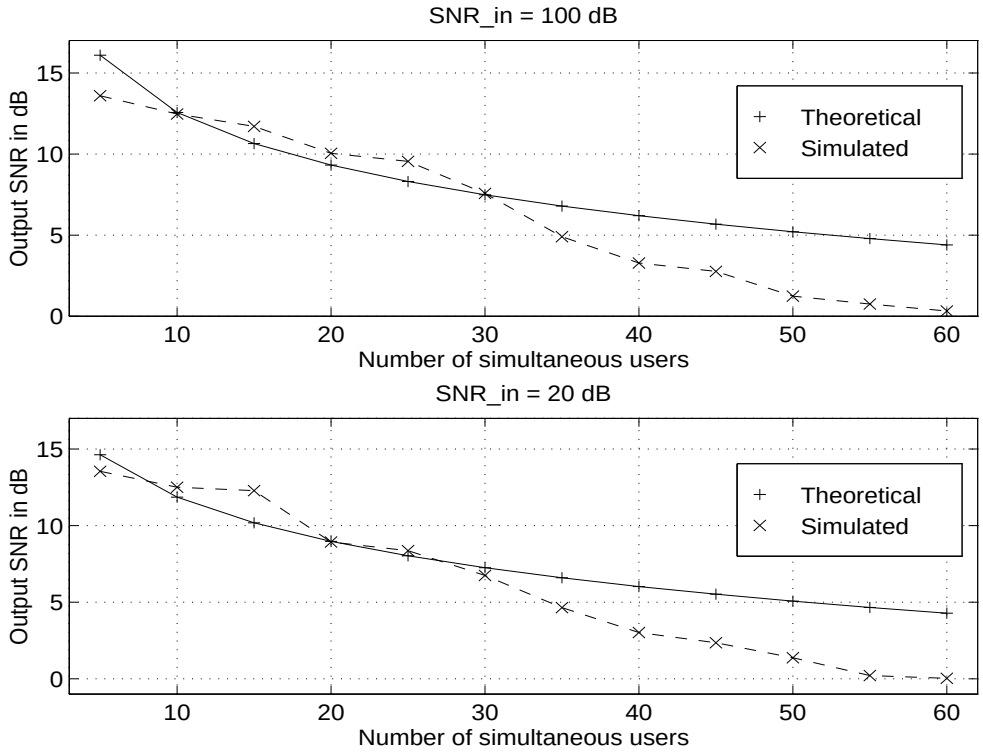

Figure 5.7: Capacity of the FM CDMA System

Hence, the SNR at the output of the FM CDMA system may be approximated as

$$SNR_{out} \approx \frac{\left(\frac{kD_f}{2\pi}\right)^2 \overline{m^2(t)}}{\frac{2}{3}\left(\frac{k}{A_c}\right)^2 [N_o + (N_u - 1)T_c A_c^2] B^3} \tag{5.29}$$

$$= \frac{3A_c^2 \beta^2 B_T \overline{\left(\frac{m}{V_p}\right)^2}}{2B\left[\frac{N_o B_T}{A_c^2} + \frac{(N_u - 1)}{N}\right]}. \tag{5.30}$$

The output SNR values for the FM CDMA system with FM bandwidth B_T=25 KHz, and spread bandwidth B_s = 8 MHz are shown in Figure 5.7. The figure also compares the simulation results with the theoretical estimates in presence of additive white Gaussian noise floor at the input to the FM demodulator. For high values of additive Gaussian SNR at the input to the FM demodulator, and for low and

moderate multiple access interference, a close match between analytical and simulation results is observed. Note that the theoretical expression for the FM CDMA system capacity does not consider signal processing imperfections faced during the simulation, resulting in a small difference between the theoretical and the simulation results.

5.2.2 Performance Estimations for the Digital CDMA System

The block diagram of a simple digital CDMA scheme is shown in Figure 5.8. The analog speech signal is quantized using adaptive differential pulse coded modulation (ADPCM) scheme [Jay86], [Pro95]. The output of the quantizer is converted to a binary polar NRZ signal which forms the input sequence to the convolutional encoder. The structure of rate r=1/2, constraint length K=4 convolutional coder is shown. The output of the encoder is spread using a binary PN code. The resulting spread signal is RF modulated before the transmission. At the receiver, the CDMA signal is demodulated, and despread using the desired user's spreading code. The binary information sequence is recovered using *Viterbi* algorithm with the *hard decision decoding* of the despread signal. The desired user's speech signal is recovered by adding the adaptive predictor output to the binary information signal at the output of the Viterbi decoder.

Flanagan et. al. [Fla79] indicate that toll quality speech transmission (SNR $\geq$ 30 dB, Total Harmonic Distortion $\leq$ 2-3 % in frequency range 200-3200 Hz) is possible with ADPCM operating at 32 kbps. Even for low data rates such as 16 kbps, ADPCM achieves communications quality speech. The authors assign the ADPCM coder a relative complexity count of 1 which compares well with the formant vocoder, and the vocal-tract synthesizers whose complexity counts fall in the range 500-1000. The authors also mention that the terrestrial telephone links perform satisfactorily with bit error rates (BER) less than 10^{-3} at such data rates. Such considerations lead to the choice of the ADPCM voice coder, with the design constraint of achieving moderate BER's.

The suggested channel encoding scheme is moderately complex, but achieves a slight performance improvements as compared to the uncoded CDMA system. The

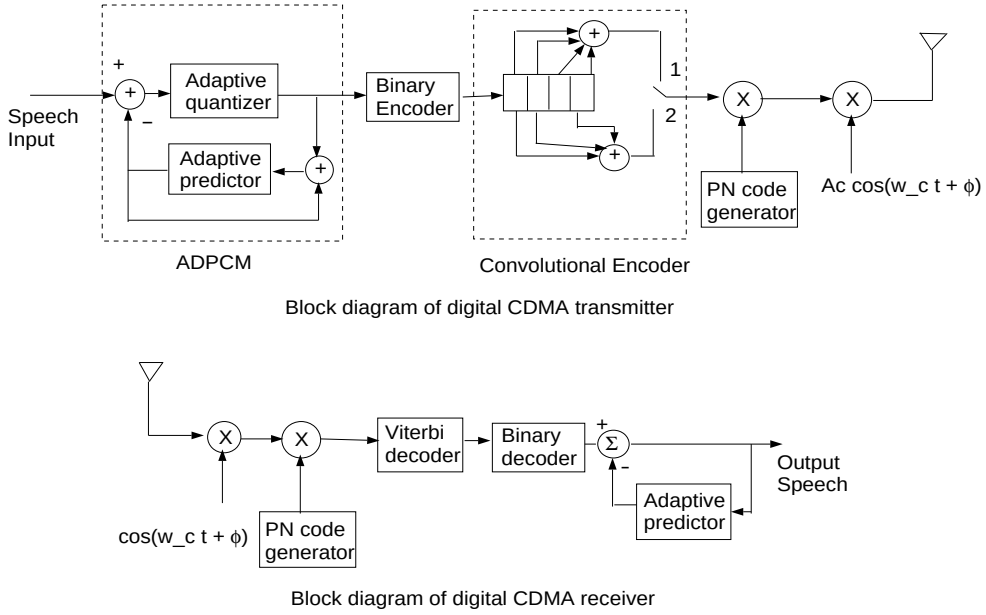

Figure 5.8: Proposed Digital CDMA System Architecture

transfer function of the convolutional encoder, shown in Figure 5.8, is

$$T(D) = 2D^6 + 7D^7 + 18D^8 + \cdots \tag{5.31}$$

The free distance (minimum Hamming distance with respect to an all-zero received sequence) of the code is 6. Equation 5.31 is useful in deriving codeword error probability, P_E, for the hard decision decoding of the received signal, since [Pro95]

$$P_E = T(D)\big|_{D = \sqrt{4p(1-p)}}, \tag{5.32}$$

where p, the BER for a similar uncoded system, may be approximated using Gaussian approximation for the BER of DS-SS CDMA system.

$$p = Q\left[\sqrt{\frac{1}{\frac{N_o}{2rE_b} + \frac{N_u - 1}{3rN}}}\right], \tag{5.33}$$

assuming equal received powers from all users. In order to factor for the increase in the energy per symbol and the data-rate required with the convolutional code, the SNR per bit E_b/N_o, and the processing gain N in the Gaussian approximation for

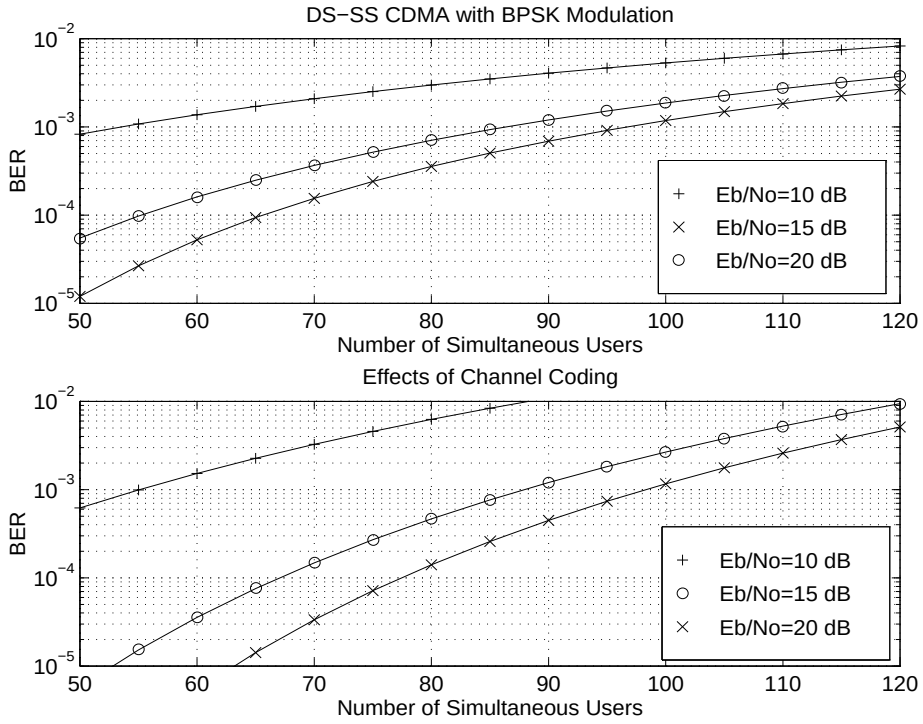

Figure 5.9: Capacity of the Digital CDMA System

bit error rates of an uncoded CDMA system are multiplied with the code-rate r to obtain the above expression for the probability of the bit errors for a coded CDMA system.

The performance of the proposed digital CDMA system architecture is compared with that of the FM CDMA system under a similar set of the parameters. The ADPCM voice coder, for the sake of comparison, is assigned a data rate of 25 kbps. If we select random spreading codes at chip frequency of 8 MHz, the digital system processing gain N remains same as the FM CDMA processing gain that falls in the range 300-400. The BER's for these values of system parameters are shown in the upper graph of Figure 5.9. The uncoded CDMA system achieves a capacity of 75-80 simultaneous users even with a low E_b/N_o value of 10 dB.

The coded CDMA system performs better for high values of E_b/N_o. The probability of the bit error for the coded CDMA reduces significantly if E_b/N_o is greater than 15 dB.

5.2.3 Performance Comparisons

As can be observed from the Figure 5.7, and Figure 5.9, the capacity supported by the FM CDMA system is significantly less than the capacity of the digital CDMA system. With the random spreading codes, the FM CDMA system starts exhibiting poor performance if the number of simultaneous users exceed 40. Even with a very high input SNR of 100 dB, the performance curves for the FM CDMA system are not very encouraging. Whereas, for the digital CDMA system, the BER values remain within the 10^{-3} bound with up to 100 simultaneous users, without any error control coding, and with E_b/N_o values greater than 15 dB. The bit error probabilities of the system are significantly reduced with a rate $r = 1/2$, constraint length[1] 4, convolutional coding scheme, however the system capacity does not increase beyond 100 users. With moderate system loads, the channel coding scheme has the potential of improving the resistance to more severe channel distortions; however, this advantage comes at the cost of an increased receiver complexity. This is the primary trade-off involved in the selection of channel coding scheme.

5.3 Chapter Summary

This chapter discussed some of the future upgrades for the FM CDMA WLL system. As the user demand for WLL subscription increases, either the CDMA interference cancelation techniques, or the migration to the digital CDMA may be considered. The results in this chapter also indicate the performance improvements possible with such techniques in hostile channel conditions.

[1]Selecting a convolutional code with a lower value of the constraint length reduces the decoder complexity. However, even the best convolutional codes, shown in [Zie92], do not cause significant performance improvement, if the constraint length is less than 4.

Chapter 6

Conclusions

This chapter summarizes the research effort conducted for evaluating the performance of the FM CDMA based WLL system. The significant results are outlined, and various assumptions and limitations pertaining to the scope of the research are noted. The chapter concludes with the suggestions on the future work in this area.

6.1 Summary

Exploring the performance and the dynamic ranges of various DSP algorithms for the FM demodulation is the first major task of the research. The results pertaining to the differential FM detection, the quadrature FM detection, and the arctangent FM detection are presented in the third chapter. More advanced FM demodulation algorithms, such as the PLL based FM detection and the zero crossing detection, are also developed and their output SNR characteristics are compared with the three basic FM receiver structures. We observe that the differential and the quadrature method are simple and robust FM demodulation techniques, the arctangent method is a more elegent DSP technique (since it does not require an explicit phase extraction), and the PLL and the zero-crossing detectors have a greater complexity, but they also offer the potential of the threhold extension.

The performance improvements achieved by the PDE and the companding operations are noted, and the limitations on output SNR gains obtained using these methods are understood. It is observed that the companding technique causes the

SNR characteristics to saturate at a low level due to the nonlinear processing. However, it improves the system performance when the speech signal power decreases. The PDE technique shows a slight performance improvement near the threshold region, however it does not exhibit significant gains above the threshold due to the signal processing imperfections in the simulation model.

The fundamental problem of an accurate determination of the output SNR for the simulated analog system is investigated. The results obtained by the four different approaches for the SNR calculations are presented and their significance is outlined. It is noticed that the MSE method is a simple and a fairly accurate method. Theoretically, the cross-correlation coefficient method and the gain-delay method have a better reliability at moderate and high values of SNR, however at the cost of a significantly greater computation load. The noise power ratio (NPR) method is used to validate the results of the MSE, and the cross-correlation based SNR calculation methods. While the general SNR characteristics obtained by the NPR method match with those of the first three methods, the NPR method shows a difference above the threshold. This is due to the fact that the NPR method estimates the signal *plus* noise to noise ratio (SNNR), unlike the other methods which estimate the SNR. Moreover, the NPR method tends to disregard the temporal distortion effects in the time domain waveform.

The performance of the FM CDMA system is studied by developing a DSP based system level simulation test-bed. Using the transmitter and the receiver models of the FM CDMA system, its performance trends are determined. The FM CDMA system capacity in somewhat ideal conditions is greater than even the design goal of 60 simultaneous users in a cell. The voice quality of the FM CDMA system is satisfactory with excessive MAI (upto 150 simultaneous users), if the system users are perfectly orthogonal. The performance of the system in less ideal, more practical conditions is also investigated. A significant reduction in the system capacity due to non-orthognal, random, spreading codes is noted. Infact, with the random spreading codes the system capacity drops to 40 simultaneous users. The FM CDMA receiver threshold in terms of input AWGN floor also increases by 2-4 dB with the random spreading codes.

The impact of the time and the frequency dispersive channel models is greater on the orthogonal system link. However, a mild flat fading channel does not inflict

appreciable performance degradation even for the orthogonal link. With the frequency selective fading channels, and with the frequency dispersion effects, the performance of the orthogonal as well as the non-orthogonal link suffers drastically. Based on the results obtained, we can conclude that in moderate channel conditions, the orthogonal link has a potential of supporting at least 30 simultaneous users. The non-orthognal link is less robust, and may support upto 25 users. However, if the system operates in bad RF channel conditions, such as those specified in the COST 207 standard for the urban hilly area and the hilly terrain, neither the orthogonal link nor the non-orthogonal link can support even 5 simultaneous users.

Besides the channel degradation effects, the effects of the system imperfections such as a nonlinear FM CDMA signal amplification at the base-station transmitter are estimated. The effects of the nonlinearity on the performance of the user phone receiver are observed to be non-significant for the orthogonal and the non-orthogonal links.

The effect of the power control algorithm on the base-station receiver is also shown in Chapter 4. The received power levels from different users at the base-station receiver are varied in accordance with the power control algorithm, and the resulting speech quality is studied for different degrees of MAI. The convergence and the stability of the power control algorithm, and the reliability of the pilot tone in conveying the closed loop power control instructions is also discussed.

The final chapter of the thesis describes the FM CDMA performance improvement strategies. A single user, fractionally spaced, adaptive FM CDMA receiver structure is proposed and its ability in combating the MAI, the multipath fading, and the received power mis-matches is demonstrated. The blind FM CDMA adaptive receiver improves the non-orthogonal system performance by 3-7 dB. The non-blind complex weight fractionally spaced adaptive receiver also gains 2-4 dB advantage over the conventional receiver. The improvements possible with alternate non-blind adaptive structures are not pursued further, since the comparatively simple, blind technique gives a good performance improvement.

The digital CDMA system is also proposed in the final chapter as an option for the future system upgrades. The capacity of the proposed system is estimated as approximately 70-100 users with moderate noise levels. A channel coding scheme is also suggested to further reduce the error event probabilities and thus improve the

ADPCM speech quality.

One improtant point needs a mention in the concluding chapter of the thesis. The FM CDMA system performance predictions, in terms of the capacity, the perceptual speech quality, and the output SNR measure, shown in Chapter 4 and Chapter 5 do not consider the improvements in the CDMA system performance achieved by the interference reduction techniques such as cell-sectorization and voice quality expoitation. If these advantages of the CDMA technique are practically realized, the FM CDMA system may perform better than the predictions in this thesis. On the other side, if the system implementation faces difficulties, for example, in the spreading code acquisition and its reliable tracking, or in the pilot tone detection for the power control, the actual system performance can turn out to be worse than the simulation based estimates.

6.2 Future Work

Eventhough, the work on the FM CDMA system evaluations encompasses the major study aspects, there are many limitations on the scope of the research.

This research focused on the physical link of the FM CDMA system. An equally challanging task is to develop and optimize the network layer issues associated with the WLL systems. Investigations pertaining to the transcoder algorithms at the base-station or at the system switch, the call set-up and termination procedures, and the interface of the WLL system with existing digital telephone network are the examples of important practical work that may be very helpful at the time of the system deployment.

The simulation models of the FM CDMA system are the only source of the performance estimations shown in this thesis. The results shown in this thesis are based on many simplifying hardware related assumptions, such as an ideal, almost infinite precision, signal processor and ADC/DAC transformations, and an efficient code acquisition and tracking scheme. The future work in this area may deal with the development of a hardware prototype of the FM CDMA WLL system, and the study of its performance in real wireless channels.

As expained in Chapter 2, the simulation models for the FM CDMA system are

based on either an orthogonal set of spreading sequences, or random, Gaussian distributed, non-orthognal spreading codes. Due to large length of the spreading code, it is difficult to determine a set of non-orthogonal seqeunces with impressive cross-correlation, and auto-correlation properties. The system performance with maximal-length sequences, or with more specific examples of the Gold and the Kasami sequences is also not studied. Although, with a large length of the spreading code the properties of different spreading codes become very similar, determining the optimum short spreading code for the FM CDMA system and comparing its performance with the performance obtained with a large spreading code may form an interesting future work.

Almost all of the above issues related to the future work in this area may require study at the time of system tests and field trials. The importance of these trials before the final deployment can not be overstated.

Appendix A
A Summary of Speech Quality Measures

Ensuring a good voice quality at the output of communications systems is an important design requirement. The speech quality tests help in identifying distortions due to nonlinear signal processing, such as quantization, speech compression algorithms, and companding. These tests also provide a better handle in accessing the quality of the speech affected by uncorrelated wideband noise components, and in distinguishing improvements achieved by performance enhancement techniques. Information regarding relative quality of speech may be obtained either by subjective tests wherein human listeners gauge the speech quality, or by objective means which are based on signal fidelity parameters.

A.1 Subjective Speech Quality Tests

Subjective tests for voice quality accessments have early origins that date back to the period before development of digital signal processing techniques. Such tests can be classified as either intelligibility tests or quality tests.

A.11 Intelligibility Tests

Rhyme tests (RT) form the main body of intelligibility tests. They aim at determining ease of correctly interpretating the reproduced speech. The human listeners in these tests "fill in blanks" after listening to specific words. The test scores are formed using the correct number of responses from different listeners. *Modified Rhyme Test*

(MRT), and *Dynamic Rhyme Test (DRT)* are examples of more structured RT's, and provide a more suitable base in accounting for different listeners' interpretations, and also serve as a partial quality tests [Del93].

A.12 Quality Tests

Traditionally, *Mean Opinion Score (MOS)* has been the most popular subjective speech quality accessment method. A number, usually between 15 to 50, of trained human listeners hear segments of speech usually 20-60 seconds long in a quiet area, and score the perceptive speech according to an index in a five point standardized scale (with rating of 1 corresponding to unsatisfactory quality, 2 corresponding to poor quality, 3 corresponding to fair quality, 4 corresponding to good quality, and 5 corresponding to excellent quality). In order to average different listeners perceptions, the mean of the scores of all the listeners is taken, hence the name mean opinion score of the test. MOS is intuitively the most reliable technique, since it does not depend on an uncertain transformation between a measured parameter and the speech quality preceived by listners. However, the MOS test results suffer from variations in perceptions by different listeners. Such variability in MOS results is reduced by employing the same group of trained listeners for many tests, and observing individual listner's scoring pattern. MOS variations also reduce if the number of listeners increase, since the standard deviation of MOS estimate, σ_{MOS}, is related to the standard deviation of individual listener's score σ_L as [Kub91]

$$\sigma_{MOS} = \frac{\sigma_L}{\sqrt{n}}$$

Diagnostic Acceptability Measure (DAM) is an alternate, more organized method for differentiating various listeners' interpretations [Del93]. In such tests, the subject evaluates the speech signal on 16 separate scales, divided into three categories, namely signal quality, background quality, and total quality.

Either DAM tests, or increasing the number of listeners for MOS tests tends to be inefficient in terms of time, effort and money. This is the primary reason behind the research in the direction of alternate, less manual, solutions to the problem of voice quality accessment.

A.2 Objective Speech Quality Tests

A.21 Time Domain Tests

Mean Squared Error (MSE), and SNR are two, related, simple approaches for speech quality measurements. These approaches have been described in Chapter 3, where a number of methods for determining mean squared error, and signal to noise ratio for a generalized class of signals were described.

However, the MSE based SNR is a poor estimator of the speech quality for a broad range of speech distortions [McD78]. Measures based on segmented SNR examine the speech signal in a greater detail, and provide an improved measure of the quality of voice, since they better emphasize small-time variations in the speech signal [Del93]. Segmented SNR is defined as the SNR over small subframes of speech each usually 20 to 22 ms long[1].

$$SNR_{seg}(i) = 10\log_{10}\left(\sum_{k=0}^{L-1}\frac{x(Li+k)^2}{[x(Li+k)-y(Li+k)]^2}\right)$$

where $x(k)$ is the discrete time reference speech signal, $y(k)$ is the recovered discrete time speech signal, and L is the number of samples in i-th speech sub-frame.

Averaged segmented SNR is determined by taking average of segmented SNR values for all N subframes, i.e.

$$SNR_{seg} = \frac{1}{N}\sum_{i=0}^{N}10\log_{10}\left[\sum_{k=0}^{L-1}\frac{x(Ni+k)^2}{[x(Ni+k)-y(Ni+k)]^2}\right]$$

Averaged segmented SNR is thus the mean of the individual segmented SNR values.

A better option is to determine the distribution functions of the segmented SNR values. The Cumulative Distribution Function (CDF) of the segmented SNR values $F[\mathbf{SNR_{seg}}]$ is defined as

$$F[\mathbf{SNR_{seg}}] = Prob\{\mathbf{SNR_{seg}} \leq SNR_{seg}\},$$

where SNR_{seg} denotes a specific value taken by the variable $\mathbf{SNR_{seg}}$. The CDF $F[\mathbf{SNR_{seg}}]$ is useful in determining the percentage of the speech frames whose quality, in terms of the SNR measure, is less than the desired value. The CDF of the segmented

[1]The 20-22 $m\,s$ interval is akin to an "acoustic packet", an interval that can contain a distinctive sound. This is the same interval of encoded by a voice coder.

SNR for the differential FM detector is shown in Figure 3.20. As observed from the Figure, this method offers a richer source of information as compared to the MSE based SNR measure.

A.22 Frequency Domain Tests

Mean Squared Error (MSE), and signal to distortion ratio (SDR), computed by taking Fourier Transform of the speech signals, offer an alternate way of measuring the distortion in the speech signal. Segmented SDR values, calculated over many sub-bands of the Discrete Fourier Transform (DFT) of the speech signal, provide a more accurate measure of distortions in different frequency bins.

$$SDR_{seg}(i) = 10\log_{10}\left(\sum_{k=0}^{L-1}\frac{X(Li+k)^2}{[X(Li+k)-Y(Li+k)]^2}\right)$$

where N is the total number of frequency sub-bands, each with L bins, for the DFT $X(w)$, and $Y(w)$ of the reference and recovered signals.

Averaged SDR, and distribution functions of segmented SDR may also be determined to gain detailed information regarding distortion in the frequency domain. Frequency weighted averaged SDR, and a similar parameter *Information Index (I_d)* developed by a French researcher [Lal90], are other popular techniques in which the average over segmented SDR values is taken after assigning different weights to different speech sub-bands.

$$I_d = \sum_{i=0}^{N} W_2(i)\frac{3}{0.1+10^{-[SDR_{seg}(i)+W_1(i)/10]}}$$

$W_1(i)$, and $W_2(i)$ are tabulated weighting functions that account for criticalness of i-th speech sub-band in determining perceptual voice quality.

An another advanced frequency domain speech quality accessment technique developed by researchers at Bell Northern Research (Canada) is based on calculating *coherence function* between the reference speech signal, and the recovered signal [Bnr86]. In this method, instead of averaging over sub-bands of the DFT of the speech signals, time-domain speech samples are first divided into four groups according to their amplitude levels. The squared coherence function $\gamma^2(f,i)$ is calculated for each of the groups by determining the spectral densities, i.e.

$$\gamma^2(f)(i) = \frac{|S_{xy}(f,i)|^2}{S_{xx}(f,i)S_{yy}(f,i)}$$

where $S_{xx}(f,i)$, $S_{yy}(f,i)$, and $S_{xy}(f,i)$ denote input, output, and cross power spectral densities, variable f denotes the frequency bin whose value ranges from 0 to 4000, and i denotes the group number varying from 1 to 4. Signal to Distortion measure using the squared coherence function, $\gamma^2(f,i)$, is then evaluated as

$$SDR(f,i) = \frac{\gamma^2(f,i)}{(1-\gamma^2(f,i)) + K_1(f,i))}$$

where $K_1(f,i)$ is a frequency weighting function. The averaged SDR is calculated by taking weighted sum of $SDR(f,i)$,

$$SDR_{avg} = \sum_{i=1}^{4}\{K_2(i)\sum_{f=0}^{4000}[K_3(f)SDR(f,i)]\}$$

where $K_2(i)$, and $K_3(f)$ are the perceptual error weighting functions.

A.23 Parametric Distance Measures

This method offers an appropriate tool for evaluating the quality of the speech reproduced by linear predictive speech coders [Del93]. An example of this method is *Ikatura measure* which is based on the dissimilarity between all-pole LPC models of the reference and encoded speech signals. Another parametric distance measure employs em log-area ratio (LAR) coefficients of the reference and encoded speech frames to determine the synthesized speech quality. *Cepstral distance*, developed by Nippon Telephony and Telegraphy (NTT), is the third example of this method and it uses cepstral coefficients of the original and coded speech determined from the LPC method [Kub91].

Bibliography

[Age83] J. Treichler, B. Agee, "A New Approach to Multipath Correction of Constant Modulus Signals," *IEEE Transactions on Acoustics, Speech, and Signal Processing–ASSP-31,* pp. 459–472, April 1983

[Arm36] E. Armstrong, "A Method of Reducing Disturbances in Radio Signalling by a System of Frequency Modulation," *Proc. IRE,* Vol. 24, pp. 689–740, May 1936

[Aue94] V. Aue, J. Reed, "An Interference Robust CDMA Demodulator that Uses Spectral Correlation Properties," *IEEE Vehicular Technology Conference,* pp. 563–567, 1994

[Bes84] R. Best, *Phase-Locked Loops: Theory, Design, and Applications,* McGraw-Hill Book Company, 1984

[Beg93] M. Begley, E. Kempton, "One per Customer Digital Radio Systems," *Proc. of 4th European Conf. on Radio Relay Systems, IEE Conference Publication*, n 386, 1993

[Bla76] A. Blanchard, *Phase-Locked Loops: Application to coherent receiver design,* John Wiley and Sons, 1976

[Bnr86] Bell Northern Research, "Objective Evaluation of Non-linear Distortion Effects on Voice Transmission Quality," *Contribution to CCITT*, COM XII-46-E, March 1986

[Bue93] M. Buehrer, B. Woerner, "Teaching Spread Spectrum for Commercial Wireless Communications, " *To appear in IEEE Transactions on Education,* 1996

[Bun96] R. Bunce, "FM Performance Summary," *A technical note from SigTek Inc.,* January 1996

[Car22] J. Carson, "Notes on theory of modulation," *Proc. IRE,* Vol. 24, pp. 57–64, Feb. 1922

[Cha93] S. Chandler, J. Braithwaite, "Analysis and Simulation of a Distributed Radio Telephone Network," *Proc. of 4th European conf. on radio relay systems, IEE Conference publication,* n 386, 1993

[Cla95] V. Classens, "Transmitting Effectively in Local Loop," *Telecommunications, International edition*, V 29, n 2, Feb. 1995

[Cos89] "Digital Land Mobile Radio Communications: COST 207," *Cost 207, Final report,* Commission on European Communities, Brussels, Luxembourgh 1989

[Cou93] L. Couch, *Digital and Analog Communication Systems,* MacMillan Publishing Company, 4th edition, 1993

[Cox91] D. Cox, W. Gifford, H. Sherry, "Low Power Digital Radio as a Ubiquitous Subscriber Loop," *IEEE Communications Magazine*, March 1991

[Cox86] D. Cox, "Research Towards a Wireless Local Loop," *Bellcore Exchange*, Vol. 2, pp. 2–7, November 1986

[Dav86] J. Davis, "Simulation Analysis of an FM Communication System with a Phase Locked Loop Discriminator In Presence of Gaussian and Impulse Noise," *Masters thesis*, University of Missouri-Rolla, 1986

[Del93] J. Deller et. al., *Discrete-Time Processing of Speech Signals,* Macmillan Publishing Company, 1993

[Dix84] R. Dixon, *Spread Spectrum Systems,* John Wiley and Sons, second edition, 1984

[Due93] A. Due-Hallen, "Decorrelating Decision-feedback Multiuser Detector for Synchronous Code Division Multiple Access Systems," *IEEE Transactions on Communications*, Vol. 41, No. 2, pp. 285-290, February 1993

[Erd95] A. Erdogan et. al., "The Effect of Directional Antennas in CDMA Wireless Local Loop Systems" *Proc. Symposium on Wireless Personal Communications*, Virginia Tech, pp. 71–80, June 1995

[Fla79] J. Flanagan et. al., "Speech Coding" *IEEE Transactions on Communications*, Vol. COM-27, No. 4, pp. 710–735, April 1979

[Gar87] W. Gardner, *Statistical Spectral Analysis: A Non-probabilistic Theory,* Prentice Hall, New Jersey, 1987

[Gil91] K. Gilhousen et al., "On the Capacity of a Cellular CDMA System," *IEEE Transcactions on Vehicular Technology,* Vol. 40, No. 2, pp. 303–311, May 1991

[Git81] R. Gitlin, S. Weinstein, "Fractionally spaced Equalization: An Improved Digital Transversal Filter," *Bell System Technical Journal,* Vol. 60, No. 2, pp. 275–296, February 1981

[Har87] F. Harris, "Exact FM Detection of Complex Time Series," *Signal Processing Theories, Implementations, and Applications*, ISSPA, pp. 70–73, August 1987

[Hau94] R. Haugen, B. Olsen, B. Eskedal, "Radio in Local Loop In Rural and Suburban Environments," *Proc. 1994 IEEE Conference on Personal Wireless Commmunications,* pp.12–16, 1994

[Hay91] S. Haykin, *Adaptive Filter Theory,* second edition, Prentice Hall, New Jersey, 1991

[Jas95] J. Hale, "DSP Implementation of an FM Demodulator," Memorandum to Grayson Electronics, October 1995

[Jav94] A. Javed, P. O'kelly, K. Dick, "Wireless Technology Evoluation and Its Impact on Access Networks," *Proc. 1994 IEEE Conference on Personal Wireless Commmunications*, pp.12–16, 1994

[Jay86] N. Jayant, "Coding Speech at Low Bit-rates," *IEEE Spectrum Magazine,* pp. 58–63, August 1986

[Jer92] M. Jeruchim et. al., *Simulation of Communication Systems,* Plenum press, 1992

[Kor85] I. Korn, *Digital Communications,* Van Nostrand Reinhold, New York, 1985

[Kau95] A. Kaul, "Multi-user Receivers for CDMA Systems," *Masters thesis*, Virginia Polytechnic Institute and State University, 1995

[Kid95] P. Kiddle, "Rural and Urban Wireless Local Loop – DECT Potential," *Proc. 5th IEE Conf. on Telecommunications,* n 404, pp. 65–68

[Kub91] R. Kubichek et. al., "Advances in Objective Voice Quality Accessment," *Proceedings of IEEE Globecom Conference,* pp. 1765–1770, 1991

[Lal90] J. Lalou, "The Information Index: An Objective Measure of Speech Transmission Performance," *Annals of Telecommunications,* Vol. 45, No. 1–2, pp. 47–65, 1990

[Lat89] B. Lathi, *Modern Digital and Analog Communication Systems,* second edition, Holt, Rinehert, and Winston, Inc., 1989

[Lee91] W. Lee, "Overview of Cellular CDMA," *IEEE Transactions on Vehicular Technology*, Vol. 40, No. 2, May 1991

[Lee85] O. Lee, W. Tranter, "Estimation of Signal-to-Noise Ratio in Communication Systems Using Complex Envelope Signal Representation," Department of Electrical Engineering, University of Missouri-Rolla, 1985

[Lup89] R. Lupas, S. Verdu, "Linear Multiuser Detectors for Synchronous Code-division Multiple Access Channels," *IEEE Transactions on Information Theory*, Vol. IT-35, No. 1, pp. 123–136, January 1989

[Maj96] M. Majmundar, "Single User Adaptive Receivers for DS-SS CDMA System," *Masters thesis*, Virginia Polytechnic Institute and State University, 1996

[Mar80] F. Marvasti, *A Unified Approach to Zero Crossing Detection*, 1980

[McD78] E. McDermott, et. al., "Perceptual and Objective Evaluations of the Speech Processed By Adaptive Differential PCM," *Proc. of IEEE International Conference on Acoustics, Speech, and Signal Processing*, pp. 581–585, April 1978

[Mer93] R. Merrett, R. Warburton, A. Rolls, "Wireless Access based on CT-2 System," *Proc. of 4th European Conf. on Radio Relay Systems, IEE Conference Publication*, n 386, 1993

[Owe93] F. Owens, C. Geoffrey, "DECT Standard in Local Loop Applications," *Proc. of 4th European Conf. on Radio Relay Systems, IEE Conference Publication*, n 386, pp. 103–107, 1993

[Pic92] A. Pickholtz, D. Schilling, L. Milstein, "Theory of Spread Spectrum Communications: A Tutorial," *IEEE Transactions on Communications*, Vol. COM-30, No. 5, pp. 855-884, May 1982

[Pis93] A. Pistoia, G. Ettore, R. Pompili, "Technical and Economical Accessment of Radio Relay Systems in Local Loop Distribution Networks in Italy," *Proc. of 4th European Conf. on Radio Relay Systems, IEE Conference Publication*, n 386, 1993

[Pur77] M. Pursley, "Performance Analysis for Phase-Coded Spread-Spectrum Multiple-Access Communications-Part I: System Analysis," *IEEE Transactions on Communications*, Vol. COM-25, No. 8, pp. 795–799, August 1977

[Pro95] J. Proakis, *Digital Communications,* 3-rd Edition, McGraw-Hill Book Company, New York, 1995

[Pro88] Committee report on radio propagation, "Coverage Prediction for Mobile Radio Systems Operating in the 800/900 MHz Frequency Range," *IEEE Transcations on Vehicular Technology*, Vol. 37, No. 1, February 1988

[Ram94] B. Ramamurthy, C. Mathiazhagan, "DECT based WLL System," *Proc. 1994 IEEE Conference on Personal Wireless Commmunications*, pp.55–59, 1994

[Rap95] T. Rappaport, *Wireless Communications: Principles and Practices,* Prentice Hall, Inc., 1995

[Rud90] M. Rude, L. Griffiths, "A Linearly Constrained Adaptive Algorithm for Constant Modulus Processing," *Signal Processing V: Theories and Applications*, pp. 237–240, 1990

[Sch94] D. Schilling, "Broadband CDMA: One Phone for a Wireless 21st Century," *Proc. 1994 IEEE Conference on Personal Wireless Commmunications*, pp.1–5, 1994

[Set94] A. Seth, Y. Rao, "Technology Choices for PCN/PCS Development in India," *Proc. 1994 IEEE Conference on Personal Wireless Commmunications*, pp.115–118, 1994

[Sig95] "Telelink CDMA System Description Document", *SigTek's report on FM CDMA WLL*, May 1995

[Sig95b] Discussions during SigTek's monthly visits to Virgnia Tech, 1995-1996

[Smi75] J. Smith, "A Computer Generated Multipath Fading Simulation For Mobile Radio," *IEEE Transactions on Vehicular Technology* , Vol. VT-24, No. 3, pp. 39–40, August 1975

[Tau86] H. Taub, D. Schilling, *Principles of Communication Systems,* McGrow-Hill Publishing Company, 2nd edition, 1986

[Voe72] H. Voelcker, "Zero Crossing Properties of Angle Modulated Systems," *IEEE Transactions on Communications*, Vol. COM-20, pp. 307–315, June 1972

[Var90] M. Varanasi, B. Aazhang, "Multiuser Detection in Asynchronous Code Division Multiple Access Systems," *IEEE Transactions on Communications*, Vol. 38, No. 4, pp. 509–519, April 1990

[Ver86] S. Verdu, "Minimum Probability of Error for Asynchronous Gaussian Multiple Access Channels," *IEEE Transactions on Information Theory*, Vol. IT-32, No. 1, pp. 85–96, January 1986

[Wer94] M. Werner, "Radio Propagation for Local Loop Applications at 2 GHz," *Proc. 1994 3rd annual int. conference on universal personal commmunications*, pp.119–123, 1994

[Wel96] M. Welborn, "Model based FM Demodulation for Cochannel Interference Rejection," *Masters thesis*, Virginia Polytechnic Institute and State University, 1996

[Whi94] D. Whipple, "The CDMA Standard", *Applied Microwave and Wireless*, pp. 24-39, Winter 1994

[Woe94] B. Woerner, J. Reed, T. Rappaport, "Simulation Issues for Future Wireless Modems," *IEEE Communications Magazine*, July 1994

[Woe96] B. Woerner, *Digital Communications Class Notes,* 1996

[Zie92] R. Ziemer, R. Peterson, *Digital Communications and Spread Spectrum Systems,* Macmillan, 1992

Vita

Yash was born on March 6, 1972 at Ahmedabad, India (Ahmedabad is the sixth largest city of India with a population of approximately 4 million). His went to school at the city of Rajkot where he lived with with his parents, Dr. Munindra P. Vasavada and Mrs. Panna M. Vasavada, and sisters, Mss. Sheetal and Amee Vasavada.

In 1988, after a very competitive entrance examination, he was admitted to the prestigious Electronics and Communications program at L. D. Engineering College, Ahmedabad. He graduated with a Bachelor in Engineering (B.E.) degree in September, 1992. In October, 1992 Yash joined Essar Gujarat Ltd. which is one of the top ten organizations of India. Yash worked there as a member of automation group. He assisted the software development activity for the automation system of a manufacturing plant.

Yash joined Virginia Polytechnic Institute and State University in August, 1994 for an M.S. degree in Electrical Engineering. He interned at L.C.C., Inc. in Arlington, Virginia during the summer of 1995. In September, 1995 Yash joined Mobile and Portable Radio Research Group (MPRG) under the tutelage of Dr. J. H. Reed.

Yash likes playing cricket, badminton, volleyball, table-tennis, and chess. In addition, he enjoys drawing pencil sketches, flying kites, and swimming.